Chemistry

For Technological Advances

Dr. Aarti Trehan

Dr. Rajesh Trehan

Chemistry for
Technological Advances

NEX GEN PUBLICATIONS

India | UAE | Nigeria | Uzbekistan | Montenegro | Iraq | Egypt | Thailand | Uganda | Philippines | Indonesia

www.nexgenpublication.com

Chemistry for
Technological Advances

Edited By:

Dr. Aarti Trehan
Associate Professor, Chemistry Department, Arya Kanya Mahavidyalaya, Shahabad (M)-136135, Kurukshetra (Haryana) India

Dr. Rajesh Trehan
Associate Professor and Head, Chemistry Department, DYSP Govt. P. G. College, Nahan-173001 (H.P.) India

First Impression: January 2023

Chemistry for Technological Advances

ISBN : 978-81-959870-7-8

Rs. 650/- ($18)

Published by:
Nex Gen Publications

PREFACE

One of society's most difficult challenges is to decouple economic growth from environmental impact and many of the emerging technologies are developed by keeping this in mind. Our society faces unprecedented challenges. The ongoing COVID-19 pandemic is perhaps the one at the forefront of our minds, but there are many other critical global issues that also require urgent action, such as the climate crisis, the growing instability and cost of energy, economic and technological developments during the present scenario of warfield conflicts and the scarcity of natural minerals and resources. Chemistry plays a vital role in tackling today's challenges and ensuring a sustainable future. Chemists are identifying technologies with the potential to advance our society and improve the quality of life. The role of chemistry is central for finding and implementing innovative solutions that enable a more sustainable future. Climate and energy are two of the most pressing global challenges and chemists need to help find solutions.

The world is adopting revolutionary digital tools such as artificial intelligence, robotics, big data and supercomputing and so are chemists in academia and industry. These technologies will transform our society and have already yielded significant breakthroughs and created previously untapped opportunities. Each of the technologies gives us a glimpse of what chemistry can achieve and how creativity and commitment for a more sustainable future can yield the solutions we so urgently need. There is also a need for multidisciplinary approach and a more holistic way to teach, carry out and apply chemistry.

One of the main goals of the present work is to implement a systems-thinking approach to the education, research and practice of chemistry. In future years, the aim is to build broader and more diverse innovative ideas owing to suggestions made by chemists from around the world. The book- "Chemistry for Technological Advances", meets the needs of an extensive community of students as it is broad in scope, rather than deep. It is,

therefore, appropriate for a wide audience, including all practising scientists, technologists and economists.

The editors are grateful to all the learned contributors for their cooperation and support in compiling very useful information on various facets of chemistry for technological advances. We are sure that the information compiled in this volume will prove helpful in understanding the role of chemistry for sustainable technologies and to ensure their use for the benefit of mankind. This book will serve as an excellent reference material for academicians, researchers, industrialists and students in the field of chemistry, chemical industry, technology, energy, material science, environment, economics etc.

Contributors are fully responsible for the authenticity of their work and the concepts/views presented by them through this book and the editors has no role or claim or any responsibility in this regard. We apologize unreservedly for any mistakes, omissions or failure to fully acknowledge any source. Any suggestions for improvement in this book are also welcome.

ACKNOWLEDGEMENT

We would like to express our sincerest gratitude to **Maa Saraswati**, who has been our guiding light throughout this project. Without Her divine intervention, this book would not have come to fruition. We most gratefully acknowledge the help of many sources in the preparation of this book. It is impossible to mention all of them, as every book on the subject that we have read has left its impression upon our memory. We would also like to acknowledge the contributions of our colleagues, friends, and students who have generously shared their knowledge and expertise with us. Their invaluable insights and feedback have helped shape the content of this book. We admire the blessings and sweet memories of our parents for guiding us during the present work and always. To our family members and loved ones, we extend our heartfelt thanks for their unwavering support and encouragement. Their love and encouragement have been a source of inspiration and motivation throughout this project. Additionally, special thanks to our cute cats and kittens, for cheering up our mood. We express our immense gratitude to Nex Gen Publications for publishing this book in time. We appreciate your commitment and fast response in publishing this book. Finally, we would like to extend our appreciation to all the contributors to this book who have shared their research, experience, and wisdom with us. Your contributions have been invaluable, and we are grateful for the opportunity to collaborate with such talented scholars and researchers. In conclusion, we express our deepest appreciation to everyone who has played a role in the creation of this book. Your support and encouragement have been essential to its success.

Dr. Aarti Trehan

Dr. Rajesh Trehan

Table of Contents

EFFECT OF ENERGY INTENSITY ON COMPONENT QUALITY THROUGH LASER METAL DEPOSITION (LMD) PROCESS

S. Sheikhi, E. Mayer and K. Bronstein
Institute of Materials Science and Welding Technology, Berliner Tor 13, 20099,
Hamburg University of Applied Sciences, Hamburg, Germany

ABSTRACT

The ability to quickly produce complex structures of a unique design and with reduced waste are the main advantages of the additive manufacturing (AM) of metal-based components. Various AM processes are used in the industry and have been subject of research. Nevertheless, the correlation of energy input, heat balance and quality of components is still a point of research. This study will introduce an affordable method to control the height of each layer as a mechanism to assure the reproducibility of AM products. Moreover, the fundamentals of energy input and heat balance will be discussed in order to demonstrate that the general requirement for constant parameters as demanded by certification authorities actually increased the production time and reduced the quality of the parts. The research has been carried out by means of laser metal deposition with powder, which is one process of additive manufacturing for metal-based components.

Keywords: LMD-P, Laser metal deposition, additive manufacturing, Robot based manufacturing

INTRODUCTION

The competitiveness of an industrial company is linked intrinsically to the production process, organization and means of production. Manufacturing industry and its associated production technology are therefore crucial to the further development of industrial society. Meanwhile, globalization ensures ongoing improvement in production technology so as to meet product requirements in terms of costs, quality, manufacturing time and complexity. Due to application of new technologies and digitization approaches, it is imperative to constantly re-evaluate production structures, on the one hand to guarantee reproducible quality and on the other hand to reduce the cost and complexity of procedures [1]. Additive manufacturing offers the potential to blaze new trails in production and to occupy new markets and niches. Additive manufacturing is the generic term for technologies that generate new components through a contiguous or rather additive operation (addition of material by elements or layers) [1,2].

Additive Manufacturing (AM) is a process whereby a component is fabricated using a 3D digital model. The process consists of the addition of layers of material to a substrate

surface to create an object [2,3]. It has the advantage of customised components which are topologically optimized, and it may substitute for many assembly processes [4].

There are several AM processes, categorized according to different aspects. The classifications are based on: (I) the material types including metals, polymers, and ceramics; (II) the bonding method i.e., direct or indirect; and (III) the form of the materials, which may be powder, wire, sheet, or liquid [2]. Additive manufacturing techniques are classified into seven general categories (binder jetting (BJ), directed energy deposition (DED), material extrusion (ME), material jetting (MJ), powder bed fusion (PBF), sheet lamination (SL), vat photopolymerization (VP)) by the International Standardization Organization (ISO) and the American Society for Testing and Materials (ASTM) 52900:2015 [5]. DED and PBF are the two main technologies used for AM of metal materials. PBF selectively melts regions of a powder bed using thermal energy. In DED, thermal energy is used to melt AM materials while being deposited on a previous layer [5]. This paper will focus on laser-based directed energy deposition, also known as laser metal deposition (LMD). LMD has been used since the 1980s to recondition components by means of laser cladding or laser coating. Developments in the field of laser source technologies have enabled LMD to be competitive with other cladding and coating technologies based on arc welding [6,7].

Originating in the principle of build-up welding, a volume/component is generated through a multilayered repetition of a welding layer assisted by the LMD process. In comparison to subtractive manufacturing, advantages can be gained regarding use of resources, integration of functions, and manufacturing time, depending on the kind of construction [8]. The reproducible quality of an additive-manufactured component and therefore the process capability relies on a variety of parameters. Next to the welding parameters there are further influencing factors such as the machine operator, material, geometry, and the production plant, all of which may impact the manufacturing process. Following the observation of Reinhardt *et al.* and Sehrt, the operator of a plant has a significant influence on the quality and economic efficiency of additive-generated components [9,12]. Human performance is liable to natural fluctuations and cannot be treated as constant in the course of a working day. This variation has to be taken into consideration for the executed activity. Further variables are the influence of method as a function of the parameter set, and the filler material. [10]. A need for standardized parameter sets for serial production has been determined in various scientific studies, as those are applied to the qualification of a process and to the properties of a component. The effect of powder used on the reproducibility of component quality has been examined in multiple research facilities. It was discovered that a high process capacity depends on consistent material properties. Influencing factors like batches, supplier, chemical composition, morphology, grain size and distribution as well as humidity all

affect the outcome of additive manufacturing process, in other words build-up welding, and act on the controllability of the process [1, 2, 8, 10-14].

Those examined interactions in the additive field are already taken into account in manufacturing that uses welding technology, by means of the codification of welding instructions and qualifications, for example ISO standard 15614 (for arc-based manufacturing) [15]. The necessary parameters are specified depending on material in a tolerance range and visualized as energy per unit length. In the context of this work the LMD process will form the primary focus. The procedures applied can be transferred to other arc-based processes as well.

METHODS

The use of laser-based build-up welding is designated in the literature as LMD (laser metal deposition), DMD (direct metal deposition), DLC (direct laser cladding), and LRM (laser rapid manufacturing) [2-3,5]. The different terms result from the development history and lead to near-net-shaped components. In the context of this study solely the term laser metal deposition (LMD) shall be understood.

LMD manufacturing essentially consists of a laser beam, device for the supply of the material (powder or wire), protective gas cover, a substrate and a handling system. Depending on the material, the laser beam is focused on a point with a defined diameter. The material is supplied into this focus point in the form of powder or wire. The energy density of the laser causes a melt pool which ideally consists of 98% of the supplied material. Argon is used to carry the powder onto the workpiece and simultaneously protects the melt pool from reacting with atmospheric gases. The laser spot and the powder nozzles are guided over the surface of the specimen along a predefined path, resulting in a weld bead (Figure 1). The surface of the workpiece is coated by offsetting the weld bead in the plane, as described below. The system is then moved upwards by the resulting layer height and the process is repeated until the required number of layers, and thus the required layer height, has been reached [16, 17].

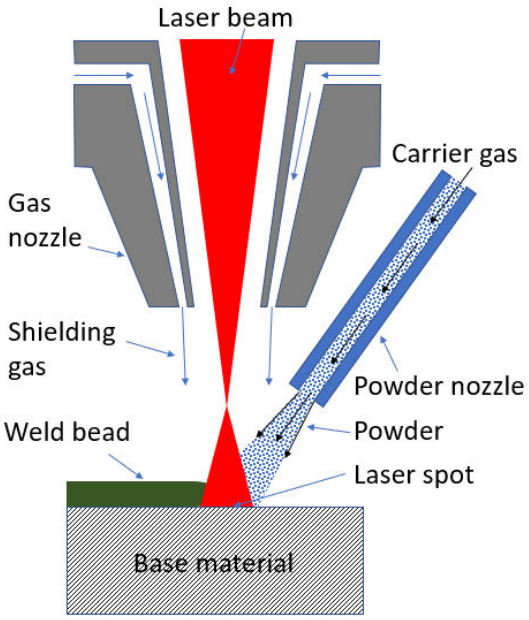

Figure 1: Schematic visualisation of the laser metal deposition (LMD) process [16]

The necessary absorbed intensities during LMD are approximately around 10^5 [W/cm²] or even less and the required exposure time is in the range between 0.01 – 1s to achieve a sufficient connection, consequently the process takes place consistent with the phenomenon of heat-conduction welding. The introduced energy intensity has to ensure a safe melting of material without reaching the boiling point of the alloy. The latter is necessary to reduce pore formation [18].

In the LMD process, the material is supplied in the form of powder or wire, and depending on the operating production plant it can be supplied laterally and/ or coaxially to the laser spot on the surface of the component. The process takes place under a protective gas atmosphere which consists of argon or a mixture of argon and helium. If powder is used in LMD, a conveying gas for the transport of the particles is added. The conveying gas usually matches the composition of the protective gas. The flow rate has to be coordinated so that no turbulences occur, simultaneously it has to be high enough to ensure a sufficient protective gas cover. Further, the applied gas influences the formation of the melting pool, since the physical properties of the gas may result in a higher possibility of cultivating disruptive plasma. Plasma formation is hampered by using helium; however, the eight times higher thermal conductivity of helium leads to a radical heat transfer and consequently to an effect on the weld bead [17].

The laser beam is focused through the use of an optic on a specific point (beam narrowing w_0). For LMD a defocused point outside of the Rayleigh length Z_r is used.

The diameter of the laser spot results from a circular point with the radius 'r' according to the following equation (1).

$$A = \pi r^2 \tag{1}$$

By that approach the process is guaranteed to be carried out as heat conduction welding. Therefore, the power density J of the material will be treated according to equation (2).

$$J = {}^{P}/_{A} \tag{2}$$

The spot size is determined by the distance of the welding head relative to the surface of the base material. The laser spot diameter $d_L(z)$, e.g., is described by Equation (1) as a function of the Rayleigh length z_r, and the defocusing distance, which is reduced by z relative to the optic-specific smallest focal spot diameter d_f.

$$d_L(z) = d_f \times \sqrt{1 + \left(\frac{z}{z_r}\right)^2} \tag{3}$$

Theoretically the distance z between the welding head and the surface of the material remains constant, assuming a constant building rate. However, in reality height variations between each layer have been observed. Therefore, in some cases z represents a mean value determined experimentally from multiple welding layers.

Experimental setup

The Institute of Materials Science and Welding has developed a robot-based additive manufacturing system consisting of a robot as a handling system in conjunction with a laser, arc and plasma depending on the use of a direct energy source. An automatic tool exchanging system has been developed, enabling a fast and reproduceable change of the direct energy systems. As a handling system an industrial robotic arm of type KUKA KR 125/3, controlled by a KR C2 controller is used. It is a 6-DOF robotic arm with a payload of 125 kg, a maximum reach of 2410 mm and a repeatability of ±0.2 mm. The large work envelope of the robot enables its usage for welding as well as additive manufacturing applications.

A turning and tilting table is attached to the robot, providing two additional DOFs. All welding guns and optical sensors are mounted at the sixth axis of the robot in a way that minimizes the occurrence of singularities, as shown in figure 2. The LMD process has been carried out using a 'HL 4006D' 4 kW lamped pulsed Yttrium-Aluminium-Granet (YAG) laser with a wavelength of 1064 nm. The control of the laser is embedded in the robot control, allowing for differentiated use of the laser power and laser operation

mode (continuous wave or pulsed). The laser beam is coupled into an optic with a focal length of f=300 mm.

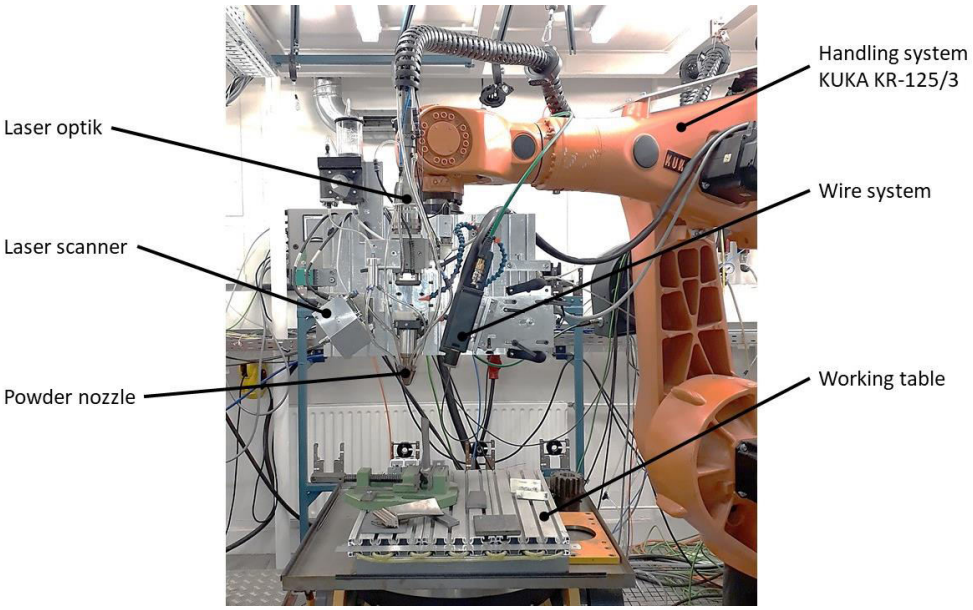

Figure 2: KUKA KR125/3 with the laser optic and nozzles for LMD

A commercially available laser scanner made by Micro Epsilon detects the surface to be reconditioned. The technical specification of the scanner is depicted in Table 1.

Table 1: Technical specification of the Micro Epsilon scanner

Technical specification	**Value**
z-axis measuring range	290 mm
x-axis measuring range	120 mm
Profile frequency	up to 4,000 Hz
Measuring rate	up to 2,560,000 points/sec
z-axis reference resolution	12 µm
x-axis resolution	1,280 points/profile
Permissible ambient light	10,000 lx
Laser source	semiconductor laser 658 nm (red)
Laser power	8 mW (class 2M)

As described on the homepage of Micro Epsilon [19], "The laser scanner uses the laser triangulation principle for two-dimensional profile detection on different target surfaces.

By using special lenses, a laser beam is enlarged to form a static laser line and is projected onto the target surface (red line on the specimen). The optical system projects the diffusely reflected light of this laser line onto a highly sensitive sensor matrix. In addition to distance information (z-axis), the controller also uses this camera image to calculate the position along the laser line (x-axis). These measured values are then output in a two-dimensional coordinate system that is fixed with respect to the sensor. In the case of moving objects or a traversing sensor, it is therefore possible to obtain 3D measurement values."

This scanner enables internal data pre-processing without the need for additional software. The system is first configured in accordance with the desired selection criteria, such as maximum or minimum value. Automatic data acquisition in accordance with the selected criteria then takes place. Further, this system has an interface suitable for integration of the scanner into the robot's control, which makes this integration process less complex and reduces the cost of the investment.

The laser scanner was incorporated into the robot's control. In order to incorporate the scanner into the welding head, a construction was created with an appropriate level of stability and robustness alongside flexibility which allows for the scanner to be set up and dismantled as necessary. It is important to ensure that vibrations from the robot's motion profile do not affect the location of the scanner. In addition, the scanner must be protected from exposure to heat during the welding process in order to avoid thermal congestion of the sensors. For this purpose, an integrated pneumatic protective device was designed to shield the scanner during welding [20]. Typically, the sensor is protected from thermal stress due to an offset between the scanning beam and the melting pool. However, this offset can negatively affect the accuracy of repositioning in the case of filigree components, and therefore needed to be avoided in this project.

Materials

The powder applied in the LMD process is Stellite 21 (CoCr28MoNi with the material number 2.4979). The material is a cobalt alloy with a density of 8.33 g/cm³, a hardness between 290 and 430 HV and a melting range between 1,295°C and 1,435°C. The alloy can be metallurgically processed powder, cast or applied through welding technology [21]. The chemical composition of Stellite 21 is shown in Table 2.

Table 2: Chemical composition according to data sheet

Co	Cr	Ni	Fe	Mo	Others
Bal.	27.0	2.5	1.5	5.5	C, B, Si, Mn

Stellite 21 has a good resistance against thermal or mechanical shock. Even during stress, the alloy can harden even further through an abrasive effect. The material is resistant against oxidizing or reductive gaseous atmospheres up to 1150°C [21].

The powder is introduced into the weld pool using a three-beam nozzle. The three powder beams intersect 12 mm below the nozzle creating a powder focus of approximately 3 mm, defining the powder density [g/min mm²] of the LMD system. The powder nozzle has been implemented in the optic and represents a unit for laser cladding, or LMD in the case of additive manufacturing. This arrangement results in the powder spot lying in the same plane as the laser spot, ensuring maximum powder efficiency. The influence of the powder beam on the quality of LMD has been investigated in [22].

RESULTS AND DISCUSSION

A parameter study was executed beforehand with the described additive manufacturing plant for the multilayer coating of components by means of LMD. In the course of preliminary tests, the parameter set as shown in Table 3 has produced flawless weld beads with an average height of 0.5 mm.

Table 3: Welding parameter

P / [W]	S / [mm]	p / [g/min]	F / [l/min]	L / [l/min]	a / [mm]	v / [mm/min]
2500	3	15	7	10	12	800

P = laser output; S = laser spot; p = powder feed rate; F = carrier gas flow; L = shielding gas flow; a = working distance; v = welding speed

The visual and dye penetrant inspection as well as the metallographic examination of the weld seams have shown reproducible and flawless seams. In the cross section, four layers arranged on top of each other with a total height of 2 mm can be seen. No discontinuities in the form of pores or cracks were detected. Thereby the principal applicability of the parameters as starting parameters for the LMD process has been proved.

It ought to be possible to additively-manufacture thin-walled structures based on the parameter set presented in Table 3. For the parameter-finding exercise, a sample with a wall thickness of 1.5 mm and a height of 10 mm was chosen. Theoretically the application of 20 overlaying weld beads should suffice to realize this geometry. Parameters determined from previous tests are applied as initial values for the process variables.

20 weld beads have been applied without regulation of the working distance. The working distance between the powder nozzle and the substrate was increased by 0.5 mm each layer. The parameters produced very good results for the first layer, but after the third layer no application could be ensured. The cause was the excessive heating of the substrate. Similar observation had been made by Eisenbarth et al and Pirch et al [25]. As a new approach, the laser output was reduced for each layer by 10%. The power reduction could only create reproducible results as low as a laser output of 900 W. Therefore, an experimental lower limit of 980 W was preset for the laser outcome in the control system of the robot. As can be seen in figure 3-a, this strategy produced 20 overlaying layers, whereby the last 5 layers do not show a regular structure.

The experiments were executed repeatedly under consideration of a constant initial temperature per layer, thereby realizing an evenly distributed build-up of the structure. The additive-manufactured bridge as shown in figure 3-b presents a higher build-up, even though the surface of the final layers could not be generated to be sufficiently even. As self-regulating mechanism as described by Sun in [26] could not be observed.

The averaged width of the bridge amounts to 1.8 mm and the height to 9.7 mm. Therefore, the created bridge has a width half the size of the spot diameter and the total height divided by the number of applied layers results in an averaged layer height of 0.49 mm. The laser spot and laser output were reduced so that the laser density stayed constant on the surface for a more evenly distributed build-up. Subsequent experiments with the new parameters show an even and reproducible build-up under consideration of the adjustment of the laser output for each layer as well as consideration of the initial temperature for each layer; figure 3-c.

Figure 3: Seam build-up a) without control b) optimized initial conditions c) optimized parameters and initial conditions

The anticipated height of 0.5 mm per layer has been nearly met, however those deviations will appear more noticeable in the upper layers with higher or more complex structures. It has been experimentally proven that an alteration of the distance of 0.4 mm leads to a significantly uneven layer build-up. It is caused by the resulting variation of the laser and powder spot density, since there is already a difference of 2 mm between the real and the theoretical surface heights at the fifth layer. The facts of this situation are illustrated schematically in figure 4; it should be considered that the real material surface represents the real working distance and not the theoretical one.

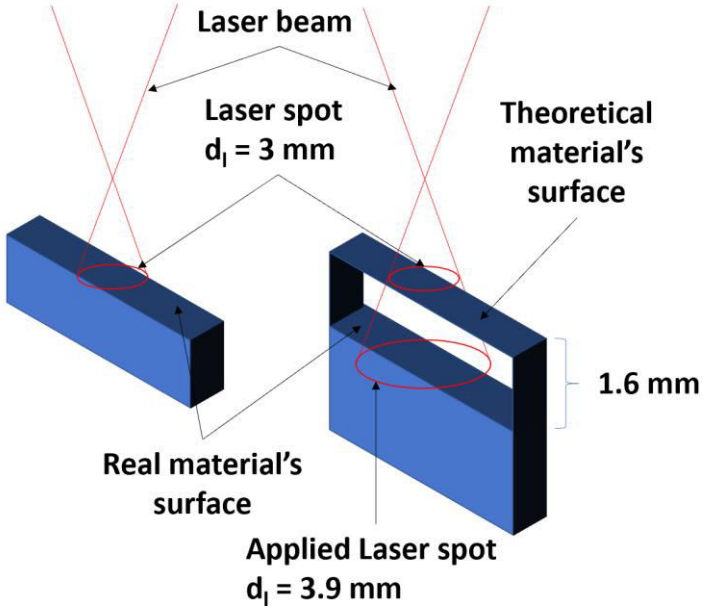

Figure 4: Comparison between the theoretical and actual layer build-up

The optimal case between process control and layer build-up is portrayed on the left-hand side of figure 4. The z-coordinate of the actual surface results from the sum of the respective layer heights. The z-coordinate of the LMD optic has been adjusted for each layer by a predetermined value. The difference between the calculated and the actual z-coordinate results from the deviation between the programmed and the measured layer heights. The laser spot diameter *dl* is a function of *z*, as is shown in equation 1, therefore the effective laser spot increases continuously over the required laser spot diameter and that causes the energy density to decrease squarely. Starting from a laser output of 2,500 W and a spot diameter of 3 mm, an energy density of 354 W/mm^2 results. Provided the actual layer height is lower than the originally determined layer height, the laser spot is too large after a certain height and thereby the energy density is not enough to create an even melting pool. Further, the powder focus increases, and the powder efficiency correspondingly decreases, causing less powder than required to enter the melting pool. This leads to an unintentional reduction of the layer height which is repeated each layer.

Over 8 layers, a reduction on a single layer height of 0.2 mm leads to a deviation of 1.6mm between the theoretical and actual material surface. This leads further to a growth of the laser spot diameter of approximately 0.9 mm and a total spot diameter of 3.9 mm for the same laser output at 2500 W, which results in an energy density of 209 W/mm^2. The outcome of a distinct difference between the actual and the programmed layer height (0.8 mm) is illustrated in figure 5.

Figure 5: Influence of the working area on the structure build-up through LMD

In order to determine the current height position of the layer surface and to transfer the input value into the handling system as a z-coordinate, a sensor is implemented into the control of the robot. This approach ensures an equal distance for each layer between the position of the powder focus and the laser spot relative to the surface. This can be accomplished by scanning the current z-coordinate of each layer and transferring the position to the robot control system. The integration of the scanner into the control system has already been described and presented by Mayer [20]. With this implemented z-control system it is possible to create greater heights. A structure with a total height of 40 mm is illustrated in figure 6-a. The z-offset varies between 0.4 and 0.6 mm for the manufacturing of that structure. A height deviation in the course of the walls can only be seen in the corners of the structure which is due to the process caused by the change of orientation, hence a co axial powder nozzle is necessary to minimize this effect.

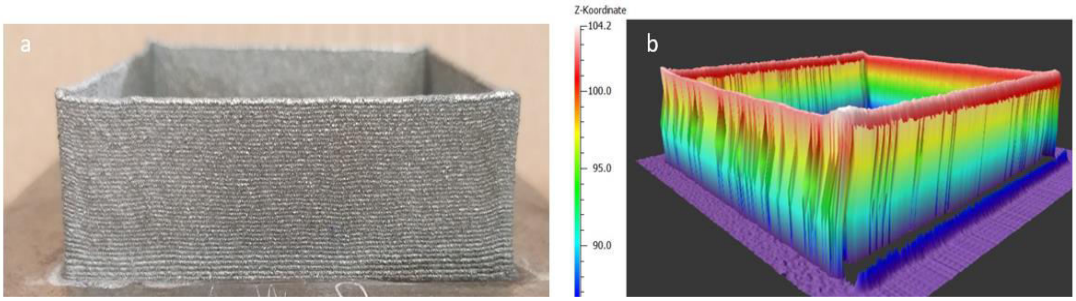

Figure 6: a) LMD manufactured component using height control; b) z-coordinates of a LMD component with optimized height control

The height of the generated component as depicted in figure 6-b has been retrospectively determined through the scanner. The maximum z-coordinate with a

value of 104.2 mm has been found at one of the edges. A height difference of 1 mm equals a delta-z of 0.49. In the illustrated example, the height difference between the highest and the lowest part of the upper surface is around 0.7 mm. The height difference within one wall is approximately 0.3 mm.

The same structure has been generated by applying regulation of the working distance to only two sides (left side and background wall) and by applying a constant height to the working distance to the other two sides (front and right wall). The result of the experiment is shown in figure 7-a. The left and the back wall clearly show an even build-up, whereas the front and the right wall are distinctly irregular. Due to the uneven build-up, the manufacturing process was terminated after a total height of 15 mm.

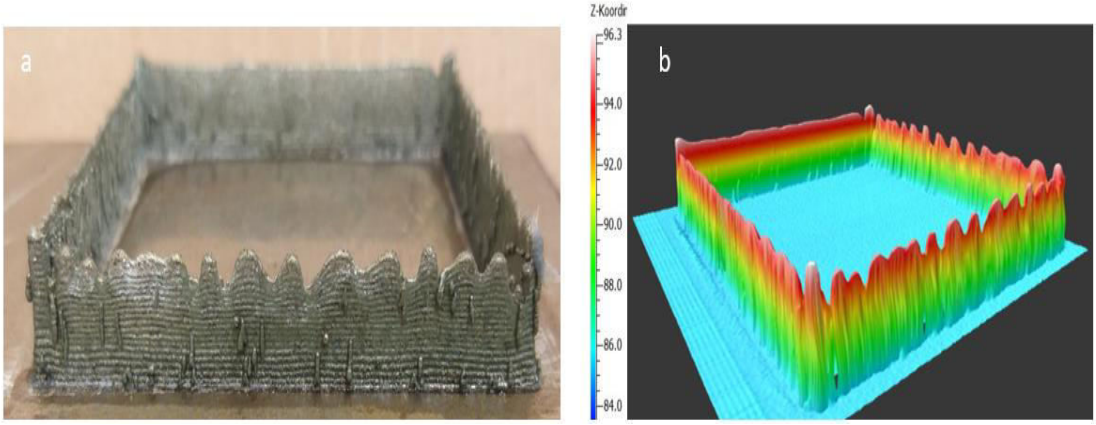

Figure 7: a) Interrupted use of height control; b) z-coordinates of a LMD-component

The outcome of the height measurement (figure 7-b) shows a delta-z of 4.5 in the z-coordinate which has a height difference of 2.1 mm along the front wall. The height difference in the area of the left wall is in the same order of magnitude (0.3 mm) as has been shown in figure 6-b.

The acquisition of the height profiles shows a need for an integrated height regulation to ensure an evenly distributed build-up through application of the LMD process.

A metallographic examination proves the quality of the illustrated component. The cross sections were examined in retrospect of pores, porosity and cracks. An image of the cross section along the vertical length of the structure (figure 8) shows several exemplary detailed views. The walls of the structure have no apparent cracks, enclosures, bonding flaws or cavities, only individual pores at maximum 50 µm have been found. The deviation of the wall thickness especially between the lower layers can be derived from the change in the heat transfer.

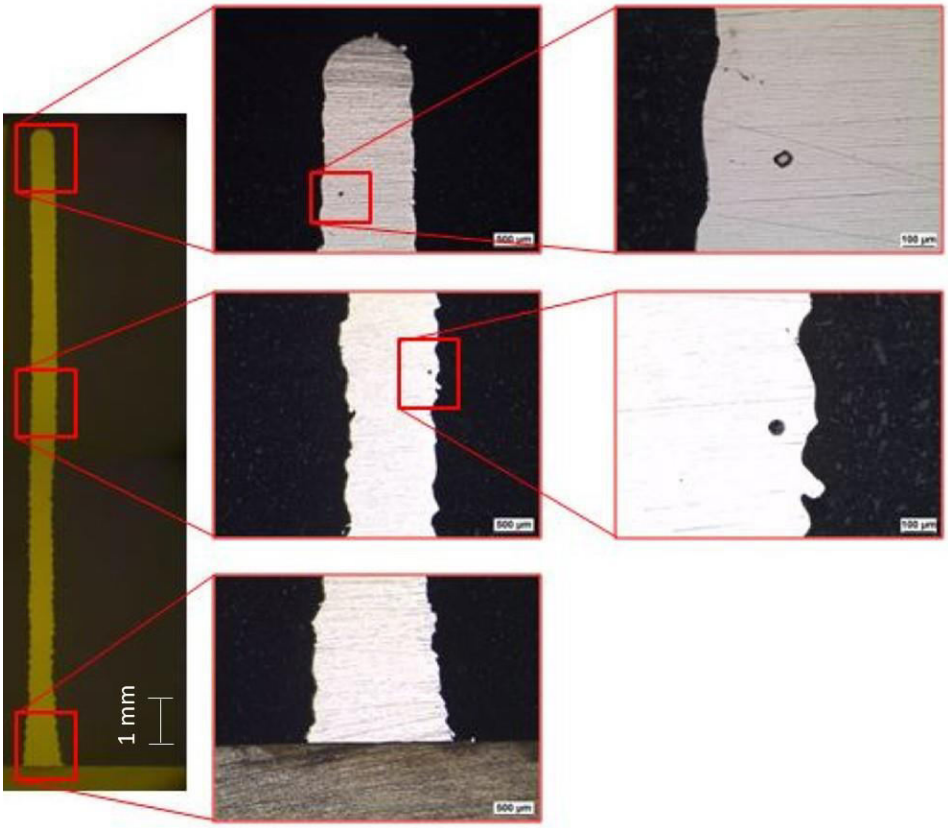

Figure 8: Metallographic examination of the manufactured component

CONCLUSION

This study showed a clear correlation between energy density and cooling rate of LMD structures. Due to the temperature of the substrate plate, it is necessary to produce the first layers with a higher energy input. However, only three layers could soundly be produced without external interaction. Further layers using the same parameters as the first three layers showed the formation of a wavy appearance on the surface of the beads, which got worse with an increasing number of layers. Consequently, a usual production strategy as executed by industrial partners was applied and analyzed. The strategy involved a 10% reduction in laser power for the next layer. However, 980 watts represented the lower limit of the required laser power, which was reached after the 12th layer. This way it was possible to produce 20 layers without external interaction such as cooling. Best results had been produced after optimizing the z-offset of the printing head, considering a 10 % reduction of heat input for each layer and considering a constant starting temperature of max. 50 °C for each layer. The effect of z-offset showed most impact on the quality of the layer: height variations of up to 1.6 mm within one layer were recorded. Similar observations have been reported in the literature. According to Eisenbarth et al and Pirch et al, the LMD process parameters

have been set for achieving mainly pore- and crack-free deposits, however they can fail when used for AM of complex parts. This is due to heat accumulation during the process, leading to a lower deposit height. Hence the part may fail during build-up. Consequently, an optimized parameter set of it has been suggested from preliminary studies [24,25]. Sun *et al.* described the height variation within the LMD process since the initial layers are characterized by a certain kind of process instability [26].

Therefore, it is essential to implement an active height and temperature regulation in the control of LMD machines.

List of Abbreviations

The following abbreviations are used in this manuscript:

AM Additive manufacturing

ASTM American Society for Testing and Materials

BJ Binder jetting

DED Directed energy deposition

DLC Direct laser cladding

DOF Degrees of freedom

ISO International Standardization Organization

KUKA Keller und Knappich Augsburg

LMD Laser metal deposition

LRM Laser rapid manufacturing

ME Material extrusion

MJ Material jetting

PBF Powder bed fusion

SL Sheet lamination

VP Vat photopolymerization

WAAM Wire arc additive manufacturing

YAG Yttrium-Aluminium-Granet

Summary and outlook

During the execution of this study, the application of welding parameters to the LMD process for additive manufacturing has been examined. It has been proven that an adjustment of the parameters is significant for additive manufacturing. It has further

been shown that the laser output has to be reduced for each layer to reach the desired height. The consideration of the initial parameters and the resulting actions show an additional measure to generate the intended heights. Particular attention must be paid to the actual height (real working distance) of the object during manufacturing, since this directly influences the diameter of laser spot and the powder focus. The wrong working distance leads simultaneously to a reduced laser output density [W/mm^2] and a powder output density [g/mm^2]. The study shows a contradiction to the literature [1] which demands constant parameters. In the case examined, reproducible flawless structures could not be derived from constant parameters. It has been determined that especially the deviation of the laser output and the control of the layer height are significant factors for the generation of flawless structures using LMD. The constant temperature per layer is an additional measure to keep layer height discrepancies within a small tolerance window. Efforts were made to keep the starting temperature at beginning of each layer at the same level, however these efforts would lead to an eight-fold increase in manufacturing time, hence either to a decrease in productivity or to an increase of residual stresses due to active cooling. The main aim of this work was to develop a simple and cost- efficient system to assure more efficient additive manufacturing using DED processes (direct energy deposition; LMD, WAAM etc.) This aim has been fully achieved.

Availability of data and material: All data generated or analyzed during this study are included in this published article.

Competing interests: The authors declare that they have no competing interests.

Funding: This research received no external funding.

Authors' contributions: Conceptualisation, Project administration, Writing - Original Draft, S.S; Investigation, Validation, Methodology, E.M.; Software, Visualization, Writing - Review & Editing, K.B. All authors have read and agreed to the published version of the manuscript.

REFERENCES

[1] Christian Eschey; Maschinenspezifische Erhöhung der Prozessfähigkeit in der additiven Fertigung; Forschungsberichte IWB Band 274; Herbert Utz Verlag München; 2013.

[2] A Review of Metal Additive Manufacturing Technologies. Mostafa Yakout, M. A. Elbestawi, Stephen C. Veldhuis. July 2018, Solid State Phenomena, Vol. 278, pp. 1-14.

[3] I. Gibson, D. Rosen, and B. Stucker. Additive Manufacturing Technologies; 3D Printing, Rapid Prototyping, and Direct Digital Manufacturing. New York, USA: Springer, 2015.

[4] Yao X, Moon SK, Bi G (2016) A cost-driven design methodology for additive manufactured variable platforms in product families. J Mech Des 138(4):041701. https://doi.org/10.1115/1.4032504

[5] 5. Standard Terminology for Additive Manufacturing - General Principles - Terminology. ASTM. ISO/ASTM 52900, ed. West Conshohocken, PA, 2015.

[6] Williams SW, Martina F, Addison AC, Ding J, Pardal G, Colegrove P. Wire + Arc additive manufacturing. Mater Sci Technol 2016; 32:641–7. https://doi.org/10.1179/1743284715Y.0000000073

[7] Gu J, Cong B, Ding J, Williams SW, Zhai Y. Wire Arc additive manufacturing of aluminium. USA, Texas: SFF Symp Austin; 2014. p. 451–8.

[8] Dubourg L, Archambeault J. Technological and scientific landscape of laser cladding process in 2007. Surf Coatings Technol 2008; 202:5863–9. https://doi.org/10.1016/; j. surfcoat.2008.06.122

[9] Reinhart, G.; Glonegger, M.; Egbers, J.; Schilp, J.; Göritz, A.; Weikam, J.; Taktzeitadaption unter Berücksichtigung der zirkadianen Rhythmik; Werkstatttechnik online 101 (20119 9, S 595-599).

[10] R. Vollmer; Optimierung mittels Laserauftragschweißen hergestellter Beschichtungen für die Blechumformung; DISSERTATION; Technische Universität Graz; 2016.

[11] Murr LE, Gaytan SM, Ramirez DA, Martinez E, Hernandez J, Amato KN, *et al.* Metal fabrication by additive manufacturing using laser and electron beam melting technologies. J Mater Sci Technol 2012; 28:1–14. https://doi.org/10.1016/S1005-0302(12)60016-4

[12] Sehrt, J.T.; Möglichkeiten und Grenzen bei der generativen Herstellung metallischer Bauteile durch das Strahlschmelzverfahren; Dissertation; Universität Duisburg-Essen; 2010.

[13] Schneider M.F.; Laser cladding with powder effect of some machining parameters on clad properties; Ph.D. Thesis, University of Twente, Enschede, The Netherlands; March 1998; ISBN: 90 365 1098 8

[14] Sexton, L.; Lavin, S.; Byrne, G.; Kennedy, A. (2002): Laser cladding of aerospace materials; Journal of Materials Processing Technology 122 (1), S. 63–68. DOI: 10.1016/S0924-0136(01)01121-9

[15] Anforderung und Qualifizierung von Schweißverfahren für metallische Werkstoffe –Schweißverfahrensprüfung – Teil 1: Lichtbogen- und Gasschweißen von Stählen und Lichtbogenschweißen von Nickel und Nickellegierungen (ISO/DIS 15614-1.2:2015)

[16] Nowotny S, Scharek S, Beyer E, Richter KH. Laser beam build-up welding: precision in repair, surface cladding, and direct 3D metal deposition. J Therm Spray Technol 2007; 16:344–8. https://doi.org/10.1007/s11666-007-9028-5

[17] K. Boivie, K. Sørby, V. Brøtan, P. Ystgaard, Development of a Hybrid Manufacturing Cell; Integration of Additive Manufacturing with CNC Machining, in: Twenty- Second Annual International Solid Freeform Fabrication Symposium - An Additive Manufacturing Conference, The University of Texas, Austin, TX, USA, 2011, pp. 153-163.

[18] Fahrenwaldt H. J.; Schuler S.; Praxiswissen Schweißtechnik; Vieweg Teubner Verkag, 2009; ISBN 978-3-8348-0382-5

[19] Available online: https://www.micro-epsilon.com/service/glossar/Laser-Linien-Triangulation.html (accessed on 6 January 2020).

[20] Shahram Sheikhi, Eduard Mayer, Jochen Maaß and Florian Wagner; Automated Reconditioning of Thin Wall Structures Using Robot-Based Laser Powder Coating; Sustainability 2020, 12, 1477.

[21] Available online: https://www.deloro.com/fileadmin/users/redakteur/006_Downloads/Data_Sheets/Deloro_MDS_Stellite21_rev00.pdf (accessed on 6 January 2020).

[22] Kuschinski, S.; Qualifizierung des Laserpulverauftragschweißens als Verfahren der generativen Fertigung sowie als Rekonditionierungsmethode; Bachelorthesis; Institut für Werkstoffkunde und Schweißtechnik, HAW Hamburg; 24.07.2017

[23] Sheikhi S., Mayer E.; Applied Digitalization in the Field of Robotic Reconditioning of Structures; Proceedings 9th International Conference Production Engineering and Management; 03. -04.10.2019, Trieste, Italy, ISBN 978-3-946856-04-7

[24] D. Eisenbarth, F. Soffel, K. Wegener, Geometry-Based Process Adaption to Fabricate Parts with Varying Wall Thickness by Direct Metal Deposition, in: H. A. Almeida, J. C. Vasco (Eds.), Progress in Digital and Physical Manufacturing, Lecture Notes in Mechanical Engineering, Springer International Publishing, Cham, 2020, pp. 125–130. doi:10.1007/ 978-3-030-29041-2_16

[25] N. Pirch, S. Linnenbrink, A. Gasser, H. Schleifenbaum, Laser-aided directed energy deposition of metal powder along edges, International Journal of Heat and Mass Transfer 143 (2019) 118464. doi: 10.1016/j.ijheatmasstransfer.2019.118464.

[26] Z. Sun, W. Guo, L. Li, In-process measurement of melt pool cross-sectional geometry and grain orientation in a laser directed energy deposition additive manufacturing process, Optics & Laser Technology 129 (2020) 106280. doi:10.1016/ j. optlastec.2020.106280.

NOVEL NANO AND MICRO SCALE COPPER (II) COMPLEXES: SYNTHESIS, SPECTROSCOPIC CHARACTERIZATION, PHARMACOLOGICAL AND CYTOTOXICITY ANALYSIS AGAINST HUMAN BREAST CANCER CELLS

Rehab K. Al-Shemary
Department of Chemistry, College of Education for Pure Science (Ibn Al-Haitham), University of Baghdad, Baghdad, Iraq

ABSTRACT

Introduction: *Although the azomethine group in Schiff base triazoles is considered to be bioactive component and its complexes with metals, copper has been a subject of interest; it is bound with ligands creating complexes that interact with biomolecules. The application of nano scale organic compounds has many advantages, as well as high volume/surface percentages and important biochemical applications.*

Objectives: *The primary goal of this study was to characterize cytotoxicity assays of novel micro and nano scale copper (II) complex ligands towards cancer cells of human breast.*

Methods: *In this paper we created a Schiff base triazole derivative (HL) with a 1,2,4-triazole ring by condensation of 4-(benzyloxy)-2-hydroxybenzaldehyde with 5-methyl-4-(naphthalen-1-yl)- 1,3- triazole-2- amino, and then used elemental analysis, NMR spectra, (FTIR), mass, and UV-vis spectroscopic techniques to characterize the ligand (E)-5-(benzyloxy)-2-(((5-methyl-4-(naphthalen-1-yl)thiazol-2-yl)imino)methyl)phenol (HL). CuCl2.2H2O was used as a ligand to synthesize novel micro and nano complexes with the new asymmetrical Schiff base (HL). Elemental analysis, flame atomic absorption, and Fourier-transform infrared and ultraviolet visible spectra were then used to characterize the structure of the micro complex. The metal complex's magnetic susceptibility properties and conductometric measurements were also determined; the structure of the nano complex was characterized using Fourier-transform infrared, (AFM), and (SEM). Examined novel compounds for DPPH scavenging activities and tested novel compounds by MTT Assay, utilizing 96-well microtiter plates containing RPMI medium for cell seeding (1 X10^5 cells/mL).*

Results: *In the inhibition of human breast cancer cells, the antioxidant and cytotoxic activities of the ligand (HL) and complexes (nano, micro) were investigated. MCF-7 of nano complexes > micro complexes > ligand (HL)*

Conclusions: *The findings show that the Schiff base triazole ligand (HL) and nano ligand (HL nano) act as a bidentate chelating agent, bonded to the metal ion via the N atom of the azomethine and the O of the phenolic groups. At low concentrations, these*

compounds demonstrated potent anti-proliferative activity against MCF-7 cells. According to our findings, the novel synthetic compound may be a potential breast cancer inhibitor.

Keywords: *Pharmacological, Cytotoxic, Nano complexes, Schiff base, MCF-7.*

INTRODUCTION

A thiazole rings are formed naturally by the water-soluble vitamin thiamine (also known as vitamin B1), which aids in the release of energy from carbs during the process of cellular respiration. The presence of a thiazole ring in vitamin B1 and its coenzyme plays important roles in electrolytes and alpha-keto acid decarboxylation, respectively. It also contributes to the normal functioning of the nervous system through its role in the synthesis of acetylcholine, a neurotransmitter. The thiazole ring system is found in antibiotics such as bacitracin and penicillin, as well as a variety of synthetic drugs. The thiazole family of synthetic drugs includes the antimicrobials acenetrazole and sulfathiazole, the antidepressant penicillin, the antitumor agent's bleomycin and tiazofurine, the anti-HIV drug ritonavir, and the anti-ulcer drug nizatidine cinalukast. Furthermore, the nonsteroidal immune-modulating drug vanitzol and the anti-inflammatory drug Meloxicam are both thiazole derivatives that are widely used. Antifungal activity has been demonstrated in thiazole derivatives with an oxidizing phenyl unit. Antitumor and antiviral properties have been discovered in thiazoles found in microbial and marine strains. Thiazoles are a type of adenosine receptor antagonist and an estrogen receptor ligand. Copper is one of the metals that has intrigued people. It also has a significant biochemical certification; it is linked to various types of bonds to form complexes that primarily interact with nucleic acids, biomolecules, and proteins. Copper complexes have intrigued researchers due to their potential applications as anti-inflammatories, antimicrobials, chemical nucleases, antivirals, antitumor agent's enzyme inhibitors. Nanoscale use of organic materials and compounds has a number of advantages including high surface/volume ratios, adaptable volumes, and adjustable structures, making them suitable for a variety of applications including industrial, electronic and medical. The Schiff base (HL) and its nano and micro copper complexes were synthesized and investigated using various chemical techniques in our research. MCF-7 cells were used to test the cytotoxic activity of the compounds synthesized (ligand and its complexes). The goal of this study is to synthesize the ligand (HL) and its nano and micro copper complexes in order to demonstrate the effect of adding an azomethine group to HL and compare the cytotoxic activity of the ligand and its complexes with the main ring structure.

MATERIALS AND METHODS

The chemicals used to synthesize were obtained from mercantile sources. Gallenkamp MF B600 instrument was used to record melting points. EA-034.mth was used to do elemental analysis for ligand and its complex. For flame atomic absorption (Shimadzu-670 Atomic Absorption Spectrophotometer) was used to estimate metal contents. The infra-red spectra were detailed for all complexes using (8400 S-FTIR SHIMADZU) spectrophotometer. Electrolytic conductivity calculating set mode (MC-1-Mark V) was used to measure molar conductivity. Magnetic Susceptibility Balance of Sherwood Scientific was used to measure magnetic susceptibilities of complex, electronic spectra (The ultraviolet [UV]– visible) were recorded using (1800-UV SHIMADZU) spectrophotometer. The spectra of 1H and 13C NMR were documented on 400 MHz MR spectrometer Bruker, Germany, using the internal standard tetramethyl silane and dimethyl sulfoxide (DMSO)-d6 as a solvent, and the mass spectrum was measured on a Shimadzu model GCMS-QP2010Ultra. The size and morphology for the nano complex were characterized using a field emission scanning electron microscope ([FE-SEM] TESCAN, MIRA3, France) and the morphology of coated surfaces was characterized using atomic force microscope (AFM) (Model AA3000, Angstrom Advanced Inc.).

Synthesis of Ligand HL

The synthetic path followed different procedures and modified methods that were used to design for the preparation of the label compounds were completed, as below:

Synthesis Schiff base (HL)

An equimolar amount of 4-hydroxy benzaldehyde with few drops of glacial acetic acid and 5-methyl-4-(naphthalen-1-yl) thiazol-2-amine were added in the round bottom flask and stirred the reaction mixture for 18 h without heating (to avoid gummy product). The precipitate was filtered to get 4-(benzyloxy)-2-hydroxybenzaldehyde and then was washed with petroleum ether and recrystallized with ethanol.

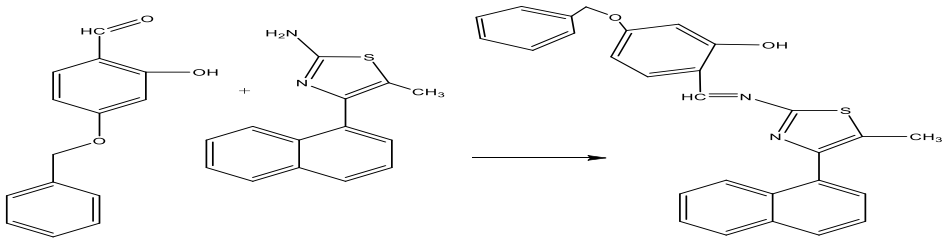

Scheme 1: Synthesis rule of ligand HL

Synthesis of Schiff Base Micro Complex

To the methanolic solution of HL, solution of the Cu (II) was added and refluxed at 75°C for 5 h, after cooling the mixing at room temperature, the solid was formed. Then, the product was filtrated, dried, and recrystallized from ethanol.

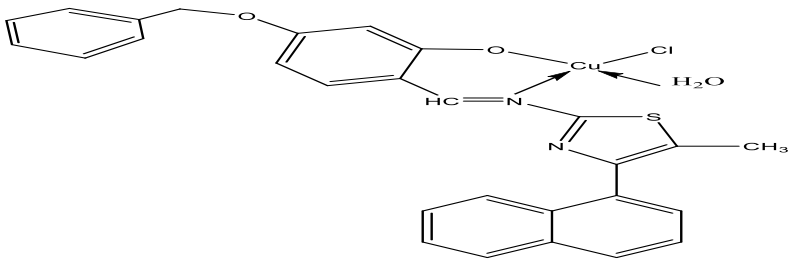

Scheme 2: Structure of complex

Synthesis of Nano Complex

Synthesis nano ligand of the methanolic solution of HL by ultrasound instrument, then mixed with the methanolic solution of the Cu (II) to prepare nanoparticles complexes by ultrasonic method, the suspension was ultrasonically irradiated with a high-density ultrasonic probe inglorious straight into the solution. The precipitate was formed and filtrated from the liquid then dried at 50°C in the oven.

Antioxidant Activity (DPPH Assay)

The tested novel compounds were evaluated for the DPPH scavenging activities; each sample was mixed with DPPH solution and made up to the required volume using ethanol. The scavenging activity of the compounds was computed using the formula:

$$\text{Scavenging\%} = [(\text{Absorbance of Control} - \text{Absorbance of Sample})/\text{Absorbance of Control}] \times 100$$

The absorbance of the samples was measured at 517 nm.

MTT Assay

By using 96-well microtiter plates containing RPMI medium for seeding of the cells (1× 105 cells/mL), and incubated overnight, after that, treated with tested novel compounds, and incubated for 72 h. Then, washing with phosphate-buffered saline (PBS) for 4 times, they were stained with MTT (2 μg/mL) and incubated (3 h at 37°C). Using a microplate reader, DMSO was added and the absorption was measured at 492 nm. Inhibition rate (cytotoxicity percentage) using the equation below:

$$\text{Inhibition rate \%} = (A - B/A) \times 100$$

Where A = control optical density, B = sample optical density.

Acridine Orange-ethidium Bromide (AO/EtBr) Staining

According to our previously published study, AO/EtBr staining was performed. Novel micro and nano compounds at IC50 concentration were used to treat the MCF-7 cells in 96- well plates. After incubation for 24 h, washing with PBS 2 times and added 100 μL of AO/EtBr for 2 min, fluorescence microscopy was applied for cell visualisation.

Statistical Analysis

The data are represented as mean ± standard error of means which were analysed using Graph Pad Prism 5 (GraphPad Software, USA) and statistically significant differences, as tested by unpaired t-test, were set at a probability level of *P < 0.05.

RESULTS AND DISCUSSION

Physical Characteristics and Analytical Data of Ligand HL and its Copper Complex

Elemental analysis and physical properties of the synthesized Schiff base ligand and its copper complex are tabulated in Table 1. These compounds were synthesised in powder, the Cu complex is stable in air, it is soluble in DMF and DMSO but insoluble in other organic solvents. Elemental analysis suggests that the molar ratios for the complex are 1:1 (metal: ligand), the results were in agreement with the suggested formula.

Table 1: Physical characteristics and elemental analysis of the ligand and its complex

Compounds	Compound formula	Molecular weight	M. p °C	Colour	Found (Calc.)				
					C	H	N	Cu	Cl
HL	$C_{28}H_{22}N_2O_2S$	450.56	189-191	yellow	73.32 (74.64)	5.12 (4.92)	6.45 (6.22)	-	16.97 (17.01)
[CuLCl (H_2O)]	$C_{28}H_{21}ClCuN_2O_2S$	548.54	230-332	Dark green	61.08 (61.31)	3.23 (3.86)	5.80 (5.11)	11.06 (11.58)	6.11 (6.46)

Electronic Spectra, Conductivity Measurements, and Magnetic Susceptibility

The (UV-visible) absorption spectrum of ligand (HL) presented two bands at 295 nm, 33898 cm^{-1} allocated to π→π* transitions and 308 nm, 32468 cm^{-1} owed to n→π* transitions and is shown in Figure 1. The spectrum of [CuLCl (H_2O)] complex in $CHCl_3$ shows one broadband (648 nm, 15432) which agrees to $2B_1g \rightarrow 2A_1g$ transition and shoulder band at 435 nm, 22989 cm^{-1} allocated to $^2B_1g \rightarrow {}^2B_2g + {}^2Eg$ (ν2) transitions, the position of these bands is to approve with configuration square planer. At room temperature, the value of the magnetic moment was found to be 2.12 B.M, which approve with distorted octahedral geometry for Cu (II) complex, the conductivity mentions to the non-ionic showing for this complex. The spectroscopic data for each ligand and complex are shown for maximum absorption in Table 2.

Table 2: Molar conductivity, electronic spectra, (μeff), and suggested geometry of complex

Compound	μ_{eff}	Λm. $S.cm^2/mol$	λ nm	ύ cm^{-1}	Assignments	geometric
HL	-	-	295 307	33898 32468	π→ π* n→ π*	-

[CuLCl (H_2O)]	2.12	17.32	643 435	15534 22943	$^2B_1$ g→ $^2A_1$g $^2B_1$ g→ $^2B_2$g +^{2}Eg	Square Planar

Mass Spectrum

The mass spectrum of ligand (HL) presented a mass to charge ratio (450 M/Z) of 80% relative abundance and 323 M/Z is 40% abundance, that is evidence that the ligand (HL) was prepared, as shown in Figure 1.

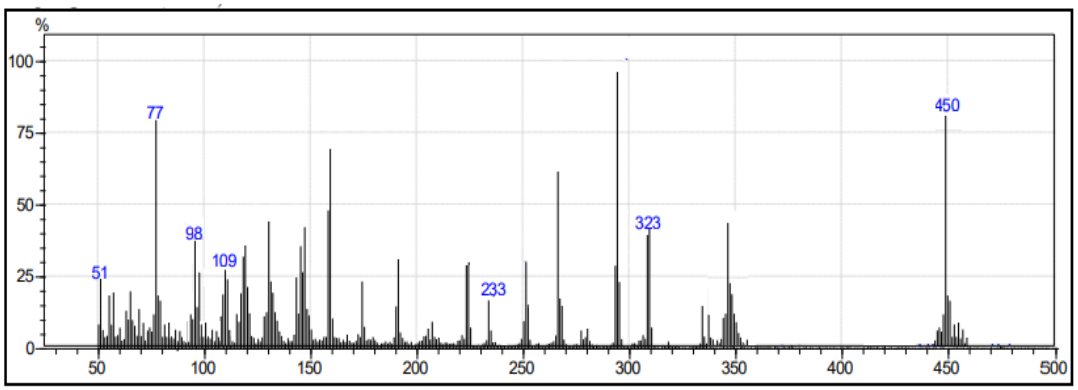

Figure 1: The mass spectrum of ligand (HL)

Infrared (IR) Spectra Fourier-transform IR for the Free Ligand (HL) and its Complexes

The IR spectra of the Schiff base ligand (HL) and its metal complex were carried out in range of 4000–400 cm^{-1}. In the spectrum of the ligand HL, the strong and broadband at 3343 cm^{-1} may be attributed to the υ(OH) of phenolic ring; as well as the υ(C=N) of azomethine band appearing at 1672 cm^{-1} and (1627) due to υ(C=N) of thaiozole ring. In the micro complex spectra, υ(C=N) of azomethine and υ(C=N) of thaiozole ring observed with a little change in shape and shifted to lower frequencies at 1660 cm^{-1} and 1620 cm^{-1}, respectively. The IR spectrum of nano ligand exhibited stretching bands at approximately 3317cm^{-1} for υ[O-H] While (1670 and 1625 cm^{-1}) due to υ(C=N) of azomethine and υ(C=N) of thiazole ring. Nano complex exhibits bands at 1666 and 1622 cm^{-1} due to υ(C=N) of azomethine and υ(C=N) of thiazole ring, respectively as shown in Table 3. Accordingly, the ligand (HL) and nano ligand (HL nano) act as a bidentate chelating agent, bonded to the metal ion through the N atom of the azomethine and O of phenolic groups. Other new weak bands of micro complex and nano complex appeared which were supported by the appearance of υ (M-N, M-O and M-Cl) bands, Table 3. A band observed around 3467–3488 cm^{-1} in the spectra of micro and nano complexes assigned to the υOH and nano metal complex.

Table 3: IR spectra vibrations (cm^{-1}) for the nano and micro ligand (HL) and their nano and micro metal complex

Compd.	**ν (O-H)** **ν (O-H)H_2O**	**ν (C=N)** **(aminic)**	**ν(C=C)** **aromatic**	**υ(M–N)**	**υ(M–O)**	**υ(M–Cl)**
HL	3343	1672 1627	1595	-	-	-
[CuLCl (H_2O)]	3467	1660 1620	1611	553	441	359
HL nano	3317 -	1670 1625	1595			-
[CuLCl (H_2O)] nano	- 3488	1666 1622	1595	550	439	368

Nuclear Magnetic Resonance (^{1}H NMR and ^{13}C NMR) Spectra of Ligand (HL)

^{1}H NMR spectrum of compound HL assignments of chemical shifts is characterised by the presence of N=CH group of azomethine at δ (9.34) ppm, aromatic protons exhibit at δ(6.56–8.42) ppm, phenolic proton appeared at δ (11.23) ppm, (CH_2) presented at δ (4.78) ppm, and (CH_3) group showed at δ (2.87) ppm.13C NMR spectrum of HL peaks is characterized by δ (N=CH), δ (N=C) of azomethine / thiazole group which appeared at δ (165.7) ppm and δ (156.7) ppm , the aromatic carbon rings exhibited at range δ (128.1–135.6) ppm, (C=C) exhibit at d (158.2) ppm, (C-O) assigned at δ (163) ppm while (CH2-/CH3) appeared at δ (30.1) and δ (11.5) ppm .

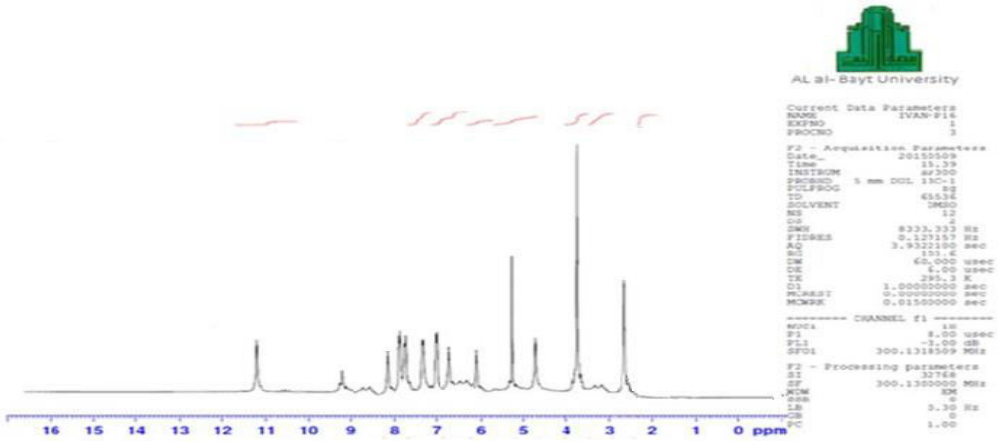

Figure 2: The ^{1}HNMR spectrum of ligand (HL)

General Proposed Stereo Chemistry Structure of Micro and Nano Complexes

According to the results, the general structure of the above mentioned prepared new complexes is shown in Scheme 2.

AFM for Nano Complex

The nano complex (Cu complex nano) has semi ball-shape with perfect, grains, identical dispensability, and aligned perpendicularly, the estimated values of average grain size root mean square of the surface is 7.33 nm and roughness average 6.35 nm. The nano complex is conglomerate to form larger particles 69.18 nm.

SEM for Nano Complex

SEM of the nano complex (Cu complex nano) images are shown in the Figure 3. SEM images enhance the diverse morphology, unsymmetrical and consists of many small irregular nanoparticles, it looks like rocks shape with average size ranging from (21.23 to 5.31) nm.

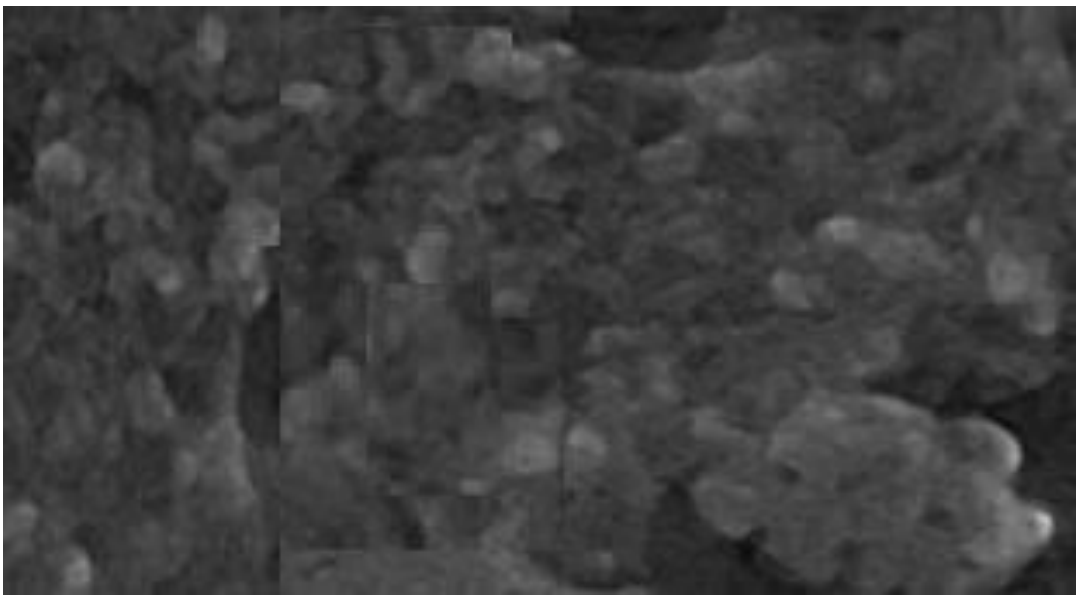

Figure 3: Scanning electron microscope of nano complex

DPPH Radical Scavenging Assay

The DPPH radical scavenging (%) activity of the tested novel compounds absorption band at 517 nm is shown in Figure 4. The result revealed that tested compounds can donate hydrogen atoms and remove the unstable electron from DPPH and can be useful for the management of numerous deleterious diseases. Free radicals of (DPPH) delocalize over the entire molecule, barring its dimerization, while a solution of DPPH can blend with a substrate that can donate a hydrogen atom, this may give an upward push to the reduced form with a color change from violet to yellow.

 ISBN: 978-81-959870-7-8

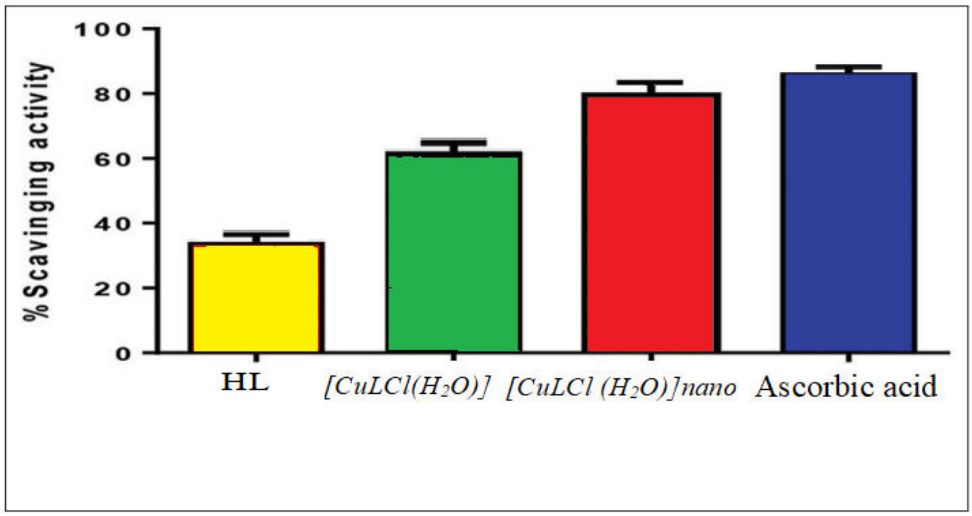

Figure 4: Antioxidant activity of indicated compounds, and ascorbic acid

Anticancer Activity of Novel Tested Compounds

The viability of MCF-7 cells was reduced after treated with tested compounds in all used concentrations, as shown in Figure 5. After incubation with tested novel compounds at (IC50), cell imaging demonstrated extensive cellular morphological changes, using crystal violet stain furthermore clumping and inhibition of the communication of the cells. However, such alterations were not seen in the control group.

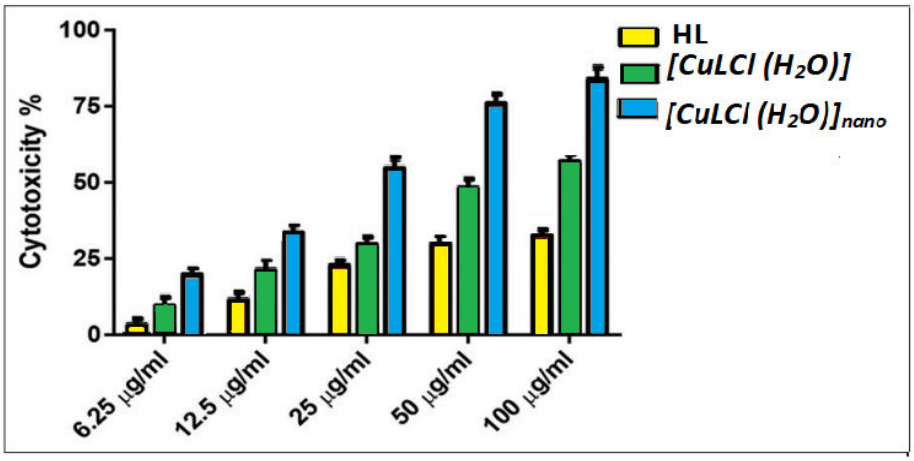

Figure 5: Cytotoxicity effect of indicated compounds on MCF-7 cell line. Cell treated with ligand HL, cell treated with micro and nano Cu complex

Role of Tested Compounds in Induction of Apoptosis

Apoptotic cells commonly show nuclei that are characterised by red to green color while the condensation of their chromatin varies in level. A combination of AO/EtBr dyes is shown in Figure 6 with the aim of further examining the ability of tested

compounds, to induce the death of cancer cell lines. The structure of the nuclei of the cells was observed to be intact, with a stable bright green color. The membranes of cancer cells treated with tested novel compound less integrity in comparison to the membranes of the untreated cells. The morphological alterations in the treated MCF-7 cells suggested that the observed cell death was caused by apoptosis.

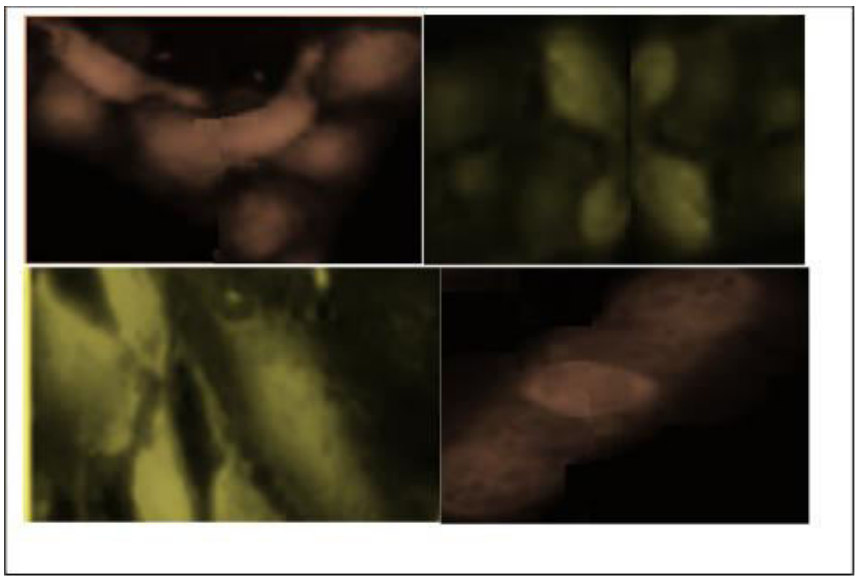

Figure 6: Fluorescence microscopic images of MCF-7 cell lines double-stained with EBr and acridine orange in the absence and presence of ligand, micro complex (a), and nano complex (b)

CONCLUSIONS

In the present research study, we synthesised new ligand from 5-methyl-4-(naphthalen-1-yl)- 1,3- triazole-2- amino. This new ligand was used to prepare the novel of micro and nanoparticles complexes that are characterized by various physicochemical and spectral analyses. The results exhibit that the Schiff base ligand (HL) and nano ligand (HL nano) act as a bidentate chelating agent, bonded to the metal ion through the N atom of the azomethine and O of phenyl groups. These compounds presented potent anti-proliferative activity against MCF-7 cells at low concentrations. Our result suggested that a novel synthetic compound may be a potential breast cancer inhibitor.

REFERENCES

1. Khedr AM, El-Wakiel NA, Jadon S, Kumar V. Synthesis, spectral, thermal analyses, molecular modeling, and antimicrobial activities of Cu (II)-complexes with 1, 3, 4-oxadiazole Schiff base derivatives. J Coord Chem 2011; 64:851-62.
2. Hussain DH, Rheima AM, Jaber SH. Cadmium ions pollution treatments in aqueous solution using electrochemically synthesized gamma aluminum oxide nanoparticles with DFT study. Egyptian J Chem 2019; 62:1-2.

3. Rheima AM, Mohammed MA, Jaber SH, Hameed SA. Synthesis of silver nanoparticles using the UV-irradiation technique in an antibacterial application. J Southwest Jiaotong Univ 2019; 54:1-2.
4. Rheima AM, Hussain DH, Almijbilee MM. Graphene-silver nanocomposite: Synthesis, and adsorption study of cibacron blue dye from their aqueous solution. J Southwest Jiaotong Univ 2019; 54:1-2.
5. Zhou J, Wu D, Guo, D. Optimization of the production of thiocarbohydrazide using the Taguchi method. J Chem Technol Biotechnol. 2010; 85:1402-6.
6. Jabir MS, Taha AA, Sahib UI, Taqi ZJ, Al-Shammari AM, Salman AS. Novel of nano delivery system for Linalool loaded on gold nanoparticles conjugated with CALNN peptide for application in drug uptake and induction of cell death on breast cancer cell line. Mater Sci Eng C Mater Biol Appl 2019; 94:949-64.
7. Ali SH, Sulaiman GM, Al-Halbosiy MM, Jabir MS, HameedAH. Fabrication of hesperidin nanoparticles loaded by poly lactic co-glycolic acid for improved therapeutic efficiency and cytotoxicity. Artif Cells Nanomed Biotechnol 2019; 47:378-94.
8. Kadhem HA, Ibraheem SA, Jabir MS, Kadhim AA, Taqi ZJ. Zinc oxide nanoparticles induces apoptosis in human breast cancer cells via caspase-8 and P53 pathway. Nano Biomed Eng 2019; 1:35-43.
9. Alsaedi II, Taqi ZJ, Hussien AM, Sulaiman GM, Jabir MS. Graphene nanoparticles induces apoptosis in MCF-7 cells through mitochondrial damage and NF-KB pathway. Mater Res Express 2019; 6:95413.
10. Khashan KS, Jabir MS, Abdulameer FA. Carbon nanoparticles decorated with cupric oxide nanoparticles prepared by laser ablation in liquid as an antibacterial therapeutic agent. Mater Res Express 2018; 5:35003.
11. Kadhim WK, Nayef UM, Jabir MS. Polyethylene glycol functionalized magnetic (Fe_3O_4) nanoparticles: A good method for a successful antibacterial therapeutic agent via damage DNA molecule. Surf Rev Lett 2019; 26:1950079.
12. Abir MS, Nayef UM, Kadhim WK. Polyethylene glycol-functionalized magnetic (Fe_3O_4) nanoparticles: A novel DNA mediated antibacterial agent. Nano Biomed Eng 2019; 11:18-27.
13. Ali AA, Al-Abdali BI. Synthesis and characterization of 4-(((3-mercapto-5-phenyl-4H-1, 2, 4-triazole-4-yl) imino) methyl)-2-methoxyphenol and its complexes with Zr (IV), Cd (II) and Sn (II) ions. Iraqi J Sci 2015; 56:1274-88.

14. Singh J, Singh P. Synthesis, spectroscopic characterization, and in vitro antimicrobial studies of pyridine-2-carboxylic acid N'- (4-chloro-benzoyl)-hydrazide and its Co(II), Ni(II), and Cu(II) complexes. Bioinorg Chem Appl 2012; 2012:104549.
15. Singh AK, Pandey OP, Sengupta SK. Synthesis, spectral characterization and biological activity of zinc(II) complexes with 3-substituted phenyl-4-amino-5-hydrazino-1, 2, 4-triazole schiff bases. Spectrochim Acta A Mol Biomol Spectrosc 2012; 85:1-6.
16. Abdulghani AJ, Abbas NM. Synthesis characterization and biological activity study of new schiff and mannich bases and some metal complexes derived from isatin and dithiooxamide. Bioinorg Chem Appl 2011; 2011:706262.
17. Barbuceanu SF, Saramet G, Almajan GL, Draghici C, Barbuceanu F, Bancescu G. New heterocyclic compounds from 1, 2, 4-triazole and 1, 3, 4-thiadiazole class bearing diphenylsulfone moieties. Synthesis, characterization and antimicrobial activity evaluation. Eur J Med Chem 2012; 49:417-23.
18. Hunashal RD, Ronad PM, Maddi VS, Satyanarayana D, Kamadod MA. Synthesis, anti-inflammatory and analgesic activity of 2-[4-(substituted benzylideneamino)-5-(substituted phenoxymethyl)-4H-1, 2, 4-triazol-3-yl thio] acetic acid derivatives. Arabian J Chem 2014; 7:1070-8
19. Abdulghani AJ, Abbas NM. Synthesis characterization and biological activity study of new schiff and mannich bases and some metal complexes derived from isatin and dithiooxamide. Bioinorg Chem Appl 2011; 2011:706262.
20. Barbuceanu SF, Saramet G, Almajan GL, Draghici C, Barbuceanu F, Bancescu G. New heterocyclic compounds from 1, 2, 4-triazole and 1, 3, 4-thiadiazole class bearing diphenylsulfone moieties. Synthesis, characterization and antimicrobial activity evaluation. Eur J Med Chem 2012; 49:417-3.
21. Rehab Khadem Al Shemary, Faeza Haseen Ghanim, and Zuhair A. Shafiq, Preparation, Characterisation and Biological Activity Studies for Some Mixed Ligands Complexes of 1, 10 – Phenanthroline and Schiff Base Ligand with Metal Ions, Diyala Journal for Pure Science July 13, 2, 2017, DOI: 10.24237/djps.1303.226C
22. Hunashal RD, Ronad PM, Maddi VS, Satyanarayana D, Kamadod MA. Synthesis, anti-inflammatory and analgesic activity of 2-[4-(substituted benzylideneamino)-5-(substituted phenoxymethyl)-4H-1, 2, 4-triazol-3-yl thio] acetic acid derivatives. Arabian J Chem 2014; 7:1070-1078.

23. Rehab. K. Al-Shemary Synthesis, Spectroscopic Characterization and Biological Studies for New Binuclear Schiff Base with Some Transition Metal Chemistry and Materials Research, 7 (5), 2015

24. Gilani SJ, Khan SA, Siddiqui N. Synthesis and pharmacological evaluation of condensed heterocyclic 6-substituted 1, 2, 4-triazolo-[3, 4-b]-1, 3, 4-thiadiazole and 1, 3, 4-oxadiazole derivatives of isoniazid. Bioorg Med Chem Lett 2010; 20:4762-5.

25. Hiyam Hadi Alkam, Wasan Mohammed Alwan, Rehab Kadhim Raheem Al Shemary, Complexes of Co(II), Cu(II), Ni(II), Pt(II) And Pd(II) with N_3O-Chelating Ligand Incorporating Azo and Schiff Base Moieties: Synthesis, Spectroscopic, Thermal Decomposition, Theoretical Studies, and thermodynamic parameters, International Journal of Pharmaceutical Research | Jan - Mar 2021 | Vol 13 | Issue 1.

26. Hranjec M, Starčević K, Pavelić SK, Lučin P, Pavelić K, Zamola GK. Synthesis, spectroscopic characterization and antiproliferative evaluation in vitro of novel schiff bases related to benzimidazoles. Eur J Med Chem 2011; 46:2274-9.

27. Noor M. Majeed, Suha Sahab Abd, Rehab Kadhim Raheem Al Shemary, Eco-friendly and Efficient Composition, Diagnosis, Theoretical, kinetic studies, Antibacterial and Anticancer Activities of Mixed Some Metal Complexes of Tridentate Schiff base Ligand, International Journal of Pharmaceutical Research, 2021, 13(1), 3358-3369.

28. Barot KP, Manna KS, Ghate MD. Design, synthesis and antimicrobial activities of some novel 1, 3, 4-thiadiazole, 1, 2, 4-triazole-5-thione and 1, 3-thiazolan-4-one derivatives of benzimidazole. J Saudi Chem Soc 2017;21: S35-43.

29. Al-Shemary, R. K., Abdul Karim, L. K., Jaafar, W. A., (2017) Synthesis, Characterization and Biological Activity of Schiff Bases Chelates with Mn(II),Co(II),Ni (II),Cu(II) and Hg(II) Baghdad Science Journal ,14(2), 390- 402.

30. Amer S, El-Wakiel N, El-Ghamry H. Synthesis, spectral, antitumor and antimicrobial studies on Cu (II) complexes of purine and triazole schiff base derivatives. J Mol Struct 2013; 1049:326-35.

31. Rehab. K. Al- Shemary, Basima Abdul Hussin Zaidan and Nibras A. Al-marsomy Synthesis, Characterization and Antibacterial Activities of Mixed Ligand Complexes of Schiff Base Derived from Benzidine and 2-Benzoyl benzoic acid, Diyala journal of pure sciences, Vol: 13 No:3, July 2017 21 DOI: http://dx.doi.org/10.24237/djps.1303.189C

ADVANCED POLYMER COMPOSITE MATERIALS FOR SPACECRAFT ELECTRONICS FOR ISRO PROGRAMS- AN INDISPENSABLE MATERIAL FOR PRESENT AND FUTURE APPLICATIONS

[1]B Muthulakshmi, [2]Lakshman Rao and [3]V. K. Padma

[1,3]Scientist/Engineer and [2]Assistant Engineer, UR Rao Satellite centre, Indian Space Research Organisation, Bangalore- 560037, India

ABSTRACT

This paper efforts to review the potential uses of Composite materials in Space industry. Composite materials have revolutionized the space industry by virtue of their multifunctional, multi-directional and tailorable properties that can sustain the extreme environment of outer space. Polymer materials are widely used for many space applications due to their many engineering designable advantages such as specific strength properties with weight saving of 20-40%, potential for rapid process cycles, ability to meet stringent dimensional stability, lower thermal expansion properties and excellent fatigue and fracture resistance over other materials like metals and ceramics. This paper emphasized the importance of Non-woven aramid-polyimide composite materials, polymeric encapsulants such as room temperature vulcanisation (RTV), used for spacecraft electronics packages along with other material systems in the major elements of a space program. In this work, polymeric composite material- Non-woven aramid-polyimide materials have been used in the electronic packages and future applications of advanced polymer potting materials e.g. Room temperature Vulcanisation (RTV) silicone sealant material is also briefly presented . An experiment has been conducted for fabrication of space grade electronic assemblies using non-woven aramid-polyimide composite materials and advanced polymeric coatings (RTV) and their properties are characterised for usage in the ISRO programs.

Keywords: Non-woven aramid-polyimide composite material, RTV, Composite Materials, Electronic packages.

INTRODUCTION

The space program and development in space research has been prime focus of many developed and developing countries. It provides the country with a broad scope of beneficial applications which includes citizen development, mass communication, agriculture, economy, defense, scientific and medical research [1, 2]. Satellite, Launch Vehicle and Space Centre are the three key components under the umbrella of any space program. The space environment affects all materials and systems of the satellite; however, external components, including thermal blankets, thermal control coatings, and optical sensors, are most affected by its individual constituents and their synergistic

effects. Thus, the key for the development of novel materials for space applications is thorough ground durability testing in order to avoid failures in the real space environment.

Composite materials are potential candidates in space applications and have dominated the space industry due to their cost-effectiveness, ease of processability, high strength to weight ratio, multi-functionality and diverse properties in terms of thermal insulation and ablation [3-6]. Polymer materials have key advantages over other conventional metallic materials due to their specific strength properties with weight saving of 20-40%, potential for rapid process cycles, ability to meet stringent dimensional stability, lower thermal expansion properties and excellent fatigue and fracture resistance.

Apart from the wide range of useful properties that polymers offer, they must meet the requirements of in-space usage. These requirements include: (a) capability to function in hard vacuum, (b) very low outgassing to prevent contamination of surrounding components, (c) resistance to extremely harsh ultraviolet light, (d) resistance to an-orbit charged particle radiation, (e) resistance to erosion from atomic oxygen, (f) endurance over wide temperature extremes and g) ability to survive the life of the mission.

Typically, the composite must display high glass transition temperatures and thermal stability, but must be combined with a good impact resistance in the event of high-speed impact from space debris or microcracking during thermal excursions. Epoxy resins, cyanate esters, and polyimides are the most commonly used composite materials in this application. with a number of space-qualified resins now commercially available, the extensive research is being undertaken to develop the next generation of polymers.

Polymers in one form or another are widely used in electronics components and electronic packaging.

These applications include the following: a) Printed Circuit Boards b) Conformal Coatings C) Miscellaneous.

Printed Circuit Boards: New dielectric materials have been introduced for printed circuit board applications, such as Thermount polyimide with the aim to match the requirements for high speed and high density of electronic devices that are planned for new space-craft electronic boards. This trend will also be followed by space technology, and there is a need to develop electronic packaging applications which are lighter, faster, and smaller. There are now commercially available high-quality composite materials like non-woven aramid-polyimide which is known as Thermount polyimide and are good candidates to replace the well-known glass epoxy composite laminate. Non-woven aramid-polyimide composite substrate" as an alternative to FR4 glass

reinforced substrate to achieve improved thermal characteristics and also weight reduction, which is desirable for space electronics.

Conformal Coatings: Coating is a thin uniform layer of insulation over a printed circuit board to protect it from adverse environmental effects like moisture, dust, dirt, corrosion, humidity etc. These coatings are usually based on two parts: urethane chemistry that are mixed and then dipped, or sprayed onto circuit boards.

Miscellaneous: Electronic application which include potting compounds such as RTV (Room temperature Vulcanisation) is used for encapsulating components capacitors, welded leaded components, Tantalum capacitors, coils and transformers. RTV is used to provide protection against vibration and shock. From the experimental results, it is evident that, introduction of thermount polyimide material has significant weight reduction and the material with stood readily six dip thermal stress tests. It is found that the usage of the above substrate has enhanced the reliability and the printed circuit boards produced have proved the ability to withstand thermal variation commonly experienced by the high-speed electronics. Polymeric encapsulants such as advanced potting materials are used in the printed circuit board assembly.

EXPERIMENTAL

2.1 MATERIALS AND METHODS:

2.1.1 THERMOUNT POLYIMIDE (NON- WOVEN ARAMID-POLYIMIDE COMPOSITE MATERIAL)

In this paper, a 14-layered multilayer Printed circuit board was constructed using non-woven aramid-polyimide composite laminate and prepreg (Arlon 85NT, T_g=250°C) as per the standard multilayer Printed circuit board fabrication process as recommended by the manufacturer.

Nonwoven aramid is more compressible and porous than E-glass, so the resin flow to lamination pressure relationship is different. Slightly higher lamination pressures might be required as compared to E-glass configurations. The heating rate should be controlled to a 3°C to 6°C/minute heat rise between 65°C to 149°C. Layup should be completed as soon as possible (within 2 hours) after drying laminate (1 hour at 250°F followed by a 90minute stabilization under desiccation), and desiccation of prepreg under vacuum for 8-12 hours for moisture removal. Lay-up operations should be kept within a two-hour time period after removing materials from vacuum or desiccation steps. Keep exposed prepreg and laminate surfaces to a minimum to reduce moisture regain. Pre-vacuum the Thermount Polyimide boards for 30 minutes. Product temperature at start of cure = 218°C. Cure time is for 3.0 hours. Cool down under pressure at (6°C/min). Full cure of polyimide is necessary to achieve optimum material

properties. This polyimide requires at least 3 hours of cure above 218ºC to complete cross-linking of the resin matrix. However, Thermount absorbs more moisture compared to standard glass epoxy materials when exposed to high-humidity and high-temperature conditions. [7]

2.1.2 RTV (ROOM TEMPERATURE VULCANISATION) SEALANT

DOWSIL™ 6-1104 Controlled Volatility Sealant is a one-part RTV Silicone sealant which is translucent. Extrudable, non-slump materials cure at room temperature; no corrosive cure byproducts; meet ISRO requirements for low outgassing; wide operating temperature range; easy repairability; good physical and electrical stability over a range of frequencies, temperatures and humidities; ensure protection of components from temperature extremes, high humidity, radiation, thermal shock, atomic oxygen and mechanical vibration. In this paper, DOWSIL™ 6-1104 Controlled Volatility Sealant is a one-part RTV Silicone sealant which is used to increase performance, reliability and safety of devices. It offers high elongation, non-flowing, no required mixing, and fast in-line processing. Features are Room temperature cure, low levels of condensable materials, proven for space-grade applications. The properties of Dowsil 6-104 CV are presented in table 3.

RESULTS AND DISCUSSION

From the table 1, it is understood that, low coefficient of thermal expansion (CTE) and high Decomposition temperature (Td) implies that, multi-layered printed circuit boards in order to use high-temperature soldering processes. After the fabrication, different properties were measured and the comparison of Thermount with regular FR-4 material is given in Table 2. It is evident from the table 2, that the operating temperature of 220 ºC is much higher in the case of Thermount compared to conventional FR-4, which is only 130 ºC. There is substantial reduction in weight to the tune of 28%. The Thermount materials are more stable during various processes as well as baking at different stages. It is found that, there is no warpage or twist caused due to thermal extremities of the process. It is also found that the Thermount has superior dimensional stability compared to regular FR-4 material in various process stages. Table-3 gives the comparison of reinforcement properties. The aramid fibers have high modulus and low axial CTE compared to other reinforcements, in fact this has negative CTE in axial direction, which helps to improve mechanical integrity. Many of the advanced ceramic-based components have CTE in the range 6 ppm/°C. This when mounted on a conventional FR4 PWB, which has CTE 18 ppm/°C, the mismatch in expansion will cause shear stresses within the solder that mounts the device on the board leading to a cracking of the solder joint after a sufficient number of thermal cycles. The micro sectioning was carried out on printed circuit board with thermount polyimide material of different samples at various stages of processes and presented in Fig 1(a) and Fig 1(b).

The properties of Dowsil 6-1104 CV are presented in Table 4 as supplied and cured. Table 5 presented the test results conducted for sample such as visual inspection of Lap shear strength samples, outgassing tests, Lap shear strength before and after environmental exposure and potting application related tests. Fig 2 depicts the components potted with DOWSIL potting material. From the test results, it is observed that material has withstood and lap shear strength properties are met as received condition, with RH, Thermal Shock cycling and thermo-vacuum cycling. As the spacecraft electronics undergo the above condition and the material is proved as space grade potting material.

Table 1. Comparison of Material properties [8]

Core Material	**Glass Epoxy Composite Material**	**Non-woven aramid-Polyimide Polyimide composite material (Thermount)**
Glass Transition Temperature T_g (ºC)	175	250 250
Decomposition Temperature Td (ºC)	300	426 407
In-plane CTE (ppm/ ºC)	10-14	6-9 16-17
Dimensional stability	+0.05%	+0.03% +0.05%

Table 2. Comparison of Thermount polyimide PCB with FR4 PCB

Property	Glass Epoxy Composite Material	Non-woven aramid-Polyimide composite material (Thermount)
Finished card thickness	2.25mm	2.31mm
Weight of the	1189 g	849 g

panel		
Continuous Operating temperature	130 ºC	220 ºC
Weight of Finished PCB	282 g	201 g
Effective Weight reduction	28.72 %	

Table 3. Reinforcement Properties

Core Material	Axial Modulus Giga (Pascal)	Axial CTE (ppm/ºC)	Specific gravity
Glass Epoxy Composite Material	70	5.5	2.4
Non-woven aramid-Polyimide Composite material (Thermount)	124	-4.5	1.44
Quartz	70	0.54	2.2

Table 4. Properties of Dowsil 6-1104 Controlled Volatility sealant

Property	Unit
As supplied	
Colour	Translucent
Specific Gravity (g/cm3)	1.10
Tack free time (hours)	0.9
Cured 7 days at 25°C (77°F) and 50%	RH
Tensile Strength (psi)	925

Elongation (%)	600
Lap Shear (psi)	500

Test Conducted	Specification	Results
Visual Inspection Lap shear strength sample	No air gaps in the bonding	No air gaps were observed No degradation observed after environmental exposure
Outgassing test	% Total Mass Loss (TML) < 1	0.245
As per ASTM E-595	% CVCM< 0.1	0.014
Lap shear Strength before and After Environmental exposure As per ASTM D1002	> 0.18 MPa	0.9,1.2,1.0,1.5

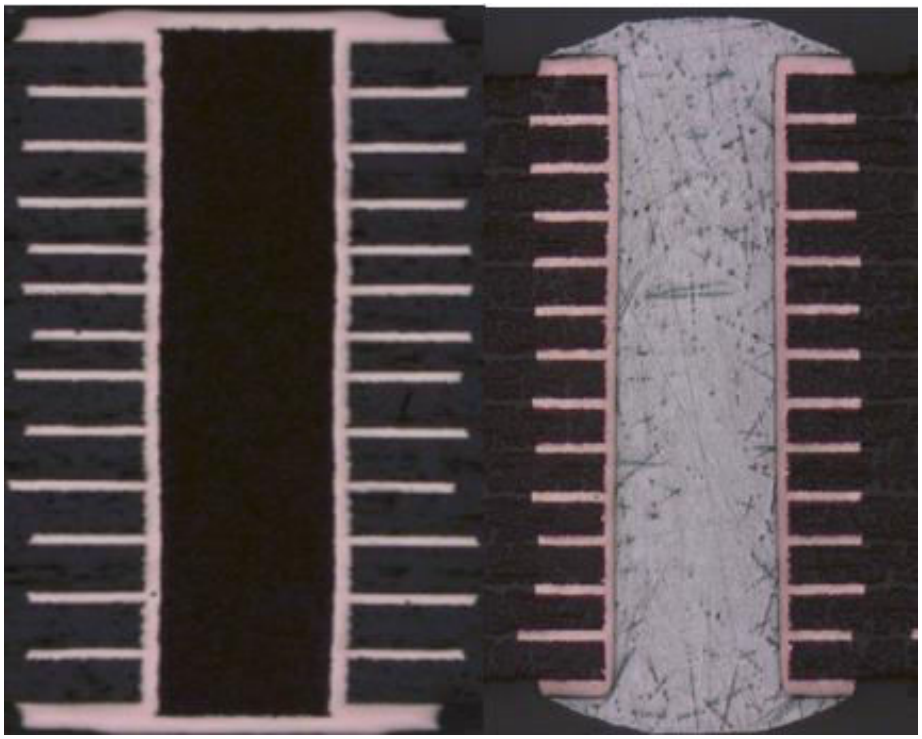

Figure. 1. (a) Microsection Image of 14 Layer Thermount Multi-Layer Board-Initial (**b)** After Thermal stress.

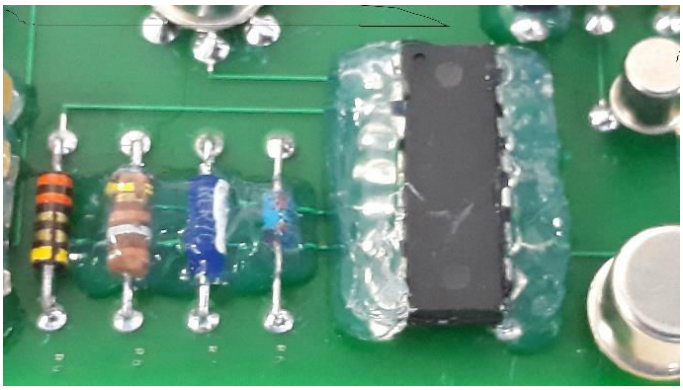

Figure. 2. Components potted with Dowsil 6-1104 CV sealant on thermount polyimide Printed Circuit Board

CONCLUSION

It is observed that operating temperatures higher than that of polyimide glass and better performance can be achieved by replacing glass reinforcement by an organic polymer and is best suited for printed circuit board substrate. The aramid (polyamide) fibre, which is an organic compound, filled with epoxy or polyimide, forms good substrate for printed circuit boards in terms of reduced weight, better thermal stability and improved dielectric properties at high frequencies. It is observed that the Aramid is having lower density value compared to traditional E-glass, which will result in overall weight reduction of 25%. The Surface smoothness for Non-woven Aramid which is also known as Thermount by brand name, is 50% better than conventional FR4 laminates, which will facilitate fine line and fine pitch for high-density interconnectivity. The aramid fibers have high modulus and low axial CTE compared to other reinforcements, in fact this has negative CTE in axial direction, which helps to improve mechanical integrity. It is found that the usage of the non-woven aramid-polyimide composite material substrate has enhanced the reliability, as printed circuit boards produced and proved the ability to withstand thermal variation commonly experienced by the high-speed electronics The MLB fabricated using Thermount material are found to have superior property owing to reduction in weight, better registration, better dimensional integrity, better process stability, better assembly performance. Hence, non-woven aramid reinforced laminates (Thermount polyimide) are better suited for the use in space electronic packages to facilitate miniaturization and weight reduction. From the test results, it is proven that advanced potting material of DOWSIL 6-1104 CV is proven as space grade encapsulant and lap shear strength properties are met as received condition, humidity, Thermal shock and thermo-vacuum cycling condition at which ISRO spacecrafts are undergoing such condition. It is proven that Thermount polyimide composite material and advanced potting materials are best suited for spacecraft electronics of ISRO programs.

REFERENCES

[1] U. M. Leloglu and E. Kocaoglan, "Establishing space industry in developing countries: Opportunities and difficulties," Advances in Space Research, vol. 42, pp. 1879-1886, 2008/12/01/ 2008.

[2] Z. S. Toor, "Applications of Aluminum-matrix composites in Satellite: A Review," Journal of Space Technology, vol. 07, pp. 1-6, 2017.

[3] D. R. Tenny, G. F. Sykes, and D. E. Bowles, "Composite Materials for Space Structures," in Third European Symp. Spacecraft Materials in Space Environment, ESTEC, Noordwijk, the Netherlands, 1985.

[4] J. R. Williamson, "Advanced materials for space structures," Acta Astronautica, vol. 24, pp. 197-202, 1991/01/01/ 1991.

[5] C. Zweben, "High-performance thermal management material," Advanced packaging, 2006.

[6] S. P. Rawal, M. S. Misra, and R. G. Wendt, "Composite Materials for Space Applications," National Aeronautics and Space Administration (NASA), Martin Marietta Astronautics Group Denver, Colorado Contract NAS1-18230, August 1990.

[7] K. Subhotosh, Comparison of the Dielectric Constant and Dissipation Factors of Non- Woven Aramid/FR4 and Glass/FR4 Laminates. Richmond, VA: Dupont Advanced Fibers Systems, 1999.

[8] S. A. Czepiela, D. Hastings, and H. McManus, “Charging of composites in the space environment,” J. Spacecraft Rockets, vol. 37, no. 5, pp. 556–560, Sep./Oct. 2004.

ACKNOWLEDGMENTS

Authors would like to acknowledge Group Director, System Power and Digital Group, Deputy Director, Systems Production Area and Director, UR Rao Satellite Centre for their constant encouragement and support for carrying out the work.

HIGH ENERGY MATERIALS: A SHORT REVIEW

Deepti Rekha Sahoo and Trinath Biswal
Department of Chemistry, VSS University of Technology, Burla-768018, India

ABSTRACT

The materials having specific properties, improved performance and high energy are termed as high energy materials (HEMs). The HEMs exhibits multidisciplinary properties and specially used in defense and aerospace without the release of any toxic contaminates. The high energy materials of different kinds are mainly used as propellants in rockets, pyrotechnics applied in the festivities, military explosives, materials applied in blasting and some of these are also used for construction activities. Since the use of these kinds of materials is increasing day by day, therefore, it is necessary to develop such kinds of eco-friendly materials. In this article more emphasis is given towards high energy materials and high density materials. For enhancing the performance of such kind of materials, it is essential to enhance the oxygen balance to mantain stoichiometry. Hence, the scientists and researchers are trying to develop popellants of chlorine and other toxic materials and explosives, which are free from lead and other highly toxic compounds. Some of the biodegradable and energetic materials and their composites are the important components of metal fuel and HEMs. This matreial was designed in such a way that, it shows superior performance with increased energies and improved mechanical properties, processability and efficiency. This review article provides knowledge regarding progress in the field of HEMs with emphasis on high-energy compact materials, oxidizers, high-energy insensitive materials, plasticizers, bio-polymers and their composites of multifunctional action.

Keywords: Propellants,Explosives.Biodegradable, HEMs, Pyrotechnics, HEDMs

INTRODUCTION

The materials which possesess the capability of releasing a huge amount of heat energy in a self-sustained chemical reaction in comparatively much faster rate and sometimes within a fraction of a second in an intense and violent manner are called as high energy materials (HEMs). These kind of materials also have the capacity to store high value of chemical energy in it and can be used successfully in different fields. These kind of materials may be a single compound such as trinitrotoluene (TNT), which contains both oxidizing groups like , -NO_2 and reducing group or both called as mixture of fuel elements and oxidizer, such as gun powder (KNO_3 + C + S). These kinds of newly developed materials can undergo stimulation by using mechanical, electrical or thermal devices and due to stimulation these materials experience quick decomposition producing light, heat, energy, sound and large volume of gaseous components [1,2] .The

energy produced from the HEMs depends upon the different characteristics of the materials, its composition, density,structural aspects, enthalpy of decomposition and formation etc. The high energy materials are mainly classified into three categories such as explosives,fireworks, propellants depending upon the properties, formability and applications.The burning of conventional fuel such as wood, coal, wax generates high energy and some gaseous components, but it is relatively a slow process, otherwise some materials on combustion even in the vacuum without air can produces a relatively less amout of energy than the conventional fuels, but, however, the energy release follows a very small interval of time. The property of fast release of various forms of energy along with gaseous products is the cause of many specific applications of high energy materials (HEMs) and hence, mostly used in propellants and explosives.The ammonium perchlorate (AP) as oxidiser and 'Al' metal as metal fuel along with the binder known as hydroxyl terminatedpolybutadiene (HTPB) forms a new propellant commonly called as composite propellants and this propellant can be effectively and efficiently used as rocket propellants, especially in space vehicles and propellant missiles [3,4]. These kinds of propellant functions are much superior (Isp 250-260s) as compared to the conventionally used propellants such as nitroglycerine (NG) and nitrocellulose (NC), which are propellants of double-base (Isp 220-230s). The composite propellants show the property of greater strain capability because of less glass transition temperature (T_g) of HTPB and one of the important advantages of this propellant is its use, even in sub-zero temperatures. Now a days these kinds of propellants are widely manufactured throughout the globe because of their huge demand. Royal, Thiokol Ordnance and SNPE are the main producer of this kind of propellants.The fuel rich propellants are a new class of propellants and its importance is enhanced due to the Renaissance of Scramjets and Ramjet [5,6] . Scheme-1 represents the structure of two important HEMs such as NG and NC.

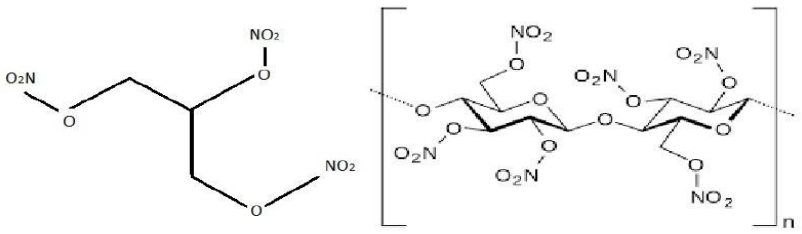

Structure of NG Structure of NC

Scheme 1: Structure of NG and NC

Now a days, the fuel-rich propellants of Mg base are in craze, but the solid propellants of boron-base are more preferred among all the metals listed fuel-rich systems because of their high energy potential but however, the problem is the eficiency, effectiveness

and pyrolyzability of boron. To increase the pyrolizability some suitable energetic binders and additives are added in it. For gun propellants normally the conventional propellants of a triple-base having the major components such as nitroglycerine(NG), nitrocellulose (NC), and picrite (nitrguanidine (NQ) are used and this propellant now occupies a key position in field gun ammunition and tank, because of its low flame temperature, low barrel erosion, less flash point for combustion, long shelf life,etc.. For the environmental point of view attenmpt was always made to replace NQ by inserting the energetic plasticizers and energetic oxidisers. In the high explosives sectors, the weapon designers and developers are facing many challenges such as clear understanding of shaped-charges having high jet velocity, devices of fragment generating high lethality and level of destruction systems with the capacity of great blast effect. To increase the lethality of the missiles, velocity of detonation and the detonation pressure are the appropriate criteria for the choice of a good explosive in the projectile application. Cyclotetramethylene tetranitramine (HMX) and cyclotrimethylene trinitramine (RDX) are generally two benchmark standard explosives used as conventional explosive compositions having the melt castable trinitrotoluene (TNT) [7,8]. The scheme-2 represents the structure of TNT, HMX and RDX

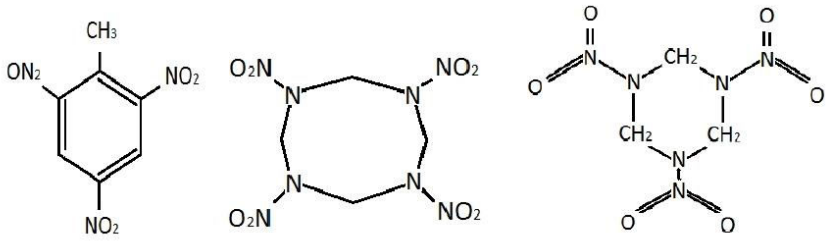

2,4,6 –Trinitrotolune(TNT) **HMX** **RDX**

Scheme 2: Structure of TNT, HMX and RDX

Criteria for High Energy Materials

A good high energy material possesses the following criteria

- These materials release huge amounts of energy with a rapid rate in the pathway of self sustained chemical reaction and the energy released is highly intense and violent.
- Such kind of materials are often undergoing combustion by using the supply of their own oxygen, which may or may not bring complete combustion of the material.
- For fast and complete combustion with production of the maximum amount of energy from its constituent atoms and molecules, some oxygen rich compounds or oxidizers have to be added in it .

- HEMs are usually a pure substance or a mixture of substances containing combustible elements or fuel along with oxidizing elements in a system of metastable state and also able to react under comparatively minor provocation along with a diversity of stimuli, producing heat energy and some gaseous byproducts [9,10]
- HEMs containing their own oxygen are releasing comparatively less amount of energy, but the energy released in the HEMs is much intense with the rapid rate of release along with some gaseous products.
- The rate of energy release for HEMs is although extremely high, but the total energy release during chemical reaction due to combustion distinguishes HEMs from other ordinary materials. If the HEMs are appropriately ignited it can release energy in a comparatively slow rate (deflagration) or in a much quicker rate (detonation), that depends upon the level of the input energy,chemical structure of the materials, chemical composition, confinement and quality of the materials.
- Hence, those explosive materials which usually have a property of detonation are termed as high explosives, but otherwise the explosives which are usually deflagrate are called as Propellants. The nature, quality, and mechanism of the chemical reactions during combustion of these materials depend upon the process of deflagration and detonation, but fundamentally have no differences, but the basic difference of both kinds of materials depends upon the rate and mode of the release of energy and the various phenomena associated with it.

Example: The process of detonation mainly involves the propagation and formation of detonation wave, which is normally an intense form of shock wave, because the energy released due to chemical reactions is extremely high. The shock wave results heating effect, which is owing to the chemical reaction during the way through the explosive medium at a comparatively much higher pressure of about nearly 10 bars and very high velocity.

- The flame anterior in the deflagrating explosive materials moves at a reduced linear velocity, normally few mm/sec, which is the cause of higher velocities with an increase in ambient pressure because of increase in degree of confinement.
- Under some favourable conditions including the release of huge quantity of energy , strong confinement, influencing initiation of the deflagration of the propellant, undergoes a transition to detonation, but, however, the occurrence of the reverse transition may also be observed. The phase due to deflagration is however, small and precedes the start of detonation in the high explosive.

- The explosives are generally treated as the materials that are capable of experiencing a self-sustained chemical reaction having rapid evolution of heat with the release of the huge volume of gaseous products in order to produce the pressure effects.
- The propellants may be found in all the three states of matter such as solid, liquid and gas. The explosives may be a single compound, which posseseses the capacity of producing an explosive reaction or mixture of compounds, which individually may or may not have explosive property.
- The molecules of most of the good explosive mixtures or materials must contain oxygen and nitrogen in their molecules of parent carbon skeleton. The role of the nitrogen atoms, present in it is to take oxygen atoms from it and initiate the chemical reaction mixing with hydrogen and carbon atoms in a suitable stress level. The unstable nitrogen-oxygen bonds sometimes may undergo unexpected disruption and initiates chain of reactions, which follows and accelerates detonation or deflagration [11,12].

High Energy Density Materials (HEDMs)

This kind of materials are a new class of HEMs, which are recently recognised and categorized. There is no united clear definition of such categories of materials but however, these generally contain a high energy density compound (HEDC) with plasticiser, binder, combustible agent, oxidiser and high insensitive agent. The major necessities of HEDMs for the stability and energy are normally as $\rho \approx 1.9$ g cm^{-3},detonation pressure P ≈ 40.0 GPa,bond dissociation energy (BDE) ≈ 80–120 KJ mol^{-1} and detonation velocity of D ≈ 9.0 km s^{-1}. These kind of materials are successfully and efficiently used as explosive, propellant, and pyrotechnic composition. The new advanced HEDMs mainly contains five substances of different categories such as nitrogen heterocyclic compounds (azine compounds, furazan compounds, azole compounds),acyclic compounds, strained materials,caged substances, oxygen cluster and nitrogen clusters molecules and materials in the excited state . In addition to all these heterocyclic compounds contains nitrogen with high density, thermal stability, insensitivity and high enthalpy or heat of formation. The compounds containing less hydrocarbon content and more number of nitrogen molecules make them easier to attain the oxygen balance and increase in the density. The degraded products of the HEDMs are usually N_2 having the least energy level, therefore, these kinds of materials are environment friendly, therefore, attention was paid by global researchers. The parent skeleton of the azine compounds are mainly the heterocyclic nitrogen containing aromatic hexagonal ring and the aromaticity of the compounds were the cause of the greater stability with less sensitivity towards friction, sparks and impact and relatively

more safe to use. Otherwise, the heterocyclic N atoms present in the substance replaces the - CH group of the benzene ring, which causes the more heat of combustion, more enthalpy of formation, and cause of accomplishing oxygen balance.Presently, more research work has been carried out on compounds of azine and primarily focussed on tetrazines (DHT, BTATz) and amino-substituted diazines or polynitrodiazines(mainly LLM-105).The research work on polyazide azo triazines (mainlyTAAT) and most of the triazines have mainly focused on the medical point of view. The central DRDO laboratory (HEMR) also carried the research work for development , design and property study of propellants, pyrotechnics, high explosives, polymeric materials, insulating materials and other high energy materials [13, 14].

Some of the major HEDMs are as follows

- 2,6-diamino-3,5-dinitropyrazine-1-oxide (LLM-105) having general molecular formula $C_4H_4N_6O_5$, molecular mass = 216.04, density ρ = 1.913 g cm^{-3} having enthalpy of formation = –12 kJ mol^{-1} are generally insoluble in most of the organic solvents except DMSO. Scheme-3 represents the structure of LLM-105, TAAT

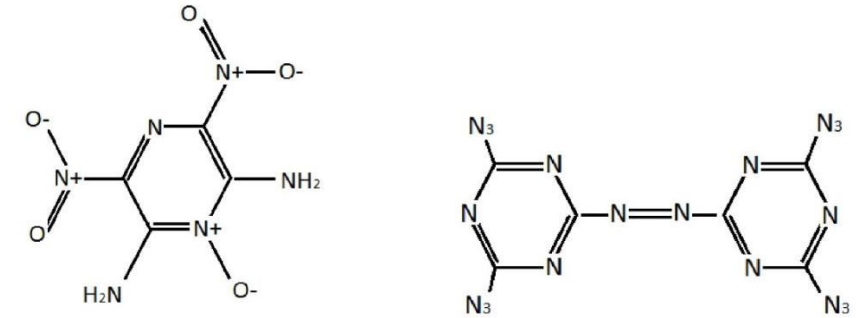

Scheme 3 Structure of LLM-105, TAAT

- 4,4′,6,6′-Tetra(azido)azo-1,3,5-triazine (TAAT) is a polyazido heterocyclic system, having many azido groups and it decomposes exothermically. The nitrogen content of TAAT is very high, up to 79.55%. It has good stability, high decomposition temperature and low friction sensitivity. The enthanly of formation of it is very high (2171 kJ mol^{-1}). The enthalpy of formation is the highest among all the known polyazide, polynitro and high-nitrogen compounds.
- 3,6-Dihydrazino-1,2,4,5-tetrazine (DHT): The compound tetrazinehas three isomers such as 1,2,3,4-tetrazine commonly known as DHT, 1,2,3,5-tetrazine, 1,2,4,5-tetrazine or S -tetrazine or homotetrazine but chemically DHT is named as 3,6-dihydr azino-1,2,4,5-tetrazine which belongs to the S –tetrazine class.

- 3,6-Bis(1H-1,2,3,4-tetrazol-5-yl-amino)-1,2,4,5-tetrazine (BTATz): From the molecular structure of this material, it was found that this compound contains two heterocyclic two high-nitrogen systems namely tetrazole and tetrazine . It is the compound of highest Nitrogen content among the HEDMs.
- 3,3′-Azobis(6-amino-1,2,4,5-tetrazine): The compound DAAT is considered as a distinctive representative of a high-nitrogen energetic compound called as azotetrazine having percentage of nitrogen up to 76.36%, low sensitivity and very good thermal stability [15,16]. Scheme-4 represents the structure of DAT, DAAT, BTATz, BTT.

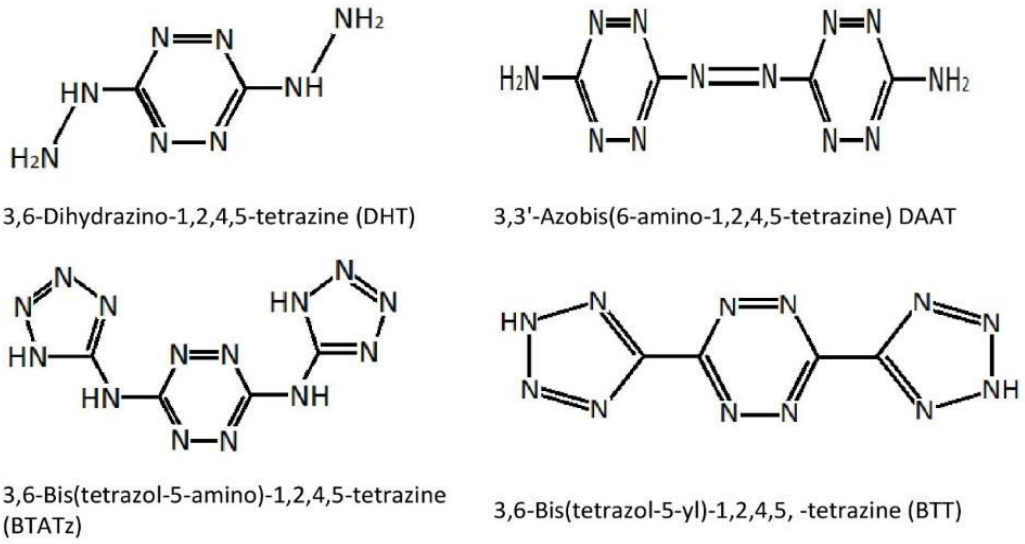

Scheme 4 Structure of DAT, DAAT, BTATz, BTT

CONCLUSION

The research work was carried out for the development of the performance levels of the high energy materials (HEMs) without affecting the sustainable environment throughout the world. A thrust was given to research in the field of force multiplying HEMs and compounds which does not contain pollution causing components. Today scientists are searching the HEMs which are eco-friendly and manufactured in a green technology by focusing on propellants without chlorine and primary explosives free from lead. This review work gives us the modification, advances in the field of high energy materials including high-energy dense materials, oxidizers, fuel materials, plasticizers, and HEDMs. The improvement of the performance of the explosives and propellants are of more concern in the programs of research in high energy materials giving priority to the space and defense sectors. The low susceptible ammunitions having potentially high performance and spin-offs are the advantages of the proposed research on the rocket

propellants which are being developed on the forefront. The energetic compounds based on azine are comparatively more stable, with high heat of formation, low sensitivity, and release high amount of heat energy at the time of combustion, producing large quantities of N_2 due to burning and are also eco-friendly to the environment. BTATz, DHT, DAAT etc. are the commonly used explosive materials. The HEDC is another class of HEMs which has a good and prospective application in the field of space engineering and national defense. But still more advance research work must have to be promoted to design and develop eco-friendly propellants and explosives that can be used both for civil and defense sectors.

REFERENCES

1. M. B. Talawar, R. Sivabalan, M. Anniyappan, G. M. Gore, S. N. Asthana, B. R. Gandhe, Emerging trends in advanced high energy materials. Combustion, Explosion, and Shock Waves, 43(1) (2007) 62–72.
2. R. William, Martin, David W., Ball Small organic fulminates as high energy materials. Fulminates of acetylene, ethylene, and allene, Journal of Energetic Materials, 37(1) (2019) 70-39.
3. S. Aguero, R. Terreux, Degradation of High Energy Materials Using Biological Reduction: A Rational Way to Reach Bioremediation, International Journal of Molecular Sciences 20(22) (2019) 5556-5578.
4. V. Anbua K., A.Vijayalakshmi, R.K Arunathan, A. David Stephen, P.V.Nidhin. Explosives properties of high energetic trinitrophenyl nitramide molecules: A DFT and AIM analysis, Arabian Journal of Chemistry, 12(5) (2019), 621-632.
5. S. Chaturvedi, N. Dave Pragnesh. Solid propellants: AP/HTPB composite propellants, Arabian Journal of Chemistry, 12(8) (2019) 2061-2068.
6. L. DeLuca “Innovative Solid Formulations for Rocket Propulsion”, Eurasian Chemico Technological Journal, 18(3) (2016) 181-196.
7. D. Trache, Thomas M. Klapötke, L. Maiz, Abd-E. Mohamed, DeLuca Luigi T. Green Chemistry 19 (2017) 4711-4736.
8. Chen Yong, Ba. Shuhong, High Energy Density Material (HEDM) – Progress in Research Azine Energetic Compounds, Johnson Matthey Technology Review, 63 (1) (2019) 51–72.
9. Adam S., Cumming New trends in advanced high energy materials, Journal of Aerospace Technology and Management, 1(2) (2009) 161-166.

10. S.M. Bobrovnikov, E.V. Gorlov, V.I. Zharkov, Remote detection of traces of high-energy materials on an ideal substrate using the Raman Effect. Atmospheric Oceanic Optics, 30 (2017) 604–608.
11. J. Keith Butler Review of Chemistry of High-Energy Materials, 2nd Edition, Journal of chemical Education, 91(2) (2014) 163-164.
12. A. S. Saikia, R. Gore, M. Girish, S. Arun, Synthesis of some Potential High Energy Materials using Metal Nitrates; An approach towards Environmental Benign, Process,73(7). (2014) 485-488.
13. Y. Wang, Y. Liu, S. Song. Accelerating the discovery of insensitive high-energy-density materials by a materials genome approach. Nature Communication 9 (2018) 2444-2455.
14. W. Zhang, J. Zhang, M. Deng, X. Qi, F. Nie, Q. Zhang. A promising high-energy-density material, Nature Communication, 8(1) (2017) 181-188.
15. J. P. Agrawal, Some New High Energy Materials and their Formulations for Specialized Applications, Propellants, Explosives, Pyrotechnics,30(5 (2005),316-328.
16. Li, X., Cao, W., Song, Q, Study on Energy Output Characteristics of Explosives Containing B/Al in the Air Blast. Combustion Explosive Shock Waves, 55 (2019) 723–731.

INCORPORATING SDGS IN WATER POLICY: PERSPECTIVES FROM JAL JEEVAN MISSION

Dr. Shruti R. Panday
Head & Assistant Professor, Economics, SIES College of Arts, Science & Commerce (Autonomous), Mumbai University, 400022

ABSTRACT
Sustainable and prudent management of water resources and its consumption plays critical role in maintaining healthy ecosystem for human survival. It is of paramount importance in improving productivity of population (UNDP- Water for LIFE-2005-15). Target 16 of SDGs clearly emphasises and recognises role of governance and political institutions in achieving the mentioned goals. In connection to the commitment towards SDG – UNO Agenda 30, Government of India has restructured and subsumed the ongoing National Rural Drinking Water Programme (NRDWP) into Jal Jeevan Mission (JJM). The present paper has two pronged objectives. Firstly, it tries to link JJM with sustainability by bringing into governance and secondly, it tracks the progress of flagship programme of the government of India.

Keywords: Jal Jeevan Mission, Water Sustainability, Participatory Approach,

1. INTRODUCTION
Water is a finite and irreplaceable resource that is fundamental to human well-being. (UNDP). Water for Life – 2005-15, UNDP campaign clearly emphasises and recognises the critical role of sustainable and prudent management of water resources and consumption for socio- economic development, healthy ecosystem for human survival and improving productivity of population. Additionally, it was also recognised that "Water is at the core of sustainable development as it is closely linked to a number of key global challenges." (The Future We Want: Outcome document adopted at Rio+20). Sufficient, safe, affordable and physically accessible sources of water are fundamental human rights.

The second populous country in the world with a population of approx. 1.4 billion (Census, 2011), the water crisis is bound to be a huge issue for the nation. With increase in population, the per capita availability of water would decline progressively, as water availability of any region depends on hydro-meteorological and geological factors which are generally constant. NITI Aayog has already stressed that there is an urgent need to consider sustainable approaches to water conservation in order to address both the immediate and future needs. The total water availability of India received through precipitation is about 4000 billion cubic meters (NCIWRD) per annum (but owing to geological and precipitation factors, the utilizable water availability is limited

to 1123 BCM per annum, which includes surface water (690 BCM) and replenishable ground water (433 BCM). The grimness of the situation can be understood by the report of National Commission on Integrated Water Resources Development, which estimated a sharp decline in the average annual per capita water availability from 2001 to 2011 as 1820 cubic meters and 1545 cubic meters respectively and which is estimated to reduce further to 1341 and 1140 in the years 2025 and 2050 respectively (NCIWRD). It is important to note that an annual per-capita water availability of less than 1700 cubic meters is considered a water stressed condition and annual per-capita water availability below 1000 cubic meters implies a water scarcity condition. Approx. 820 million people in India spread over twelve river basins across the country have per capita water availability of 1000 cubic meter, which happens to be the official threshold for water scarcity. (Central Water Statistics 2015).

Apart from the issue of per capita availability, the country has also a persistent problem of accessibility and absence of physical nearness of water resources. Out of total rural households 19, 14,48,0269 as of April 2022, only 9,37,01,502 (48.9%) have connections with PWS (piped water supply). (Jal Shakti ministry, 2022). Thus, a large population of rural households 9,77,46,5249 (51.1%) are deprived of piped water connections. It is being estimated that by 2030, India's demand will outgrow water supply two to one. (Composite water Resource Management Report, 2019). Against this background, the Indian Government flagship programme of JJM launched in 2014 is of worth mentioning.

2. OBJECTIVE AND METHODOLOGY

The present paper has two pronged objectives. Firstly, it tries to link JJM with sustainability by bringing into governance as influencing factors and secondly, it tracks the progress of Jal Jeevan Mission, a flagship program of the government of India being sloganized as Har Ghar Nal Se Jal. The paper has mainly collected data from Ministry of Jal Shakti and presented it into tables and diagrams. Chart was prepared collaging the information collected from UNDP.

3. JAL JEEVAN MISSION – A SUSTAINABLE APPROACH OF DEVELOPMENT

JJM is a participatory, decentralized, bottom-up approach of delivering assured potable tap water supply in adequate quantity with sufficient pressure and of prescribed quality on regular and long-term basis in the homes. It is perceived as a laudable initiative to provide safe and sufficient drinking water to rural households by 2024.

Two broad objectives of the JJM are, firstly to impart priority in provision of Functional Household Tap Connections (FHTCs) in areas where quality water availability is an issue, villages in drought prone and desert areas, villages under Sansad Adarsh Gram

Yojana (SAGY), Secondly, it also emphasises on children health, therefore, aims at ensuring provision of functional tap connection to not only households but also public institutes , schools, Gram Panchayat buildings, *anganwadi* centres, rural health and wellness centres and community buildings. Apart from these two main objectives, it also envisages rural community empowerment in sustaining water sources and creating awareness on different aspects of significance of safe drinking water, economical use of water resources with intention of making water everyone's business. In this respect, it is unique in comparison to earlier programs as it addresses the grave issue of water scarcity and its impact on the economy in the long run. The Jal Jeevan Mission follows a three-tier model for implementation of its objectives.

Chart 1: (Bottom Up, Decentralised, Participatory Approach of Development)

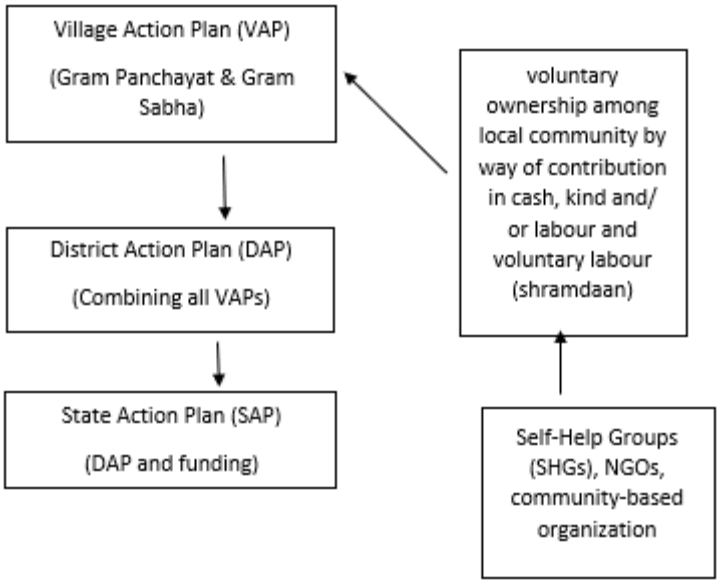

Source- compiled by the author (Information from Jal Shakti Ministry)

At the first level, there is the Village Action Plan (VAP), which is prepared by the Gram Panchayat and approved by the Gram Sabha. This is followed at second level by the District Action Plan (DAP), which combines all the VAPs prepared at panchayat level. These two are backed at third level by the State Action Plan (SAP), which considers the DAP and looks after the financing part. SAP also aims to target water security across the state by finding ways to discourage the use of tankers and handpumps in villages. It is a participatory and community approach to solve water problems at ground level. The scheme has envisaged voluntary accountability among local youths and beneficiaries by way of contribution in cash, kind and voluntary labour (*shramdaan*). It also encourages participation of NGOs, Voluntary Organizations/ women SHGs under NRLM/ SRLM, etc. to assist the village community for in-village water resource management and water supply related infrastructure augmentation. The voluntary organisations are expected

to be associated with the scheme as partners to facilitate the communities in awareness creation, capacity building, planning and implementing the schemes.

3.1 Incorporating Sustainability in Water Policy-

Central government-funded schemes like JJM targeting rural water supply are not a novel concept. In 1954, a National Water Supply Programme was initiated to provide safe drinking water to villages. Followed by the scheme, National Rural Drinking Water Programme (NRDWP) launched in 1972. In that way, JJM is unique as it incorporates a sustainable approach to the water crisis and satisfactorily fulfils SDGs and water targets as laid by UNO. The chart shows a link between development outcomes and mechanisms under JJM to fulfil SDGs target on the water front.

Chart 2: Linking SDG and JJM

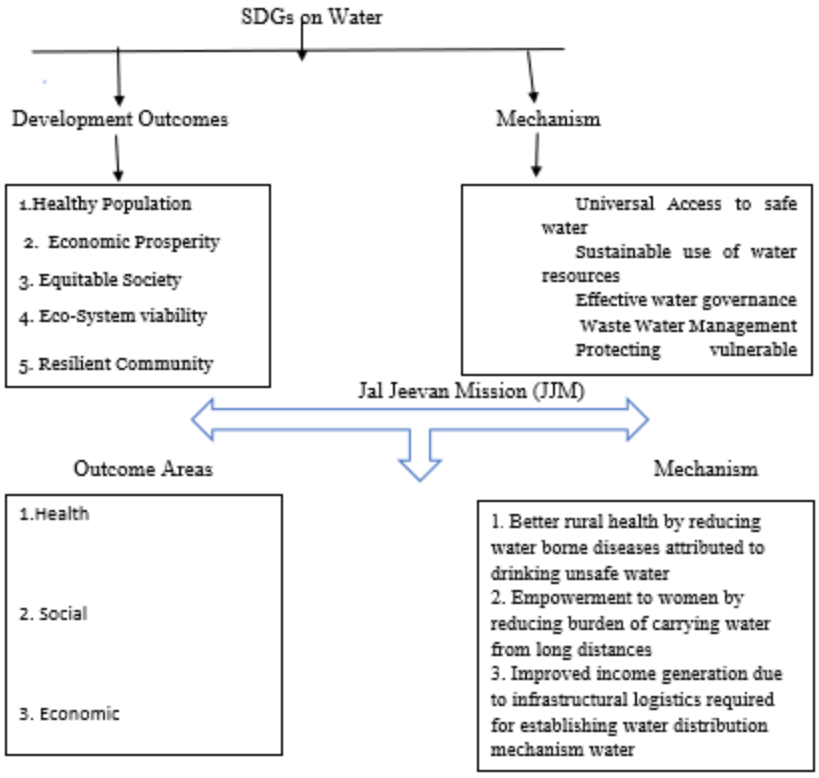

Source- adapted from "Securing sustainable water for all, UN "SDGs on water"

It can be well understood that sustainable water management is key to handle a host of development challenges and can be determinant factors in ensuring development goals. Sustainable and efficient water resource utilisation is important for ensuring a healthy, prosperous population as well as in maintaining the vitality of the ecosystem. In line with SDGs goal on water, Jal Jeevan mission has targeted rural household health by ensuring affordable access to safe drinking water and in process of building a resilient

community by protecting them from water borne diseases majorly caused by unsafe drinking water and sanitation issues. The mission has clearly targeted on ensuring tap water connection to tribal residential schools for drinking, cooking mid-day meal, hand washing and use in toilets with focus on health and well-being of children. JJM has also targeted social equality and women empowerment by addressing the issue of women members of household in (NSSO- 69th round). Approx. 50% household members in rural India has to travel a minimum distance of 0.2 km to 0.5 km to reach to the principal source of drinking water. Since the primary burden of water collection is borne by women members of the household, it means they have less time and energy for any productive works. (UN 2015, The World's Women 2015). The uniqueness of the program also lies in embracing the resolution of International Decade for Action, 'Water for Life' (2005-2015), which calls for women's participation and involvement in water-related development efforts.

3.2 Progress Assessment of JJM

As of 2022, the total number of tap water connections provided since the launch of the program in 2019 stood at 5.03 crore. (Ministry of Drinking Water and Sanitation). Out of 33 states and UTs, (figure1). In two years, the program has shown a progress of % in coverage of tap water connections, 76.93 % increase in coverage of PWS in Schools, 68.21 % increase in coverage of PWS in *anganwadi* centres (AWCs). Additionally, an increase of 36.09% and 37.83 % in ensuring tap water connections in Aspirational districts and JE/AES affected districts respectively. (Table 1).

The functionality assessment found 94% of tap water connections to be working, 84%tap connections with quantity of water supply more than 55 litre per capita per day(lpcd), 61% with potability, and in 87% households, water supply found to be regular (Jal Shakti Ministry report,2022)

Table 1- Performance of JJM on significant parameters.

Parameters	2019	2021
Budgetary allocation (in lakh crore)	10,000	50, 011
Coverage of tap water connection (crore)	3.23	8.23
Coverage of PWS in schools	48,772	7.93 lakh (76.93%)
Coverage of PWS in AWCs	25,092	7.65 lakh (68.21%)
Tap water connection in Aspirational districts (no of households in lakh)	31.30	122.62 (36.09%)
Tap water connection JE/AES affected districts	8.02	115.95 (37.83%)

Source- Jal Shakti Ministry, 2022. (Figure in parenthesis is percentage progress)

Figure 1- Percentage of Rural Household Access to Piped Water Supply

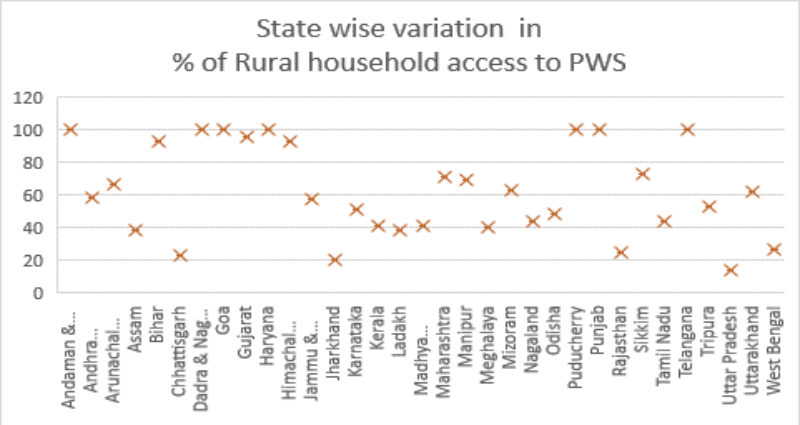

Source- Jal Shakti Ministry, 2022

Despite this impressive growth, there are challenges that need to be addressed. The coverage of tap water connection in quality affected habitats need to be expedited. A large number of 47,098 districts are still out of reach of the program. Similarly, there is regional variation in states performance in ensuring PWS to rural HHs (figure1). States like Goa, Haryana, Telangana and UTS like Puducherry, Andaman-Nikobar Islands, Dadar-Nagar Haveli & Daman -Diu have achieved 100% coverage of tap water to rural households but there are states like Chhattisgarh, West Bengal. Kerala, Maharashtra lagging far behind. This variation may pose a challenge in achieving the target and therefore, states need to be monitored and incentivised to achieve targets.

4. SUMMARY AND SUGGESTIONS

An estimate by WWF raises an alarming scenario that by 2030, 30 Indian cities will be at risk of a severe water crisis and, according to the World Bank, India will lose 6% of its GDP due to poor water management. India heavily depends on monsoon for its water requirement. Climate change is likely to make the monsoon more erratic, exacerbating pressure on water resources. Therefore, to mitigate this impending crisis, modern technology along with strong governance backed with community support are poised to play a huge role.

At the same time, it is crucially important to understand the role of clean water in fighting water borne diseases and the need for innovative solutions and technology for public water supply infrastructure. In this regard, JJM principally addresses the issues of safe, sufficient and sustainable sources of drinking water for rural households. The programme has embodied a necessary mechanism to check use and supply of water, but equally important is surveillance with regard to maintenance of infrastructure, grey water management, methodical monitoring of the plan, capturing service data for ensuring the quality of services. The mission is based on a community approach to

water; therefore, the role of IEC (Information, Education and Communication) becomes extremely important to implement a practical sustainable water management model. UN Agenda 30 with respect to SDGs has heavily relied on the governance and people participation to achieve its target and goals, therefore all the mechanism mentioned in the JJM needs to be followed in its true letter and spirit to achieve its target of proving piped water supply to every rural household by 2024.

REFERENCES

1. Biswas, A.K., & Tortajada, C. (2010). Future water governance: problems and perspectives. International Journal of Water Resources Development, 26(2), 129–139.
2. Chaudhuri, S., Roy, M., McDonald, L. M., & Emendack, Y. (2020). Water for All (Har Ghar Jal): Rural Water Supply Services (RWSS) in India (2013–2018), challenges and opportunities. International Journal of Rural Management, 16(2), 254–284.
3. Composite Water Resources Management: Performance of States NITI Aayog August 2019, http://social.niti.gov.in/uploads/sample/water_index_report2.pdf
4. https://ejalshakti.gov.in/IMISReports/Reports/Physical/rpt_CoverageIndividualHousePipConnection.aspx?Rep=0&RP=Y
5. https://jaljeevanmission.gov.in/
6. NITI Aayog, Government of India. (2018). https://prsindia.org/theprsblog/status-of-drinking-water-and-sanitation-in-rural-india.
7. NSSO 69th round, key indicators of Drinking water, sanitation, hygiene and housing condition in India.
8. Press Information Bureau, Government of India, Ministry of Water Resources, 20-July-2017 Shortage of Water, https:// pib.gov.in/ newsite/ Print Release. aspx? relid=168727
9. The world Women 2015- Trends and Statistics, UN 2015.
10. Two years of Jal Jeevan Mission, Ministry of Jal Shakti, Government of India, October 2021.
11. UNDP- Report- International Decade for Action “Water for Life” -2005-15.
12. Water as a Human Right? IUCN, UNDP, 2004
13. Water in the post-2015, Development agenda and Sustainable Development Goals. Discussion paper, World Bank, Water and Sanitation Program (WSP). March 2014

FOOT NOTES

National Commission on Integrated Water Resources Development

"NANO MEMORY"- A FUTURE OF SEMICONDUCTOR MEMORIES

[1]Shobhika P. Gopnarayan, [2]Dr. Shriram D. Markande and [3]Dr. Vaishali P. Raut

[1]Research Scholar, GHRCEM, Wagholi, Pune & (Assistant Professor, Electronics & Telecommunication Department, AISSMS IOIT, Pune)

[2]Principal, Sinhgad Institute of Technology and Science, Narhe (SITS Narhe, Pune)

[3]Assistant Professor, Electronics & Telecommunication Department, GHRCEM Wagholi, Pune

ABSTRACT

The most significant development in the area of semiconductor (microchip)circuit memory during the last decade has been the enormous rise of the flash circuit-memory market, which has been driven by wireless phones and other types of digital movable equipment such as palmtop, PC, various players etc. Because of its advantages over current rigid digital systems, the necessity for adaptable digital systems like apparel computers, digital-paper, and adaptable flexible screens take lately surged. Versatile memory is a fundamental component of digital structures for data interpretation, stowing, and communiqué, and is thus, a critical component in realising such adaptable digital systems. We have effectively scaled this fantastic technology down to 20nm, but we are now exceeding the limit. This is the time for disruptive breakthroughs, such as merging the same fundamental gadget in a vertical structure or transitioning to entirely new device designs. This article examines the various choices of nano memories in terms of their application areas. The configuration comprises silicone field effect transistor with silicone nanocrystals positioned in the oxide gate near the transposal apparent. Using deep ultra-violet lithography, the gadgets are planned for ultimate lamella together as microchip technology on 300 mm thickness silicone on insulator wafers.

Keywords: Component, Nanotechnology, Silicone Transistor, Flash Memory, MOSFET, Transistor.

1. INTRODUCTION

A standard MRAM through immense speed and sufferance-free features is an appealing contender for non-volatile RAM. It employs a present-induced magneto area for write operations, which is relational to the demagnetize area, which enhances as the magneto tunnel junction (MTJ) extent decreases (1, 2), highlighting the issues in write power depletion and surmounting. To address of these issues, we developed a new spin torque transfer magnetic switching (STS) technology that has the potential to overcome their limitations. Adaptable digital devices have gained popularity due to their greater transportability, conformal contact with rounded faces, insubstantial design, and user-

friendly edges over conservative bulk silicone technology. 1-3 Various analyst have investigated numerous flexible digital devices like as integrated circuits (Ics),4,5 organics light-emitting diodes (OLEDs), sensing nodes, and radio frequency identification reader (RFID) antennas. Though these studies established the viability of adaptable digital equipment's, their approaches were limited to few aspects of the digital, and that each electrical appliance should thus be merged into a distinct gadget to fulfil its individual purpose within an adaptable model. Volatile memories, like SRAM or DRAM, drops the data after the power source is switched off, while being immensely fast in writing and reading or very dense. The micro digital sector has almost constantly outlined the evaluated methods, for example, narrow silicone-on insulator (SOI) film rather unpackaged silicone, high-k dielectric rather than the outmoded SiO2 gate dielectric, and metallic gate in its place of the polysilicone gate for destructive MOSFET lamella to improve outcome. In contrast to EEPROM, there is very little deterioration as a result of the device's operation in direct tunnelling. The modern complementary single-electronic transistor (SET) hybrid design of metal-oxide-semiconductors (CMOS), dubbed SETMOS, is discussed, that provides Coulomb blockade oscillations [15, 16, 17, 18] and quasi-periodic negative variance resistance effects at significantly advanced recent levels compared to conventional SETs. It is a detailed threshold-shifting, single transistor circuit-memory structure with rapid read and write intervals and an extended retaining period. For more than four decades, the progress of Non-Volatile Memories has been largely dependent on the floating gate MOS transistor. We have effectively scaled this fantastic technology down to 20nm, but we are now exceeding the limit. This is the time for disruptive breakthroughs, such as merging the same fundamental gadget in a vertical structure or transitioning to entirely new device designs.

1.1. The Memory Cell

The Nano-crystals circuit-memory bank shown in Figure 1 made up of a distinct FET gadget through a disseminated floating gate area made up of an arbitrary array of silicone or germanium Nano-crystals (1-10 nm in thickness) arranged amongst the channel and the controller gate 1-5 nm distant through the channel. The distance between the Nano-crystals is kept more than 5nm, limiting any lateral charge leakage. As a result, while the transporters can be inoculated into the Nano-crystals, The atom charge is preserved in these separated nano-crystals of 2-5 nm in size that are divided from each other by more than 5 nm of $SiO_2$and less than 5 nm of SiO_2 as after the substrate surface's transposal layer. At 350 K, a hybrid circuit operation containing a single hole transistor connected to a metal oxide semiconductors-field-effect-transistor (MOSFET) is exhibited.

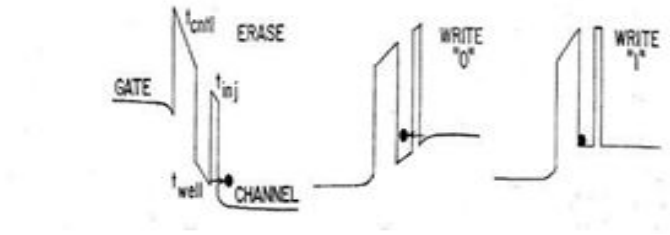

Figure 1 Read, write and erase operation [19]

1.2. Intersect Concerns and Many Value (MV) Logic

Nonetheless, not only the essential limits of the Nano scale MOSFET, but also the intersect restrictions, have threatened to slow or stop the microchip sector's past advancement, as shrinking of intersects, distinct transistors, doesn't improve their outcomes. Many challenges arise when lamella intersects into the nanometre regime, like resistivity deprivation, material combination disputes, and dependability concerns caused by electric-powered, thermic, and mechanical strains in a multi-level chain stack [14]. Today's options for reducing connection delay include the usage of Cu and low-k dielectrics. Alternative potential resolution to the intersect conundrum is to reverse-scale lengthier semi-global and global intersects to have fat cross-sectional magnitudes [14]. This method improves connectivity accuracy but reduces wired density. Simultaneously, it has been found that as chip sizes increase, so does the lot of local modules and intersects in a generally network connect [15][19].

Because device area is closely tied to cost, the area penalty of converse scaled techniques potentially impedes the augmented cost per function reductions that has powered microchip research over the last years ago.

1.3. Writing Process

With reference to Fig. 8, the physical problematic of driving an atom over or through an energy obstacle is the problematic of writing the FG cell. The question was addressed by utilizing a variety of physical impacts [11]. The three major key processes for writing the FG memory cell are depicted in Fig. 1. The CHE process occurs due to the electric arena in the transistor channel amongst the source and drain, where atoms obtain enough energy to pass the oxide-silicone energy barrier. Indeed, on the high energy side, atoms energy propagation exhibits a tail that can be controlled by the longitudinal electric arena. The photoelectric consequence, in which atoms gain adequate energy to cross the obstacle. Photon interface with energy is superior to the barricade itself. UV radiation is used to describe this for silicon dioxide. This method was originally used to remove the entire system in EPROM items. The Fowler–Northeim atoms tunnelling system is a quantum-mechanical tunnel created by an electric arena [18]. When an effective electric field (in the 8-10 MV/cm range) is applied to a thin oxide, a substantial atom tunnelling current can be driven into it

without causing it to lose its dielectric properties [16,18,19]. A NORMAL drain side of a flash circuit-memory cell is automated by CHE inoculation into the FG, and the silicone surface is erased by FN atoms tunnelling through the FG to the silicone apparent through the tunnel oxide.

1.4. The organisation of memory cells and the integration of processes

The only dissimilarity amongst Spin-RAM and a standard MRAM is in the written process, while the read system is the similar. The circuit-memory bank of the Spin-RAM is made up resistor, an MTJ, a word line (WL), a bit line (BL), and a source line (SL), depicted in Figure 2. (a). An MTJ has double magneto layers and a tunnel obstruction layer amongst them. Some of the magneto layers is a switching layer, while the further, it's magnetized in one direction only. For the appropriate resistance area (RA) produce of the MTJ, a tunnel obstruction layer is built of crystalline MgO with a thinness of fewer than 1nm. A cell array was built for memory characterizations, as illustrated in Fig. 2. (b). During the write process, a WL is chosen, and a constructive voltage is provided to a BL or SL of a chosen column. The current trend controls the magnetization direction of a switching layer. During the read procedure, a WL is chosen, and a voltage of 0.1 V is delivered to a BL of a chosen column. The write and read things were examined using mutually voltage sweep and pulse modes. The Spin-RAM scheme was built with 0.18μm CMOS equipment and a four-level metal. As shown in Fig. 3, cross-sectional SEM and TEM imageries reveal our process of combination and configuration of the 4kbit Spin-RAM device. We created a new MTJ by combining our innovative CoFeB ferromagnetic coat [7] and an MgO tunnel obstruction layer. Even though an MTJ is utilized in MRAM, Spin-RAM devices require extra development. The primary goal is to improve the efficiency of rotational torque transmission. Figure 4 is a TEM imagery of an MTJ film in cross-section. A crystal growing condition of (100) oriented thin MgO tunnel obstruction layer and magnetic material microstructure have been improved to get a larger tunnelling spin polarisation and a lesser RA product. As a result, the magneto resistance (MR) ratio increased by greater than 160 percent at a RA product of 20 $\Omega\mu m^2$.

 ISBN: 978-81-959870-7-8

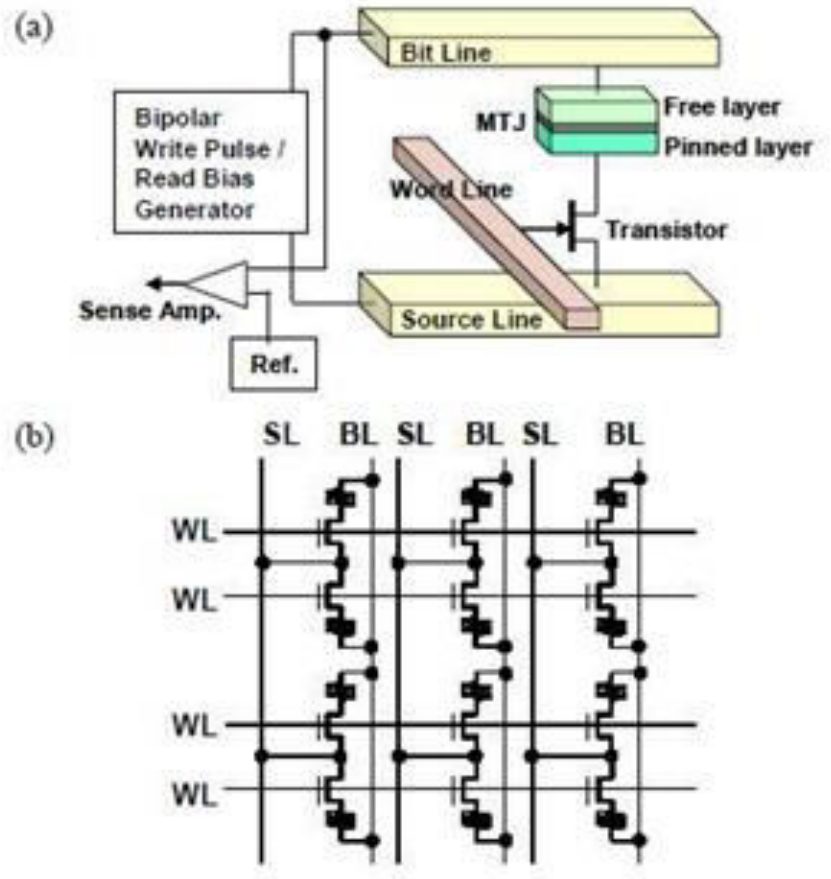

Figure 2: Memory Cell(a), memory array(b) [15]

1.5. Discussion of Memory Cell

The circuit design of the SRAM cell under evaluation is illustrated in Figure 2; this comprises a SE turnstile, a SET/MOS hybrid circuit, an SN, and a MOSFET Reset. The read word line (RWL) and the write word line (WWL) is utilized for the cell's two simple processes. The fixed-line utilized to rearrange the stowed charge in the SN. The cell's input node is the Write Bit Line (WBL), and its output node is the RBL. A SE is originally believed throughout the transfer process. In terms of the simulation outcomes of the described Memory Cell, the subsequent operating cycles are analysed at 45 nm feature size utilizing the parameters in Table I. (as in Fig. 3).

- When RWL is '0,' no read process is achieved in the SRAM, regardless of RBL value. The cell is supposed to be in reserve mode.
- Turning on the reset-FET (Tn5) and Tn2 completes the relocate operation. For illustrate, if the Wetland reset line is '1' at the same time, Tn2 and Tn5 are both ON. "All atoms in the single-electrons box (SEB) and SN flowing to the ground are saved, and the circuit-memory bank is rearranged to "0.".

- The "write" action ensures in Cycle 2; primarily, the WBL is "0" during the RWL is "1." (To turn the transistor Tn1 ON). Nonetheless, because "0" is the material to be written, no atoms are transmitted into the SEB. As a result, in Cycle 2, WWL is '1' and RWL is '0,' and Tn1 is turned off and Tn2 is twisted on. As a result, a "0" is written to the SN, indicates that voltage variance will not be there in the RBL.
- In Cycle 3 processes, has the read '0'. After Cycle 2, the knowledge (i.e., '0') is in the SN, and the charge-voltage converter (composed of Tn3, Tp1, and SET1) converts the deposited atoms into the equivalent voltage. Because there are no atoms in the SN, it has a '0.' In Cycle 3, RWL is "1," hence transistor Tn4 is turned on. The "0" will then be read by the RBL.
- The operation Write "1" is described below. In Cycle 1, RWL and WBL are both "1." (Turning ON the transistor Tn1). Because WBL is '1' in this cycle, a SE is sent to the SEB. Succeeding this scenario, WWL is "1," and Tn1 is turned off in this loop. Furthermore, when RWL is "0," Tn2 is activated. The SE is transmitted to the SN throughout this phase, i.e., the "1" procedure is performed.
- The following is the process for reading "1." As a '1' is saved in circuit-memory bank. The translator of the SET/MOS blend circuit can intellect the stowed SE in the SN by translating it into an immense voltage threshold for Tn4 to be ON. In Cycle 2, RWL is set to '1' and Tn4 is twisted on. As a result, the "1" is read and a voltage transition happens. As previously stated, it occurs via the RBL [15]

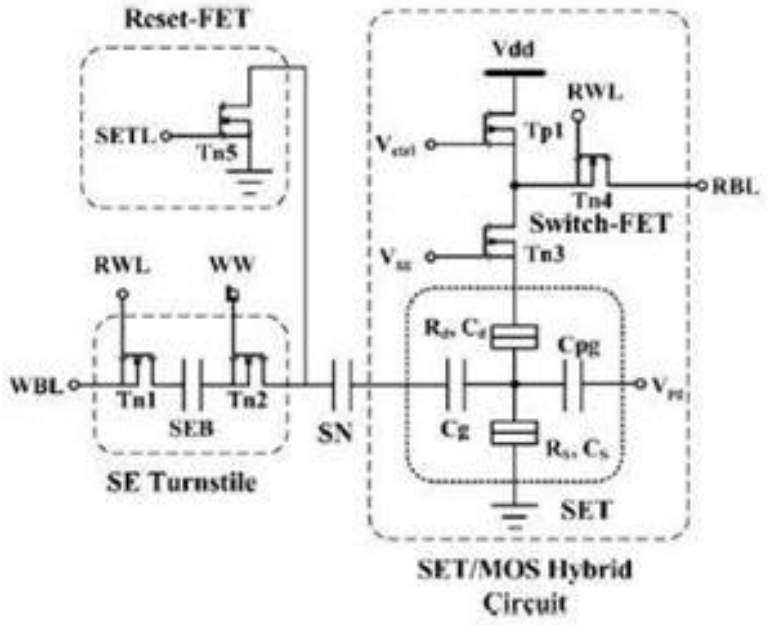

Figure 3: SRAM memory using hybrid SETMOS [20]

2. RELATED WORK

Nanomaterials for Tissue Engineering

Several nanomaterials for tissue engineering have been developed using nanotechnology. These materials have various structures, such as nanopatterns, nanofibers, and controlled-release nanoparticles. From a biological point of view, these nanomaterials are intended to imitate genuine tissues because they are manufactured to be nanometres in size, similar to extracellular fluid and other cellular components (Guan, Lifang, & Ali, 2007). Three nanomaterials for tissue engineering are discussed in this context.

Self-Assembled Nanomaterial

Electrolytic deposition, PH induction, and biometric coating are used to induce self-assembly in these materials. Chitosan, peptide amphiphilic, amylogenic/apatite, and hyaluronic acid are some of the biomolecules employed in the manufacture of self-assembled nanomaterial for tissue engineering (Guan, Lifang & Ali, 2007). In general, the presence of hydrophilic and hydrophobic sections of the peptides, along with charge shielding via the use of hydrogels, facilitates the production of self-assembled peptides (Hartgerink, Beniash & Stupp, 2002). Using peptide amphiphilic, 3D self-assembled nanofibers have recently been created. Through the coupling of peptide amphiphilic with arginine- glycine-aspartate acid, these fibers are employed to promote bone morphogenetic protein-protein adhesion. Furthermore, electrolytic deposition is used to create nanomaterials that allow collagen fibers to grow at the cathode, especially in bio compositing enamels in tooth therapy and osteo therapy. An electrolytic deposition is also used to cover self-assembled calcium phosphate and amylogenic materials. (Wang, Apeldoorn, and Groot, 2005). For the first time, a new non-volatile memory based on STS was presented. Immense speed exchanging inside a 2ns pulse was definite in a combined Spin RAM circuit. Theoretic forecasts coincided well with substituting test, proving that the transferring driving power is sourced from spin differentiated existing rather than heat-up assist or existing induced field. Conceptual predictions can then be used to aid in the development of practical memory. The 1012 cycle test also proved the reliability of the MgO tunnel barrier.

It has been demonstrated that non-volatile Spin-RAM possesses distinguishing qualities, like fast speediness, less power, and excellent scalability. A nano-crystal memory outperforms Flash EEPROM in terms of programming and endurance while maintaining the effortlessness of an individual poly-Si-gate method. The circuit-memory change is achieved by the storing of atoms in clusters created via Ge (Si) implantation or chemical vapor deposition. The use of Nano-crystals reduces charge loss, allowing for thinner tunnelling oxides, smaller working voltages, small power dissipation, and quicker write

and read operations than Flash EEPROM. Most importantly, the VT window is a little deteriorated after lo9 write/erase cycles or lo5 s retention time.

3. CONCLUSION

Charge storage in metallic or semiconductor NPs can result in two-terminal resistive switches. This equipment can be transitioned among both In and Out of it multiple times and maintain good consistency in the both states. As a result, these devices have a wide range of applications as two-terminal device applications. These storage devices may have a fast response time and a large density. They have the potential to solve the technical challenges encountered in the three foremost memory techniques: DRAMs, HDDs, and flash memory bank. They have a wide range of applications together high-end and low-end systems.

Crossbar resistive switches made of nanotubes and nanowires they can also be used as increased density and fast-responding memory bank devices. One major issue in these devices, for example, is repeatability, which stems from difficulties in precisely controlling the sizes of nanomaterials. Preparing thin films evenly distributed with nanometer materials is also technically challenging. Furthermore, the electric-powered conductivity of nanomaterials is heavily influenced by the experimental parameters. As a result, laboratories reported wildly disparate data in terms of device endurance and storage time. All of these issues are expected to be resolved in the future due to the fast expansion of nanoelectronics and nanostructures.

REFERENCES

[1] D. G. Gorden *et al.*, “Overview of nano electronic devices,” Proc. IEEE, vol. 85, 1997, pp. 521–540.

[2] D. Averin and K. Likharev, “Single electronics: A correlated transfer of single electrons and Cooper pairs in systems of small tunnel junctions,” in Mesoscopic Phenomena in Solid, IEEE Transactions on Nanotechnology. Amsterdam, The Netherlands: Elsevier, vol. 3, no. 3, 2004, pp. 173–271.382.

[3] H. Nakashima and K. Uozumi, “Negative differential resistance on single electron transport in a junction array of ultra-small islands,” J.Vac. Sci. Technol. B, Microelectron. Process. Phenom., vol. 15, no. 4, 1997, pp. 1411–1413.

[4] C. P. Heij, D. C. Dixon, P. Hadley, and J. E. Mooij, “Negative differential resistance due to single-electron switching,” Appl. Phys. Lett., vol. 74, 1999, pp. 1042–1044.

[5] M. C. Shin, S. J. Lee, K. W. Park, and E. H. Lee, “Secondary Coulomb blockade gap in a four-island tunnel junction array,” Phys. Rev. B, Condens. Matter, vol. 59, 1999, pp. 3160–3167.

[6] K. Uchida, K. Koga, R. Ohba, and A. Toriumi, "Programmable single electron transistor logic for low-power intelligent Si LSI," in Int. Solid-States Circuits Conf. Dig., 2002, pp. 206–207.

[7] H. Inokawa, A. Fujiwara, and Y. Takahashi, "A merged single-electron transistor and metal–oxide–semiconductor transistor logic for interface and multiple-valued functions," Jpn. J. Appl. Phys., vol. 41, 2002, pp. 2566–2568.

[8] M. I. Lutwyche and Y. Wada, "Estimate of the ultimate performance of the single-electron transistor," J. Appl. Phys., vol. 75, 1994, pp. 3654–3661.

[9] S. Horiguchi, M. Nagase, K. Shiraishi, H. Kageshima, Y. Takashashi, and K. Murase, "Mechanism of potential profile formation in silicon single electron transistors fabricated using pattern-dependent oxidation," Jpn. J. Appl. Phys., vol. 40, 2001, pp. L29–L32.

[10] Y. Ono, K. Yamazaki, and Y. Takahashi, "Si single-electron transistors with high voltage gain," IEICE Trans. Electron., vol. E84-C, no. 8, 2001, pp.1061–1065.

[11] C. Wasshuber, H. Kosina, and S. Selberherr, "SIMON—A simulator for single-electron tunnel devices and circuits," IEEE Trans. Computer-Aided Design, vol. 16, 1997, pp. 937–944.

[12] J. P. A. van der Wagt, A. C. Seabaugh, and E. A. Beam, "RTD/HFET low standby power SRAM gain cell," IEEE Electron Device Lett., vol.19, 1998, pp. 7–9.

[13] H. Inokawa, A. Fujiwara, and Y. Takahashi, "A multiple-valued logic and memory with combined single-electron and metal-oxide-semiconductor transistor," IEEE Trans. Electron Devices, vol. 50, 2003, pp. 462–470.

[14] H. Goto, H. Ohkubo, K. Kondou, M. Ohkawa, N. Mitani, S. Horiba, M. Soeda, F. Hayashi, Y. Hachiya, T. Shimizu, M. Ando, and Z. Matsuda, "A 3.3-V 12-ns 16-Mb CMOS SRAM," IEEE J. Solid-State Circuits, Vol. 27, 1992, pp. 1490–1496.

[15] R. Vaishali and D. Pravin. "Design and Implementation of Hybrid Multiple Valued Logic Error Detector using Single Electron Transistor and CMOS at 120nm Technology," IOP Conference Series: Materials Science and Engineering, vol. 225, 2017, pp. 012160.

[16] V. Dakhole, "Design and Implementation of Single Electron Transistor N-BIT Multiplier" [ICCPCT]-978-1-4799-2395-3.

[17] R. Vaishali and P. K. Dakhole, "Design and Implementation of Single Electron Arithmetic and Logic Unit Using Hybrid Single Electron Transistor and Mosfet at 120nm Technology," 2015 International Conference on Pervasive Computing (ICPC). 2015.

[18] M. Hosomi, H. Yamagishi," A Noval Nonvolatile Memory with Spin Torque Transfer Magnetization Switching: Spin-RAM, IEEE 2005.

[19] Hussein I. Hanafi, Fast and Long Retention, Time Nano-Crystal Memory, IEEE Transaction,1996.

[20] Wei, Jie Han, Design and Evaluation of a Hybrid Memory Cell by Single Electron Transfer, IEEE Transactions on Nanotechnology, Jan 2013.

ASSESSING GROUNDWATER QUALITY OF SAIFUL AREA, SOLAPUR USING GIS

Farhan Kazi, Farooq Ahmed Maniyar and Ameerhusain Jamdar
Department of Civil Engineering, NK Orchid College of Engineering & Technology, Solapur, India

ABSTRACT

Ground water analysis of area, is very important activity required for impact study as well as analysis of that area. Ground water sampling and analysis is an activity within projects dealing with carbon capture and storage, mineral exploration, geothermal and energy resources, as well as for ground water resource assessment and management. QGIS (Quantum Geographical Information System) is used as an effective tool for developing solution for water resources problems for assessing and mapping of ground water quality. As a part of a project we have selected Saiful as study area. We collected 50 different samples of ground water from various locations in Saiful area. As well as we take latitude and longitude of those 50 location in order to map in QGIS.

We carried out various tests on those samples such as Turbidity, pH, Hardness, Dissolved oxygen (DO), Total dissolved solids (TDS), Chloride. We map those 50 points with the help of latitude and longitude taken on the field. After getting result we started plotting above application on QGIS software.

In the next part of study we make 6 different maps using above application by using Google satellite and QGIS in order to get a clear idea about that area.

Keywords— QGIS, Groundwater, Quality, Water level, Parameter, spatial interpolation

INTRODUCTION

In India, most of the population is dependent on groundwater as the only source of drinking water supply. The groundwater can become contaminated either naturally or because of numerous types of human activities, residential, municipal, commercial, industrial, and agricultural activities can affect the ground. Groundwater quality of any specific area or specific source can be assessed using physical, chemical, and biological parameters. The values of these parameters are harmful to human health if they occurred more than its defined limits. Therefore, the suitability of water resources for human consumption has been described in terms of water quality index, which is one of the most effective ways to describe the quality of groundwater.

Saiful, Rohini Nagar, Janki Nagar is a Locality in Solapur North City in Maharashtra State, India. It belongs to Desh or Paschim Maharashtra region. Area of Saiful is about 4.23km.

Dwivedi & Pathak, 2007 studied number of methods to analyse water quality data that vary depending on informational goals, the type of samples, and the size of the sampling area [1]. Horton, 1965 initially, WQI was developed by Horton in United States by selecting 10 most commonly used water quality variables like dissolved oxygen (DO), pH, coliforms, specific conductance, alkalinity and chloride etc. [2]. Ramakrishnaiah, 2009 used water quality index to assess groundwater quality of Tumkur Taluk, Karnataka State. 17 parameters such as pH, electrical conductivity, TDS, total hardness, bicarbonate, carbonate, chloride, sulphate, phosphate, nitrate, fluoride, calcium, magnesium, sodium, potassium, iron and manganese are used to calculate water quality index and water quality is divided in 5 categories [3]. Muthulakshmi, 2013 studied correlation of water quality parameters and determined linear regression models for highly correlated parameters [4]. Chatterjee, 2010 worked on the groundwater quality assessment of Dhanbad district, Jharkhand, India. Groundwater quality assessment is important to ensure sustainable safe use of water. The overall water quality in the Dhanbad coal mining area of India is difficult due to the spatial variability of multiple contaminants and wide range of indicators that could be measured [5]. Machiwal, 2010 focused on a GIS-based assessment and characterization of groundwater quality in a semi-arid hard-rock terrain of Rajasthan, western India using long term and multi-site post-monsoon groundwater quality data. Spatio-temporal variations of water quality parameters in the study area were analyzed by GIS techniques [6].

MATERIALS AND METHODS

Study Area

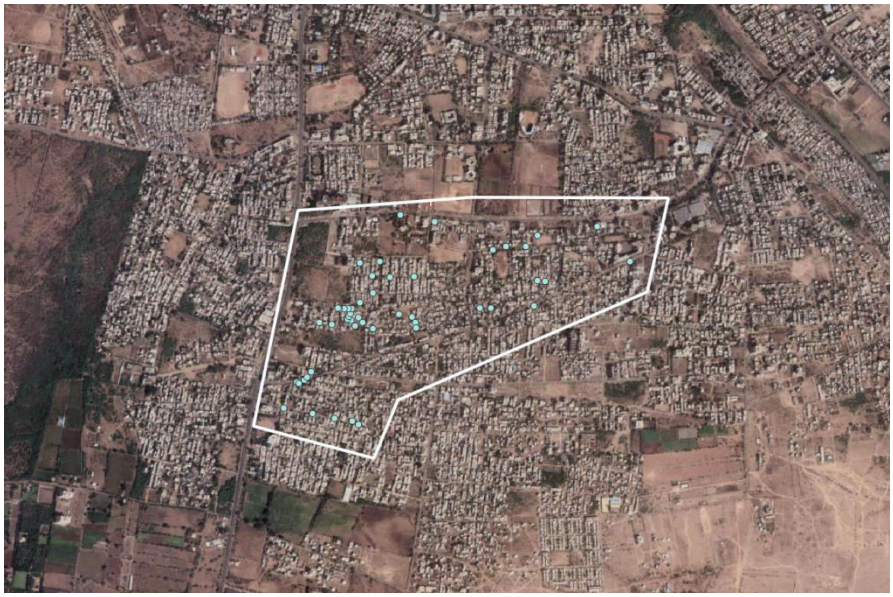

Fig. 1. Study Area

Name of area is Bank colony, Rohini Nagar, Saiful, Solapur (study area shown in fig. no. 1). Purpose of visit: Our main priority was, to collect the water samples from different locations and to get latitude and longitude. Co-ordinates are latitude: 17.6254 and longitude: 75.8981.

Climatic conditions: The climate was sunny with maximum temperature was 41 degree Celsius and min temperature 38 degree Celsius.

Data Collection

We visited to Rohini Nagar, Bank colony, Saiful, Solapur on 2-03-2022 to collect ground water sample from 50 different locations in our study area. It took 1 week to collect all samples.

Then after collecting each sample, we also took latitude and longitude of that location. After acquiring the samples, we started to test those samples in our college laboratory. After that we started identifying chemical properties such as hardness, pH, turbidity, chloride, EC, TDS, dissolved oxygen etc.

After taking the result of these chemical properties we started to plot the points on map with help of latitude and longitude in QGIS software.

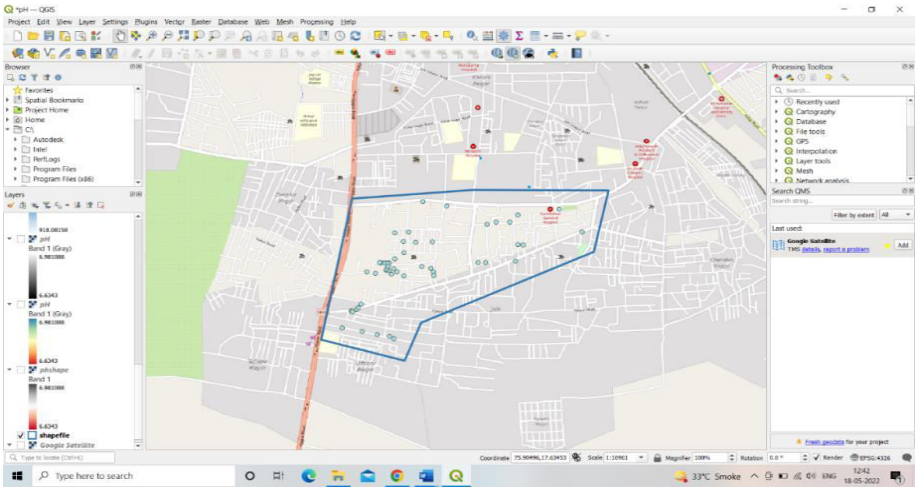

Fig. 2. Sample Points on the Map

The next step was to plot the chemical properties obtained from laboratory.

RESULT AND DISCUSSIONS

TDS in study area

In below fig. 3 shows the total dissolve solid in study area. The permissible limit of TDS in groundwater according to Indian standards is in between 500mg/l to 2000mg/l. The observed values of TDS lie within the permissible limit.

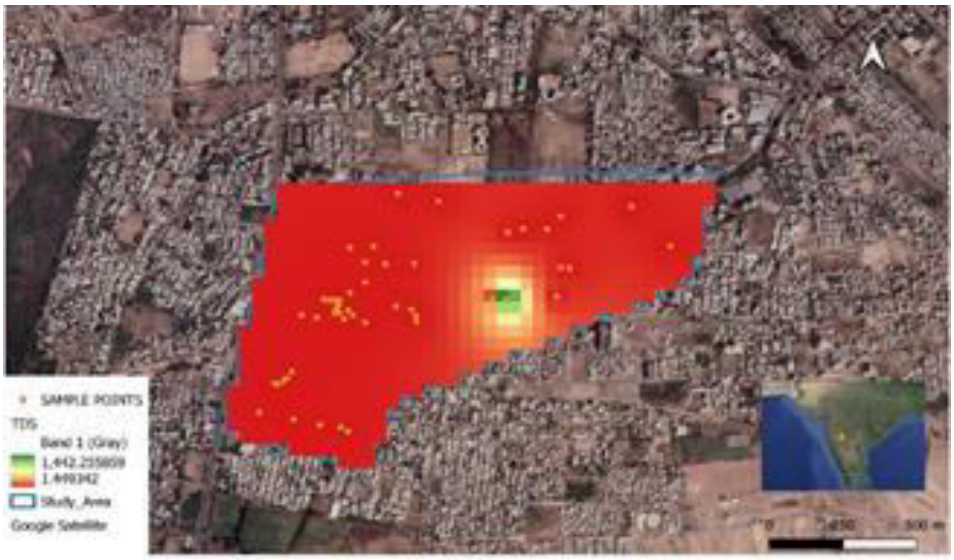

Fig. 3. TDS in Study Area

pH in study area

The below fig. 4 shows pH level in study area the permissible limit for pH in groundwater according to Indian standard is in between 6.5-8.5. The observed pH values lies within the permissible limit.

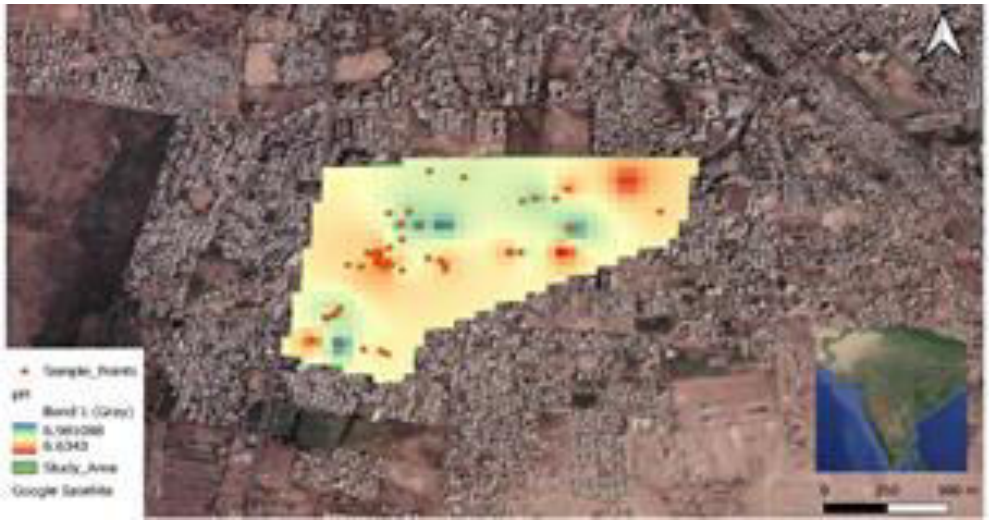

Fig. 4. pH in Study Area

Hardness in study area

The below figure-5 shows hardness in study area. The permissible limit for hardness in groundwater according to Indian standard is about 200mg/l. The observed hardness value does not lie within the permissible range of 200mg/l.

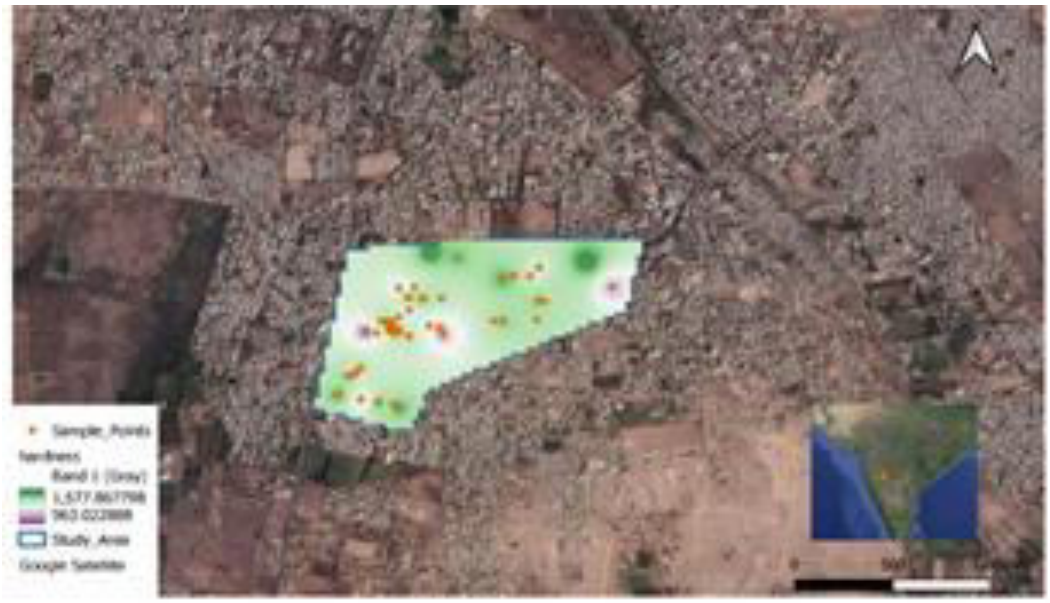

Fig. 5. Hardness in Study Area

Chloride in study area

In below figure-6 shows chloride in study area. The permissible limit for chloride in ground water according to Indian standard is in between 20mg/l to 1000mg/l. The observed chloride value lies within the permissible limit.

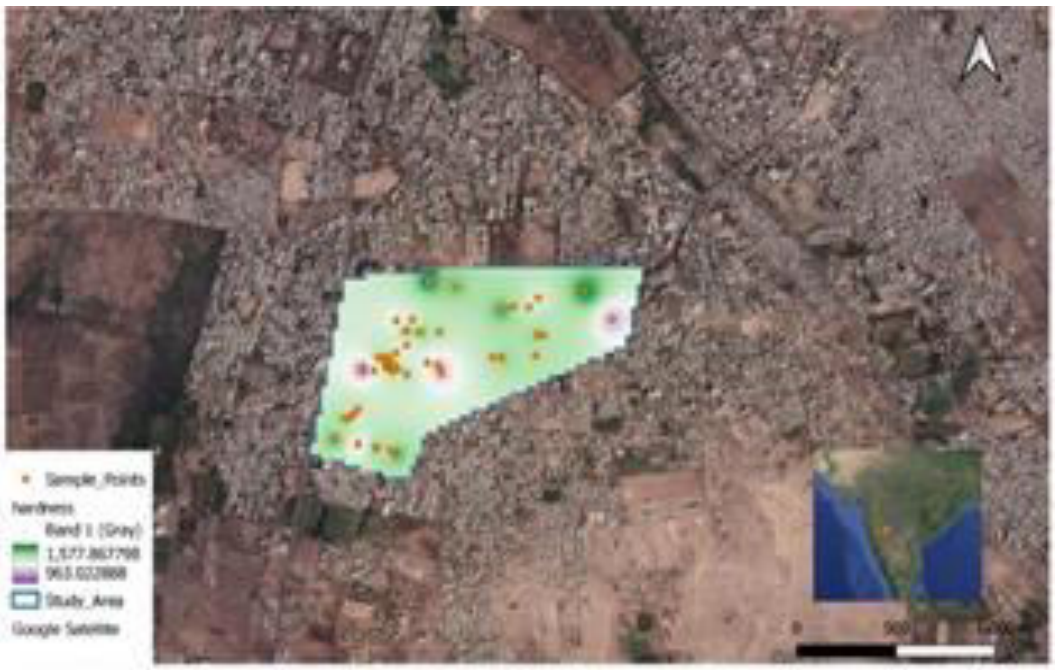

Fig. 6. Hardness in Study Area

TDS in study area

In below figure-7 shows turbidity in study area. The permissible limit for turbidity in ground water according Indian standard is in between 5NTU to 10NTU. The observed turbidity value lies within the permissible limit barring a few locations.

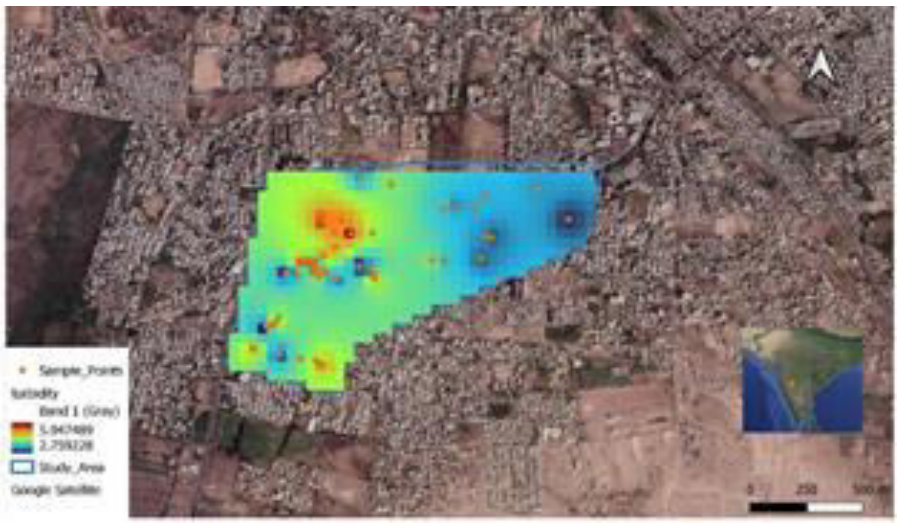

Fig. 7. Hardness in Study Area

TDS in study area

In below figure-8 shows dissolved oxygen in study area. The permissible limit of dissolved oxygen in ground water according to Indian standard is in between 6.5– 8 mg/l. The observed values of DO don't lie within the permissible limit.

Fig. 8. Dissolved Oxygen in Study Area

CONCLUSION

Based upon the tests performed in the lab as well as spatial analysis performed using QGIS it is observed that only pH, chloride, Turbidity and TDS content values of the samples are within the limit in Saiful area. For the other parameters, such as Hardness, and Dissolved oxygen, Turbidity the values were found to be above allowed limits and they can pose problem for the people using them such as:

1. Scaling
2. Excessive soap consumption
3. Calcification of arteries
4. Causes harm to aquatic life
5. Affect water quality
6. Increases growth of bacteria
7. Creates so much plant growth, which suffocates the water system.

REFERENCES

[1] Dwivedi and Pathak(2007) Water quality index for assessment of water samples of different zones in Chandrapur city. Ground Water, 3.

[2] Horton K.W. (1965), Hydrogeochemistry of ground water in Manukan Island, Sabah., The Malaysian Journal of Analytical Science, 1965.

[3] Ramakrishnaiah (2009), "An index number system for rating water quality", J. Water Pollu. Cont. Fed., 37(3). 300-305.

[4] Muthulakshmi (2013), "Status of Groundwater Development and its Impact on Groundwater Quality. Groundwater Availability and Pollution, The Growing Debate over Resource Condition in India. Monograph, Ahmedabad: VIKSAT-Natural Heritage Institute.

[5] Chatterjee, Rima. (2010), "Groundwater quality assessment of Dhanbad district, Jharkhand, India" Bulletin of Engineering Geology and the Environment, 69(1):137-141, DOI:10.1007/s10064-009-0234-x

[6] Deepesh Machiwal, Madan K Jha, Bimal C Mal 2010, "GIS-based assessment and characterization of groundwater quality in a hard-rock hilly terrain of Western India", Environ Monit Assess, Mar;174(1-4):645-63. DOI: 10.1007/s10661-010-1485-5. E-pub. 2010, May, 12.

WASTE HEAT RECOVERY FROM DIESEL ENGINE EXHAUST GAS USING HEAT PIPES FOR EMISSION REDUCTION – A REVIEW

[1]S. Ramasamy, [2]M. Thambidurai and [3]M. Sivasubramanian

[1]Lecturer in Mechanical Engineering (Deputed from Annamalai University), Government Polytechnic College, Melur, Madurai, Tamil Nadu, India

[2]Assistant Professor in Mechanical Engineering, Annamalai University, Chidambaram Tamil Nadu, India

[3]Associate Professor in Automobile Engineering, Kalasalingam Academy of Research and Education, Krishnankoil, Tamil Nadu, India

ABSTRACT

With an increasing number of vital outstanding problems regarding rapid economic development and the gradually serious environmental pollution, the waste heat recovery methods have received notable attention. The total heat energy from the fuel supplied to the engine, approximately conversion of useful power of engine from 30 to 40 % but the remaining heat is wasted to the environment through exhaust and cooling systems results serious atmospheric pollution. It is essential to recover the waste heat and convert it into useful work. In general, heat exchangers (HEXs) are used to capture unused heat energy from engine exhaust. Along this connection, various types of heat exchangers are designed and fabricated for recovering unused heat from IC engine exhausts. Among that, heat pipe heat exchanger has an important application in reducing primary energy consumption and reducing carbon-dioxide concentration due to high heat transfer capacity. It is an extremely effective device for absorbing heat from exhaust gases in the region of evaporator and transfer the heat to the region of condenser where the vapours get condensed and release heat to the coolant. This review reflects the vacancy and possibility of unused heat from the Diesel Engine, various recovery techniques for unused heat and also describes the heat energy losses from exhaust gas of a Diesel Engine. Also, this review helps to know the ultimate improvements and techniques on waste heat recovery from Diesel engine exhaust.

Keywords: Diesel Engine, Waste heat recovery, Heat exchanger, Heat Pipe, Exhaust Gas, Carbon- dioxide

1. INTRODUCTION

Awareness towards Internal Combustion Engines (ICEs) is increased due to changes in the fuel costs and the presence of stringent emission norms over the world. Hence, growing interest is generated towards expansion of useful applications heat energy and minimizing the volume of harmful emissions from the engines [1]. Although, the energy shortage and atmospheric pollutions are being identified one among largest issues in the

world of this century. In this aspect, identifying the optimum result to develop the internal combustion engine performance and also reducing harmful emissions from engines is the major role of scientists for continuous improvement [2]. The various methods are available to recover waste heat energy from engines are such that i) engine fabrication based on six stroke concept ii) Exhaust Gas Recirculation iii) automotive air conditioning iv) gas turbine cycle v) vapour absorption refrigeration system vi) Thermo Electric Generator vii) Turbo compounding viii) Organic Rankine Cycle [3][4]. In accordance with various advanced techniques, Internal Combustion (IC) engines equipped with waste heat recovery system has been proved best technique for lowering consumption of fuel and harmful emissions like CO_2 and increase engine power output [5]. By comparing traditional system of waste heat recovery from exhaust gases through turbocharger method produced fuel saving of 15 % and power increases specifically but Rankin cycle method of waste heat recovery produced of 20% fuel-saving and same power increases. Various research suggests that over 20% improvement in fuel economy can be achieved from Waste Heat Recovery [6]. Thus, 4 – 5 % of efficiency improvement is happened by waste heat recovery system, nowadays it is an emerging field [3]. Heat energy was extracted at an average of 10 - 15% and also at maximum load condition, possible heat extraction is nearly about 4 kW [7]. Out of various heat recovery methods, exhaust heat recovery using a heat exchanger plays a vital role creates dropping pressure and also effects performance of the engine, so its design is of major importance [3]. This review aims to focus various methods of waste heat recovery from engines by using heat exchangers and scope of future work also was presented. Further, the study focused on the exhaust waste heat energy in the Standby CI engine and operations of waste heat recovery system using heat pipe heat exchanger under different operating regimes of the engines.

2. HEAT RECOVERY FROM EXHAUST GASES

The exit temperature of heavy-duty diesel engine ranges from 500 to 750°C due to the existence of 35% waste heat in the exhaust gas [8]. The exhaust gas from the diesel engine had a possible more heat recovery capacity than the cold fluid because of its high energy and higher temperature [9]. Waste heat recovery technique had an impact on the performance nature of the process and indirect benefits like equipment size, supplementary air consumption, a reduction in pollution. Instead of wasting heat from exhaust gases into the atmosphere, the waste heat may be utilized by some other process or a portion of waste heat that may be wasted can be reused in the same process. The most important waste heat recovery methods are direct and indirect which are discussed below. Mhia. Md. Zaglul Shahadat *et al.* tested the effect of Diesel NO_x reduction by preheating inlet air using exhaust gas. They found that an elevated inlet air temperature after warming up the engine, carbon monoxide (CO), oxides of nitrogen and engine

noise decreases for medium load conditions using the newly designed system. This may occur due to a significant reduction in ignition delay and better combustion by the presence of higher inlet air temperature [10]. Dhruv Raj Karana *et al.* did the experimentation of new internal twisted ribs in automobile exhaust heat exchanger for waste heat recovery applications to investigate thermohydraulic performance. They found that heat transfer rate was improved by 164 % of maximum under the specifications of pitch ratio – 8, twist ratio – 4 and angle of attack - 60°. And also they inferred, the improvement in waster heat recovery in automobile was possible through the efficient heat transfer with the twisted rib.[11].

2.1 Waste Heat Recovery by Organic Rankine Cycle

A particular field of energy generation systems at low temperature uses some organic fluids except water, called as Organic Rankine Cycle (ORC). It is a one type of indirect waste heat recovery system i.e. generating power through mechanical work. Organic rankine cycle is treated as the most suitable cycles for low grade temperature resources such as exhaust of the engine. The steam is generated by using the stem expander in a secondary circuit with help of thermal energy of exhaust gases and also produces excess power. The working of ORC is presented in the Fig.1. It consists of boiler, expander, condenser, pump, and working fluid. Thermoelectric materials provide higher efficiency when residual thermal energy sources are used. Exhaust Heat Recovery system (EHR) based on rankine cycle, to produce steam from the exhaust heat a steam generator is used, then the steam is expanded in a steam turbine to generate more power [12]. Chen *et al.* conducted the experiment by comparing thirty five working fluid natures and concluded that the working fluid depends on the operating condition and does not have higher efficiency at all working conditions [13]. Saiful Bari *et al.* did the investigation on diesel engine waste heat recovery with the help of shell and tube heat exchanger and an organic rankine cycle. The experimental work was conducted to construct and design heat exchangers which operate optimally for the particular heat recovery exhaust using commercial CFD software named as ANSYS CFX 14.0. Finally, they found the maximum excess power achieved with heat exchangers by use of the exhaust heat recovery system using ORC[14].

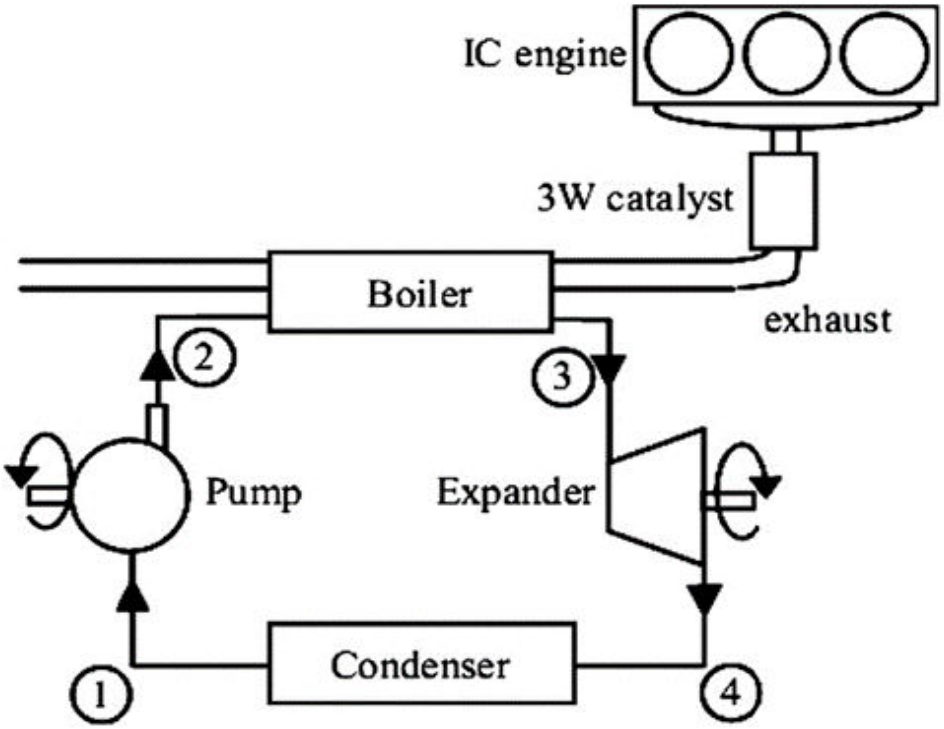

Fig. 1: Schematic diagram of Organic Rankine Cycle working

Pooja B. Surwas *et al.* conducted the experimentation in the exhaust of a diesel engine using shell and tube heat exchanger. They reveal that for exhaust recovery bottoming Rankine cycle is a better variation, which will minimize the specific fuel consumption and also thus reduces toxic emissions and greenhouse gases with respect to overall power produced per kW. [15].

2.2 Exhaust gas recirculation (EGR)

EGR is an effective technology to minimize the Nitric oxide levels. Hot EGR or cold EGR can be used in the both petrol and diesel engines. The EGR gases are cooled down to the low temperature by using a heat exchanger to recirculate a more kg of gases into the engine [16]. G.H. Abd-Alla, reviewed exhaust gas recirculation (EGR) potential to minimize the exhaust emissions, particularly nitrogen oxide emissions. He concluded that, the impact of addition of exhaust gas to the inlet air flow rate of the diesel engine through recirculation helps to replace some of the inlet fresh air which will reduce NO_X emissions in the exhaust and also lowers the air fuel ratio. [17]. P. Muthusamy *et al.* investigated a passenger's car cabin heating using waste heat recovery method with help of matrix heat exchanger. The results indicated that heat transfer rate of heat exchanger will increase with the rise of gas temperature. And also they found that exhaust gas pressure drop is little by implementation of matrix heat exchanger [18].

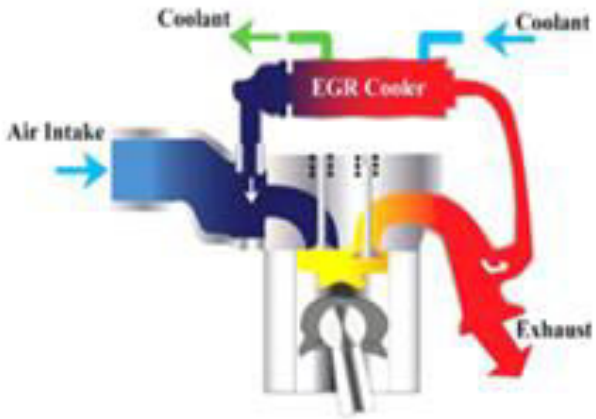

Fig.2 Operation of Exhaust Gas Recirculation System

The working principle of the exhaust gas recirculation system is presented in the Fig.2. EGR is a successful methodology for nitrogen oxide reduction. The exhaust gases broadly contain nitrogen oxides, carbon dioxide, etc. The exhaust emissions are considerably affected by reduction in the air fuel ratio with help of recirculation system. The specific heat of the intake mixture is increases due to mixing of exhaust gases with intake fresh air and also reduced flame temperature [19].

2.3 Waste Heat Recovery Heat Exchangers

The aim of heat recovery technique is used to minimize the consumption of energy and maximize the consumed energy usage. Based on the above concept, researchers tried to enhance the usage of energy either by using the dissipated heat gain for same application or other applications. Heat exchangers (HEXs) are devices that are used for efficient transfer of heat from one medium to another medium and also used for recovering the heat from engines. A typical heat exchanger is shown below in Fig.3.

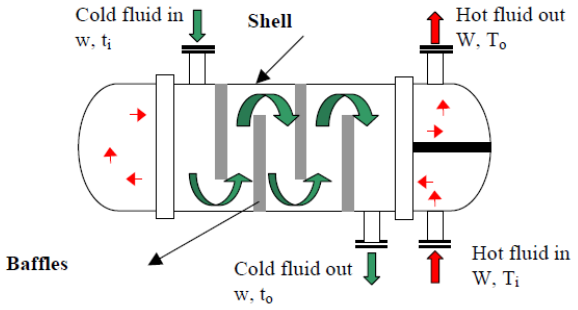

Fig. 3 Working of Shell and Tube Heat Exchanger

The shell-and-tube heat exchanger (STHE) is made up of mild steel tubes. The STHE consists of: shell, shell cover, tubes, tube-sheets, nozzles, channel, channel cover, and baffles. The outer face of the STHE shell is tightly covered insulating material like glass wool to avoid loss of heat to the atmosphere. The expelled gases of the Diesel engine

are passed through the annulus side. The pumping of water heat exchanger tube is possible through water pump. Selection of a suitable heat exchanger design is based on the limitations of each model which should be considered initially. The production cost is also the preliminary limitation, and consideration of other aspects like temperature ranges of temperature, limits of pressure limits of thermal performance, pressure drop, flow capacity of fluid, the cleanliness, maintenance, materials, etc. [16]. The major objective of the present study is to concentrate on review of different heat exchangers types which are tested in heat recovery of the diesel engine exhaust. Fortunately, a few related studies are developed in this field, so research gap was identified in this area. The following figure (Fig.4) shows the feasible technologies which are used for heat energy recovery from exhaust gas [20].

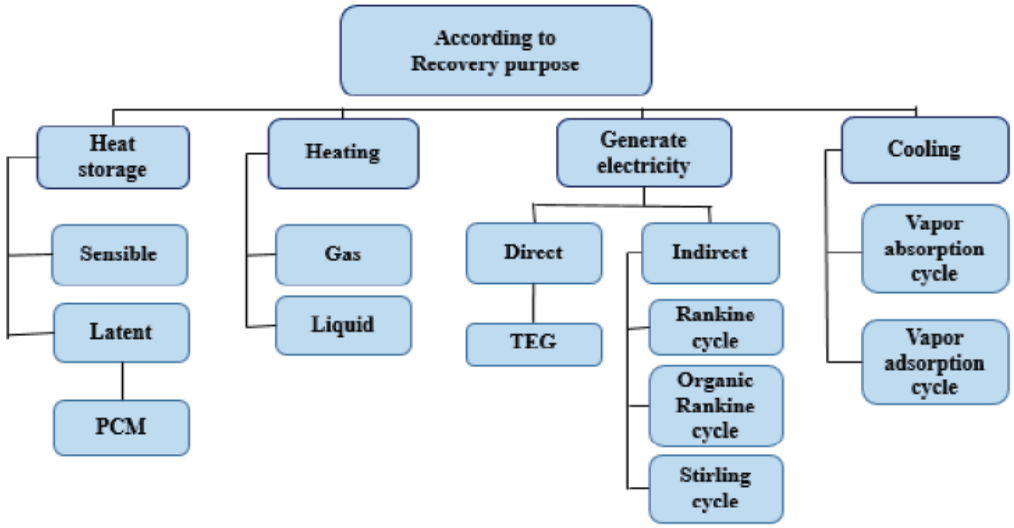

Fig.4 Heat Recovery Technologies [20]

Tanya Wang et.al, investigated exhaust energy recovery from a light-duty SI engine. Exhaust Energy Recovery system is integrated with light duty petrol engine and water is treated as the working fluid, the recovered exhaust energy efficiency in the range from 5% to 21% under different engine operating conditions was achieved [21].

M. Hatam *et al.* studied the comparative analysis heat exchangers types and their effect on exergy and performance analysis of Diesel Engine. It concludes that Optimized HEX configuration gives the improved outputs based on recovered exergy and performance of engine [22]. Rajesh Ravi *et al.* conducted the study on effective utilization of waste heat from diesel engine exhaust through computational and experimental methods by using heat exchanger with a protracted fin. The results concluded that if fin number is increased along its height, then the rate of heat transfer got increased and also further improved heat recovery and enhanced useful thermal efficiency from 32 % to 40 %. To

ensure surrounding safety and reduction in cost, the water-ethanol mixture in internal combustion engines is used for waste heat recovery. This study also resulted that the outlet temperature of working fluid, rate of transfer, effectiveness as well as overall useful thermal efficiency were increased if comparing along with conventional heat exchangers without fins. [23]. Rajesh Ravi *et al.* designed and developed a Contemporary design of Protracted-Finned Counter Flow Heat Exchanger (PFCHE) and tested its impact on exhaust emissions. The experimental results concluded that if an increase in the length and number of fins results in improved rate of heat transfer, the effectiveness of the heat exchanger and the useful thermal efficiency [24]. Vijay V. S *et al.* did the design and construction of a heat exchanger for waste heat recovery of a diesel engine exhaust. From the results, it is understood that a heat exchanger of counter flow type is more efficient than a heat exchanger of parallel flow type [25]. R. Rajesh *et al.* conducted the experiment in a single cylinder compression ignition engine for exhaust heat recovery using heat different models of heat exchanger design. From the experimental results, they found that heat energy of about 40% was wasted in the diesel engine exhaust. The optimized heat exchanger proved that additional heat energy was regained from the engine exhaust [26]. Kyungwook Choi *et al.* investigated gasoline engine performance with help of shell and fin type heat exchangers in the waste heat recovery system. Thus the investigation reveals that Rankine cycle system improves the thermal efficiency and also produces adhere impact on performance of the engine due to increment in back pressure[27]. M. Hatami *et al.*, reviewed diesel exhaust waste heat recovery using various types of heat exchanger designs. This review reports that in most heat exchange technologies, heat exchangers have a vital role to transfer based on the fact drop in pressure increases rate of heat transfer [3].

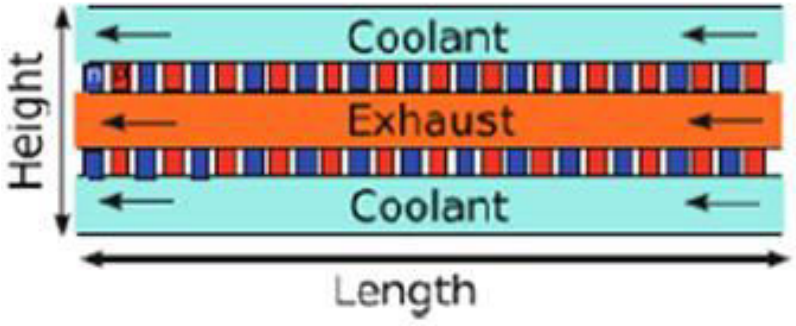

Fig.5 Cross-section of Duct type Heat Exchanger

The cross-section of duct type heat exchanger is shown in Fig.5. Here, the heat transfer takes place between coolants and exhaust gases through parallel or counter flow modes. The performance of this type of heat exchanger depends upon various factors like mode of flow, heat exchanger geometry, temperature of exhaust gas, coolant temperature,

exhaust gas flow rate and coolant, etc. D.S. Vidhyasagar *et al.* conducted an experiment on heat recovery for IC engines using shell and tube heat exchangers to do performance analysis. Results showed that shell and tube heat exchanger effectiveness was increased by providing increased contact area inside the heat exchanger between the shell and tube surface [28]. Dipak S. Patil *et al.* studied shell and tube type heat exchangers for waste heat recovery from diesel engine exhaust as a case study. The researchers also studied waste heat recovery effectiveness on performance of the engine by doing the tests on engines with and without heat exchangers. They concluded that the deviation between forecasted and experimental values of outlet temperatures of water and gas are not beyond ±8% and ±15% correspondingly [29].

2.3.1 Heat Pipe Heat Exchanger Heat Recovery

The basic working principle of heat pipes is shown in the below Fig.6. Heat pipes are non-resistant heat transfer instrument that are used for transferring large amount of heat of relatively long distance. These are effective and simple devices, compact in size and light in weight [30]. It is a safeguarded thin tube consisting of a structure of wick which is lined on the inner surface and the quantity of small fluid may be water of saturation state at vacuum pressure. The heat pipe consists of three sections such that one end is having the evaporator section in which absorption of heat and vaporization of fluid happens and similarly the other end is made up of a condenser section in which condensation of the vapour and rejection of heat occurs. The adiabatic section is placed between evaporator and condenser section on which the vapour and the liquid phase fluid flow takes place in opposite direction. The core and the wick are meant for completing cycle without significant heat transfer between surrounding medium and the fluid. To enhance heat transfer area, the evaporative section is installed in the waste heat gases duct that may be finned.[16].

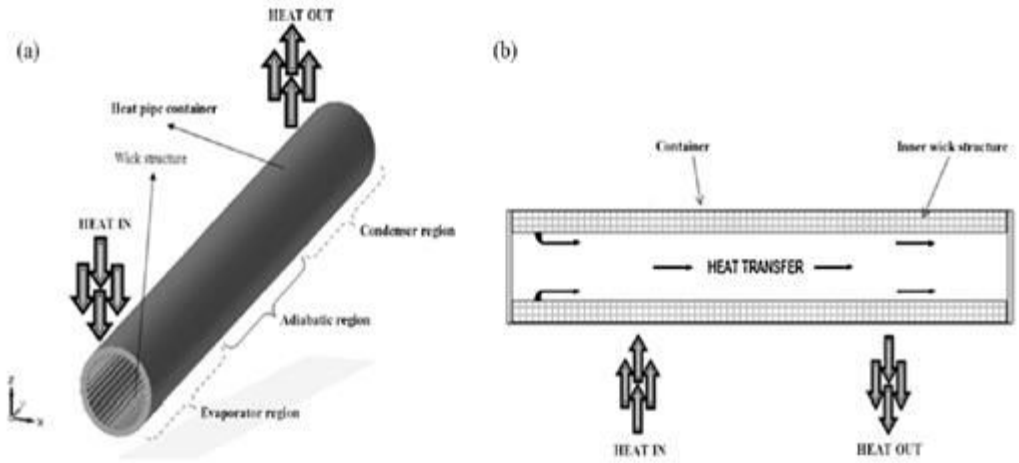

Fig.6 Basic Working Principle of Heat Pipe

The employed pressure and fluid type inside the heat pipe depends largely on the heat pipe working temperature. The heat pipe is designed and fabricated by using water as a heat transfer fluid to release heat at 100°C, the pressure must be maintained at 31 kPa inside the heat pipe like thus boiling pressure of water at same temperature. The working fluid selection is based on the property of surface tension which should be high enough to increase the effect of capillary and is also adaptable with the wick material, chemically stable, readily available, and inexpensive [31]. S. Venkatachalapathy *et al.* using nanofluids, conducted performance analysis of heat pipes of cylindrical cross section. The study reported that an improvement in heat transfer coefficient ratio of condenser and evaporator sections and also the reduction in thermal resistance were obtained. Based on the heat load and angle of inclination of heat pipes, the thermal efficiency is increased and reported that an improvement of 33% is observed for inclination angle of 60° and 120 W input heat loads as compared with the horizontal heat pipe. CuO nanoparticles were deposited and produced a coating of thin coating layer on the surfaces of the wick and evaporator section. Surface wettability improves the heat pipe performance [32]. Hassam Nasarullah Chaudhry *et al.* conducted review studies on heat pipe systems for heat recovery and applications of non-conventional energy. The review accepted that heat pipe system with standard tube provides a biggest range of operating temperatures in accordance with other systems and therefore, provides feasible development and merges into renewable energy systems [33].

Thermosyphons heat pipe: Thermosyphons are one type of heat exchanging method that circulates a substance through free convection. S.A. Shelke *et al.* conducted an experimental investigation on automobile engine exhaust using vertical thermosyphons heat pipe heat exchangers with help of hybrid nanofluid as heat transfer fluid to evaluate heat transfer performance. Heat pipe heat exchanger performance is charged with nanofluid increased with an improvement in source temperature. At condenser section, maximum effectiveness and heat gain was observed for proposed heat pipe heat exchanger design up to 0.18 and 1331 W [34]. The variables which affect heat pipe performance are nanoparticle - shape, material, size, volume concentration, temperature, pH, etc. From the various reviews about nanofluid studies, it is found that solid type nanoparticles colloids (i.e., colloids together and grains have dimensions of 10-40 nm size) are extremely stable which exhibit even after weeks or months under static conditions no significant settling. In addition, thermal-transport properties enhancements of selected nanofluids was more than coarse-grained materials of suspended nature [35]. Vikash Kumar *et al.* conducted the review on IC engine performance analysis with waste heat recovery system with help of a heat pipe and also biodiesel blends by supplying warm air with help of external attachment of exhaust heat

recovery using heat pipes and also compare the results of neat diesel with waste cooking oil biodiesel blends. An increase in useful thermal efficiency, indicated thermal efficiency and also reduced fuel consumption was obtained [36].

Vikram Singh, H Magar *et al.* conducted a performance investigation using nanofluids in waste heat recovery heat pipe heat exchanger by variable source temperatures. 82% of exhaust air heat under perfect condition was recovered in this experiment. 50 to 65% of economic heat recovery rate happened and hence also the enormous saving of energy is possible. And further, they found the heat pipes are reversible in nature and also helpful to cool outdoor air in the summer season. Heat pipe is called as year-round energy saver [37]. Bhavin Shah conducted the experiment on heat pipe heat exchanger waste heat recovery. The author concluded that there is a scope for development in the design and construction of heat pipe heat exchanger to recover the extent of maximum possible amount of heat from urban waste water, surgery rooms in Hospitals, air conditioners, cooling equipment like cooling towers as well as in various fields of thermodynamics [38]

2.4 Thermoelectric Generation

This is one type of direct electric conversion device. It consists doped n- and p-type paired semiconductors which are connected electrically in series and thermally in parallel. If one of the junctions is at a different temperature than the other, the direct current flows in the circuit and also magnitude of current depends upon the two materials specific thermoelectric properties and difference in temperature between the two junctions. Operating temperature range of TEG depends upon the materials which are employed. In case of moderate temperatures like T = 500 to 800°C, the sources of heat are such as exhaust of the vehicles and waste heat of industries [39]. An array of semiconductors is present in the thermoelectric generators if it is placed across a gradient of temperature, it will generate a voltage without releasing any emissions that are typically obtained from consumption of fossil fuels. Amit Md. Estiaque Arefin *et al.* reviewed internal combustion engines waste heat recovery systems. They concluded that the multiple research works should be needed for the betterment of waste heat recovery system and thus to enhance the efficient and effective use of fuel and maximizing environment sustainability.

3. SUMMARY OF THE REVIEW

Ref. No.	Title of the Research	Authors and Year of Publication	Design Parameters	Objective and Outcome of the Research Work
[2]	Car waste heat recovery systems by using thermoelectric generators and heat pipes- a review	B. Orr *et al.*, (2015)	The author had used both technologies such that Thermo Electric Generators and heat pipes	To recover some of the waste heat by using both technologies of TEGs and heat pipe to find an alternate method of enhancing the completed fuel efficiency used in a car. They concluded that both technologies are passive, solid-state, scalable silent and durable. The thermal resistance between the TEG and gases and also pressure losses in the gas stream due to a reduced fin surface area by heat pipes.
[3]	Heat exchangers of different designs for improving recovery of exhaust waste heat of diesel engine – a review	M. Hatami *et al.*, (2014)		From full review of report submitted by the researchers, we concluded that different heat exchangers were designed and used for increasing waste heat recovery of the exhaust. This work reports that in most heat exchange technologies, heat exchangers played a vital role to transfer heat

				in connection that when pressure drop is at the acceptable level heat transfer rate is increased.
[10]	Preheating of inlet air used for reducing Diesel NO_x	Mhia Md. Zaglul Shahadat *et al.*, (2005)	Four stroke diesel engines, Number of cylinder - 1 D x L - 95 x 115 mm Output rated power - 10 kW/2000 rpm CR – 20:1 Cooling type - Water cooling Injection pressure - 14 MPa	To test the impact of air preheating at the inlet by using exhaust gases in combustion of diesel engine and emission analysis with help of pure diesel fuel and diesel kerosene blend. They found that, an elevated inlet air temperature after warming up the engine, carbon monoxide (CO), oxides of nitrogen (NO_x) and engine noises are decreased for medium load condition in the newly designed system. The emissions are reduced due to significant reduction in delay of ignition and almost complete combustion by presence of higher inlet air temperature.
[11]	Heat exchanger for waste heat recovery applications using	Dhruv Raj Karana *et al.*, (2020)	Experiment was conducted for various pressure drops by using twisted ribs on heat exchanger. The various geometric	To investigate thermo hydraulic performance of the automobile exhaust using heat exchanger integrated with twisted ribs. They found that the

	internal twisted ribs to test thermo hydraulic performanc e of a new automobile exhaust		parameters for the experiments study such that pitch ratio – 8, twist ratio – 4, angle of attack - 60°, Reynolds number - 2300 to 25,000.	higher rate of heat transfer was enhanced by 164 % under pitch ratio of 8, twist ratio of 4 and 60° angle of attack. And also, they inferred that the excellent rate of heat transfer with the twisted rib would enhance waste heat recovery in automobiles.
[14]	Diesel engine Waste heat recovery using shell and tube heat exchanger	Saiful Bari *et al.*, (2013)	Number of cylinders: 4 Type of cooling: Water Engine model make: Toyota diesel engine Inside diameter: 102 mm Stroke length: 105 mm CR: 17.6:1 Torque: 217 N m Rated rpm: 2200 rpm Type of Injection: Direct Intake mode: Naturally aspirated	The exhaust waste heat from a diesel engine using two heat exchangers is going to be estimated. Attempts were taken to enhance the full performance by optimizing the design of the heat exchangers in the exhaust heat recovery system. Finally, working fluid pressure and the orientation of heat exchangers had optimized. They concluded that, after development, the excess power is increased from 16% to 24 % by incorporating water as heat transfer fluid. For power output of 50 kW engine, the pressure optimum was found as

				30 bar and the recovered excess power was 10 kW as maximum.
[15]	Diesel engine waste heat recovery exhaust using parallel flow shell and tube heat exchanger	Pooja B. Surwas *et al.*, (2016)	For this study, Rated Power: 3.7 kW Type of cooling: Air cooled No. of cylinders: 1 No. of strokes: 4 Type of fuel used: Diesel Type of loading Device: Eddy current dynamometer Heat exchanger used: Shell and tube Heat transfer fluid: water	To evaluate existing energy of exhaust gas in the diesel engine. Performance characteristics of the heat exchanger are to be studied. They reveal for exhaust recovery bottoming Rankine cycle is a better variation, which will minimize the specific fuel consumption and also thus reduces toxic emissions and greenhouse gases with respect to overall power produced per kW.
[18]	Heating car's passenger cabin with help of waste heat recovery system using matrix heat exchanger	P. Muthusamy *et al.*, (2016)	Engine model: Quadrajet- Make FIAT Engine type: CI Cylinder inside diameter: 1695 mm Stroke length: 3795 mm CR: 17.6:1	To investigate heat transfer of matrix heat exchanger models using different fluids of various types flow characteristic using software package of computational fluid dynamics (CFD). They used polishing material of silicon carbide material to avoid the carbon deposit in the inner flow side passage and also the heat energy wasted from this process is used for heating

				passenger cabin in the car during winter season. Results indicated that heat transferred by the heat exchanger is increased by gas temperature rise. And also they found that, implementation of matrix heat exchanger is minimized the pressure drop of exhaust system.
[22]	Performanc e and exergy analysis of a diesel engine with different exhaust heat exchangers effect - Comparativ e study	M. Hatam *et al.*, Applied Thermal Engineering (2015)	Optimized and non-optimized finned-tube, vortex generator heat exchanger is selected for the study. Investigations are carried at five engine loads (null load, 20 %, 40 % 60 %, 80 % and full load) and four water mass flow rates (20 30, 40, and 50 g/s)	Finding suitable heat exchanger for exhaust energy recovery had minimal impact on the engine performance. The range of obtained exhaust energy efficiency from 5 % to 21% under different engine operating conditions.
[23]	Conducted study on effective utilization of waste heat from diesel engine exhaust through computation al and	Rajesh Ravi *et al.*, Energy (2020)	In this research work, using binary (water-ethanol) mixtures as heat transfer fluid in Double pipe Protracted Finned Counter Flow Heat Exchanger (PFCHE) was designed, analysed, fabricated and experimented.	To investigates recovery capability of exhaust gases from ICEs to receive low quality waste heat energy. From the results, concluded that, the rate of heat transfer is also got increased when the number of fins increased along with its height. It results in enhanced heat

	experimental methods by using heat exchanger with a protracted fin.		Engine type: Diesel engine Type of cooling: naturally-aspirated and water-cooled system Rated power: 3.7 kW Rated speed: 1500 rpm	recovery performance and increased useful thermal efficiency from 32 % to 40 %.
[24]	Designed and developed a Contemporary design of Protracted-Finned Counter Flow Heat Exchanger (PFCHE) and tested its impact on exhaust emissions.	Rajesh Ravi *et al.*, (2018)	Waste heat recovery system using Organic Rankine Cycle (ORC) was investigated. Double-pipe heat exchanger with counter flow and internally–externally protruded fin for diesel engine of exhaust waste heat recovery (WHR) was contemporary designed	By altering geometric parameter of finned heat exchanger was used to find the performance of heat recovery system. The experimental results concluded that if an increase in the length and number of fins results improved rate of heat transfer, the effectiveness of the heat exchanger and the useful thermal efficiency.
[25]	Diesel engine waste heat recovery with help of newly designed and fabricated heat exchanger	Vijay V. S *et al.*, (2016)	Heat exchanger of concentric type, heat exchanger of shell and tube was designed, fabricated for retrieving waste heat of diesel engine of single cylinder and operated at different load conditions and also predicted injection timing of test engine.	Performance of concentric tube heat exchanger in comparison with shell and tube heat exchanger was done with respect to heat recovery potential in CI engines and also effectiveness of heat exchanger also studied. From the results, it is understood that a heat exchanger of counter

				flow type is more efficient than a heat exchanger of parallel flow type.
[26]	Exhaust heat recovery of a single cylinder compression ignition engine using different heat exchanger designs	R. Rajesh *et al.*, (2019)	For waste heat recovery, perforated type heat exchanger design with outer insulation was selected	To retrieve and ensure maximum possible heat transfer from exhaust gas of Internal Combustion Engine by using a heat exchanger. They found that from the experimental work, 40% of heat energy was wasted in the exhaust of the diesel engine.
[27]	Gasoline engine performance analysis by using the effect of the heat exchanger in the waste heat recovery system	Kyungwook Choi *et al.*, (2014)	Shell and fin tube-type heat exchangers heat exchangers were selected for this study. An experimental study was conducted by varying the back pressure with help of valve closing rate (i.e., full open, quarter, half and ¾ of close) by using back-pressure regulator	To harness the waste heat from the exhaust pipeline, a rankine cycle was developed and installed in a test engine to investigate back pressure impact on the engine performance. The investigation reveals that rankine cycle system which improves the thermal efficiency and also produce adhere impact in the engine performance due to increase in the back pressure.
[28]	Using shell and tube heat	D.S. Vidhyasaga-r *et al.*,	Tested engine with heat exchanger of shell and tube type	To calculate exhaust heat energy obtained from exhaust gas of the

	exchanger to conduct performance analysis and experimental analysis on heat recovery of IC engines exhaust	(2017)	through counter and parallel flow modes.	test engine by using shell and tube heat exchanger and also evaluating characteristics of performance and heat exchanger and engine effectiveness. The results showed that shell and tube heat exchanger effectiveness was increased by incorporating inside the heat exchanger larger area of contact between the shell and tube surface.
[29]	Case study of waste heat recovery from diesel engine exhaust using shell and tube type heat exchanger	Dipak S. Patil *et al.*, (2019)	In this work, heat exchanger of shell and tube type had designed, fabricated and tested for its performance.	To carry out design process of the heat exchanger by using simulation process with help of design program developed. The effect of waste heat recovery in the performance of engine had been studied by doing tests on engine with and without heat exchanger. They concluded that the deviation between forecasted and experimental values of outlet temperatures of water and gas are not beyond ±8% and ±15% correspondingly.

[32]	An experimental study of performance analysis of cylindrical heat pipe using nanofluids	Venkatachal-apathy *et al.*, (2015)	For this experimental work, Design parameters are Tube material: copper tubes of cylindrical cross section Wick size: 100 mesh/inches copper screen wick Type of working fluid: DI water Volume of saturated working fluid: 7.3 ml of fluid No. of heat pipes: 4 heat pipes with DI water Nano fluid: CuO nanofluids Heater: Ceramic of 100 mm length Mass flow rate of cooling water: Constant at 20 l/hr at 25°C inlet temperature	Using water-based Copper oxide Nano fluids to test cylindrical copper mesh wick heat pipe thermal performance. Study reported that reduced thermal resistance ratio, improvement of condenser and evaporator heat transfer coefficient were obtained. Based on change in heat load and heat pipe inclination, its thermal efficiency is increased to 33% was observed for heat loads of 120 W at an inclination angle of 60°compared with respect to horizontal heat pipes. CuO nanoparticles were deposited and produced a coating of thin coating layer on the surfaces of the wick and evaporator section. Surface wettability improves the heat pipe performance.
[33]	Heat pipe systems for heat recovery and non-conventiona	Hassam Nasarullah Chaudhry *et al.*, (2012)	Heat transfer fluids are compared with respect to its efficiency of heat pipes along the span of temperatures.	For heat recovery and non-conventional energy applications, recent heat pipe systems are tested and evaluated. The review accepted

	l energy applications – a review			that standard tubular heat pipe systems provide more range of operating temperature by comparison to other heat transfer systems and therefore it is feasible for development and merging of non-conventional energy systems.
[34]	Automobile engine heat transfer performanc e with help of a vertical thermosyph ons heat pipe heat exchanger by using hybrid based nanofluids	S. A. Shelke *et al.*, (2016)	Manufacturer: Briggs & Stratton Type: 4 stroke SI engine Cylinder ID: 79.375 mm Stroke length: 61.9252 mm C.R: 8:1 Volumetric Capacity: 305 CC RPM: 3600 BHP: @3600 7.46KW Cooling system: Air cooled	With help of recovered heat from engine exhaust, thermsyphons heat pipe behaviour was studied for fresh inlet air heating. The heat pipe performance is increased due to the presence of heat exchanger charged with nanofluid and also increase in source temperature. Proposed heat pipe heat exchanger, produced heat gain and maximum effectiveness at condenser section.
[36]	IC engine performanc e analysis by waste heat recovery heat pipes and	Vikash Kumar *et al.*, (2016)	Make: Kirloskar Engine type (model): Four Stroke, four valve Fuel Used: Biodiesel Blended Fuel Number of Cylinder: One	To conduct performance test on four stroke single cylinder diesel engine by supplying warm air with help of external attachment of exhaust heat recovery using heat pipes and also compares

	biodiesel blends: A review		Rated Power Output (kW): 3.7 Cylinder inside diameter [mm]: 87.8 Stroke length [mm]: 110 CR: 18.5:1	the results of neat diesel with bio diesel blends. Here wasted cooking oil is used to prepare bio diesel blends. Increase in useful thermal efficiency, indicated thermal efficiency and reduced fuel consumption are obtained from the experiment.
[37]	Performanc e analysis using nanofluids in waste heat recovery heat pipe heat exchanger by variable source temperature s.	Vikramsinh H Magar *et al.*, (2015)		With help of nanofluid heat exchanger of thermo syphon, to determine the performance characteristics air heat recovery system. They reveal that performance of heat exchanger coupled with heat pipes is increased by changing nanofluid instead of conventional fluid in heat pipes.
[38]	Heat pipe heat exchanger for waste heat recovery	Bhavin Shah (2017)		The aim of this research is focused on waste heat recovery by using heat pipe heat exchanger in various applications. Author concluded that there is a scope for development in the heat pipe heat exchanger design to recover maximum possible amount of heat from the

				urban waste water, surgery rooms in hospitals, air conditioners, cooling equipment's like cooling towers as well as in various fields in the field of thermodynamics.
[39]	A review of waste heat recovery systems for IC engines:	A. E. Arefin *et al.*, (2017)		Enhancing fuel effective and maximizing surrounding sustainability concluded that the research should be carried out for the improvement of waste heat recovery systems.

4. CONCLUSIONS

- Waste heat recovery from exhaust gases of Internal Combustion Engine review studies; we have concluded following suggestions and future scope of research work in particular area.
- Waste heat loss due to inefficiencies of thermodynamic limitations on processes and equipment. Waste heat recovery system evolution being a constructive technique for enhancing overall thermal efficiency and retrieving the appropriate amount of waste heat from the engines.
- If Non-conventional energy resources are not available, heat recovery is the most favourable solution mainly in those areas. The heat from cooling water and exhaust gas can be utilized to enhance of internal combustion engines thermal efficiency. Due to the above factor, the field of heat recovery had shown an enormous improvement during recent years.
- Thermodynamic efficiency of the operating cycle or by reducing mechanical losses can be utilized for higher diesel engine efficiency. Rankine cycle based thermal system is expressed as the solution for low cost with high total system efficiency, compared to other systems. Heat pipe heat exchangers are used for a broad range of applications for the reduction of energy which is a leading requirement of the growing population. Heat pipe thermal performance is being improved by conventional working fluid with high heat transport properties.

- Heat exchanger coupled with heat pipes are used to safeguard the environment contrasted to other heating systems based on oil, electricity, or coal-like fossil fuels. The use of fins is a more appropriate method due to the smaller drop of pressure and more rate of heat transfer.
- Exhaust heat recovery from the engine depends upon various parameters like exhaust gas temperature, inlet air temperature, air velocity, working pressure in the heat exchanger and engine, etc. Heat pipe heat exchangers are the better option for waste recovery from stand-alone internal combustion engines, which are used inlet air preheating in the inlet of the engine. The preheated air improves useful thermal efficiency and reduces consumption of the fuel.
- Further research work is possible by the changing design and operating conditions of engines and heat exchangers. Also, waste heat recovery on internal combustion engines may be carried through experimental and computational methods on using different binary mixtures as heat recovery heat transfer fluids. The various research gap is identified in case of PCM as heat storage source, vortex generators, nanofluids, etc., at different geometrical and operating conditions for improving rate of heat transfer.
- Waste heat energy scope can be intensified to do the research work on other applications like generating electricity, cabin heating, drying industries, refrigeration, etc.

REFERENCES

[1] D. Jung, J. Yong, H. Choi, H. Song, and K. Min, "Analysis of engine temperature and energy flow in diesel engine using engine thermal management," J. Mech. Sci. Technol., vol. 27, no. 2, pp. 583–592, 2013, doi: 10.1007/s12206-012-1235-4.

[2] B. Orr, A. Akbarzadeh, M. Mochizuki, and R. Singh, "A review of car waste heat recovery systems utilising thermoelectric generators and heat pipes," Appl. Therm. Eng., vol. 101, pp. 490–495, 2016, doi: 10.1016/j.applthermaleng.2015.10.081.

[3] M. Hatami and D. D. Ganji, "A review of different heat exchangers designs for increasing the diesel exhaust waste heat recovery," Renew. Sustain. Energy Rev., vol. 37, pp. 168–181, 2014, doi: 10.1016/j.rser.2014.05.004.

[4] R. Saidur, M. Rezaei, W. K. Muzammil, M. H. Hassan, S. Paria, and M. Hasanuzzaman, "Technologies to recover exhaust heat from internal combustion engines," Renew. Sustain. Energy Rev., vol. 16, no. 8, pp. 5649–5659, 2012, doi: 10.1016/j.rser.2012.05.018.

[5] D. A. Arias, T. A. Shedd, and R. K. Jester, "Theoretical analysis of waste heat recovery from an internal combustion engine in a hybrid vehicle," SAE Tech. Pap., no. 724, 2006, doi: 10.4271/2006-01-1605.

[6] R. El Chammas and D. Clodic, "Combined cycle for hybrid vehicles," SAE Tech. Pap., vol. 2005, no. 724, 2005, doi: 10.4271/2005-01-1171.

[7] H. G. Zhang, E. H. Wang, and B. Y. Fan, "Heat transfer analysis of a finned-tube evaporator for engine exhaust heat recovery," ENERGY Convers. Manag., vol. 65, pp. 438–447, 2013, doi: 10.1016/j.enconman.2012.09.017.

[8] T. Wang, Y. Zhang, Z. Peng, and G. Shu, "A review of researches on thermal exhaust heat recovery with Rankine cycle," Renew. Sustain. Energy Rev., vol. 15, no. 6, pp. 2862–2871, 2011, doi: 10.1016/j.rser.2011.03.015.

[9] M. He, X. Zhang, K. Zeng, and K. Gao, "A combined thermodynamic cycle used for waste heat recovery of internal combustion engine," Energy, vol. 36, no. 12, pp. 6821–6829, 2011, doi: 10.1016/j.energy.2011.10.014.

[10] M. Z. Shahadat, N. Nabi, and S. Akhter, "ICME05-TH-31 Diesel NO_X reduction by preheating inlet air," vol. 2005, no. December, pp. 28–30, 2005.

[11] D. R. Karana, "Thermohydraulic performance of a new internal twisted ribs automobile exhaust heat exchanger for waste heat recovery applications," no. May, pp. 1–17, 2020, doi: 10.1002/er.5763.

[12] D. T. Hountalas, C. O. Katsanos, D. A. Kouremenos, and E. D. Rogdakis, "Study of available exhaust gas heat recovery technologies for HD diesel engine applications," Int. J. Altern. Propuls., vol. 1, no. 2–3, pp. 228–249, 2007, doi: 10.1 504/ijap.2007.013019.

[13] H. Chen, D. Y. Goswami, and E. K. Stefanakos, "A review of thermodynamic cycles and working fluids for the conversion of low-grade heat," Renew. Sustain. Energy Rev., vol. 14, no. 9, pp. 3059–3067, 2010, doi: 10.1016/j.rser.2010.07.006.

[14] S. Bari and S. N. Hossain, "Waste heat recovery from a diesel engine using shell and tube heat exchanger," Appl. Therm. Eng., vol. 61, no. 2, pp. 355–363, 2013, doi: 10.1016/j.applthermaleng.2013.08.020.

[15] H. S. Farkade, "Waste heat recovery from the exhaust of a diesel engine using parallel flow shell and tube heat," no. 6, pp. 150–153, 2016.

[16] J. B. Heywood, Internal Combustion Engine Fundamentals, McGraw-Hill Education. 2018.

[17] G. H. Abdollah, "Using Exhaust Gas Recirculation in Internal Combustion Engines: a Review," Energy Convers. Manag., vol. 43, no. X, pp. 1027–1042, 2002.

[18] P. Muthusamy and P. S. Kumar, "Waste heat recovery using matrix heat exchanger from the exhaust of an automobile engine for heating car's passenger cabin," vol. 985, pp. 1132–1137, 2014, doi: 10.4028/www.scientific.net/AMR.984-985.1132.

[19] V. Pradeep and R. P. Sharma, "Use of HOT EGR for NO_x control in a compression ignition engine fuelled with bio-diesel from Jatropha oil," Renew. Energy, vol. 32, no. 7, pp. 1136–1154, 2007, doi: 10.1016/j.renene.2006.04.017.

[20] S. Brückner, S. Liu, L. Miró, M. Radspieler, L. F. Cabeza, and E. Lävemann, "Industrial waste heat recovery technologies: An economic analysis of heat transformation technologies," Appl. Energy, vol. 151, pp. 157–167, 2015, doi: 10.1016/j.apenergy.2015.01.147.

[21] T. Wang, Y. Zhang, J. Zhang, G. Shu, and Z. Peng, "Analysis of recoverable exhaust energy from a light-duty gasoline engine," Appl. Therm. Eng., vol. 53, no. 2, pp. 414–419, 2013, doi: 10.1016/j.applthermaleng.2012.03.025.

[22] M. Hatami, M. D. Boot, and D. D. Ganji, "Comparative study of different exhaust heat exchangers effect on the performance and exergy analysis of a diesel engine," Appl. Therm. Eng., 2015, doi: 10.1016/j.applthermaleng.2015.06.084.

[23] R. Ravi, S. Pachamuthu, and P. Kasinathan, "Computational and experimental investigation on effective utilization of waste heat from diesel engine exhaust using a fi n protracted heat exchanger," Energy, vol. 200, p. 117489, 2020, doi: 10.1016/ j.energy.2020.117489.

[24] P. C. Flow, H. Exchanger, and R. Ravi, "Exhaust Emissions," 2018, doi: 10.3390/ en11102717.

[25] V. S. Vijay, A. B. K, S. Shetty, N. V Gurudatta, and R. Sequeira, "Design and Fabrication of Heat Exchanger for Waste Heat Recovery from Exhaust Gas of Diesel Engine," vol. 6, pp. 131–137, 2016, doi: 10.5923/c.jmea.201601.25.

[26] R. Ravi and P. Senthilkumar, "Design of heat exchanger for exhaust heat recovery of a single cylinder compression ignition engine," no. July 2018, 2019.

[27] K. Choi, K. Kim, and K. Lee, "Effect of the heat exchanger in the waste heat recovery system on a gasoline engine performance," 2014, doi: 10.1177/ 095440 7014547241.

[28] D. S. Vidhyasagar, A. J. I. J. Rakesh, M. Manikandan, S. Sathyanarayanan, and M. Sridharan, "Performance Analysis And Experimental Investigation On Exhaust Gas Heat Recovery For IC Engines Using Shell And Tube Heat Exchanger," no. February, 2020.

[29] D. S. Patil, R. R. Arakerimath, P. V Walke, and R. S. Shelke, "Shell and Tube Type Heat Exchanger for Waste Heat Recovery from Diesel Engine Exhaust-Case Study," vol. 13, no. 1, pp. 1–14, 2019.

[30] M. F. Remeli, L. Kiatbodin, B. Singh, K. Verojporn, A. Date, and A. Akbarzadeh, "Power Generation from Waste Heat Using Heat Pipe and Thermoelectric Generator," Energy Procedia, vol. 75, no. August, pp. 645–650, 2015, doi: 10.1016/j.egypro.2015.07.477.

[31] P. A. Kew, "Heat Pipes 4.1," Elsevier Ltd., pp. 180–239, 2011.

[32] S. Venkatachalapathy, G. Kumaresan, and S. Suresh, "Performance analysis of cylindrical heat pipe using nanofluids - An experimental study," Int. J. Multiph. Flow, vol. 72, pp. 188–197, 2015, doi: 10.1016/j.ijmultiphaseflow.2015.02.006.

[33] H. N. Chaudhry, B. R. Hughes, and S. A. Ghani, "A review of heat pipe systems for heat recovery and renewable energy applications," Renew. Sustain. Energy Rev., vol. 16, no. 4, pp. 2249–2259, 2012, doi: 10.1016/j.rser.2012.01.038.

[34] S. A. Shelke and N. S. Gohel, "Heat Transfer Performance of a Vertical Thermosyphons Heat Pipe Heat Exchanger using Hybrid Nanofluid for Automobile Engine Exhaust Heat," vol. 5, no. 5, pp. 91–94, 2016.

[35] B. Takabi and H. Shokouhmand, "Effects of Al_2O_3-Cu/water hybrid nanofluid on heat transfer and flow characteristics in turbulent regime," Int. J. Mod. Phys. C, vol. 26, no. 4, 2015, doi: 10.1142/S0129183115500473.

[36] V. Kumar, "Performance Analysis of IC Engine with Waste Heat Recovery by Heat Pipe and Biodiesel Blends : A Review," vol. 7, no. 8, pp. 2017–2019, 2018, doi: 10.21275/ART2019902.

[37] V. H. Magar, "Performance investigation of Waste heat recovery heat pipe heat exchanger by using nanofluid with variable source temp," no. 2, pp. 1–6, 2015.

[38] B. Shah, "Waste heat recovery by heat," no. 1, pp. 1128–1131, 2017.

[39] A. E. Arefin, M. H. Masud, M. U. H. Joardder, and M. Mourshed, "Waste heat recovery systems for internal combustion engines : A review Waste heat recovery systems for internal combustion engines : A review," no. February, 2017.

A STUDY TO ASSESS THE PHYSIOLOGICAL AND BIOCHEMICAL EFFECTS OF ONLINE GAMING AMONG CHILDREN AT VEEPAMPATTU

[1]Linda Xavier and [2]Shalini. T

[1]Clinical Instructor, Department of Child Health Nursing, Saveetha College of Nursing, Saveetha Institute of Medical and Technical Science, Thandalam, Chennai, Tamil Nadu, India

[2]B. Sc. (N) IV Year, Saveetha College of Nursing, Saveetha Institute of Medical and Technical Science, Thandalam, Chennai, Tamil Nadu, India.

ABSTRACT

Aim: *the present study aims to assess the physiological and biochemical effects of online gaming among children at Veepampattu.*

Methods And Materials: *A quantitative research design was used for the present study. A total 60 samples were collected using convenience sampling technique. The demographic variable was assessed by structured questionnaire, and pretest, post test of physiological and biochemical effect was assessed by monitoring the blood pressure and blood glucose levels and samples were exposed to cognitive reconstructive therapy followed by that data was gathered and analyzed.*

Results: *The study revealed that there is a significant association between level of physiological effect with selected demographic at the level of $p<0.01$ conclusion: Thus, the present despites that factors associated with level of physiological effect with selected demographic.*

Keywords: online gaming, children, bio chemical.

INTRODUCTION

Video games have transitioned from being a subculture to being a popular entertainment during the past 30 years. Concern over how playing video games negatively impacts kids' and teens' health is growing among parents, educators, and the general public (1). Online gaming is beneficial because it helps keep people, particularly young people, from engaging in risky behaviour like using drugs or joining gangs. People get excited about playing video games online and become more competitive. Additionally, it improves a player's cerebral agility and sharpness (2). The majority of prior research on Internet gaming disorder (IGD) has been on the addiction to traditional desktop-based online gaming. But according to a new study, there are very weak links between the various types of Internet addiction (3). Violent video games can trigger adolescents' observational learning, according to Bandura's social cognitive theory (Bandura). They may not only copy the aggressive behaviour of the role model in this scenario, but their

perceptions of aggression may also shift. As a result, adolescent violence and violent video games may potentially be mediated by normative attitudes about aggression (4). Online games can distract players and interfere with crucial responses to actions taken outside of the game, such as academic performance, health, and social relationships. This can have a huge negative impact on people's lives, especially those of students (5). When a youngster spends a significant amount of time playing video games, especially online games where the goal is to defeat actual people who are skilled at the game rather than merely the computer, their potential in school is not fully realised. This is the displacement hypothesis. Online gaming can have a negative impact on academic performance by taking time away from other educational pursuits like reading and homework (6). The link between adolescent video gaming and hostility affects classroom conduct (7). Children and adolescents today live media-rich lifestyles, according to a number of recent studies: They own 83 to 97 percent of home video game consoles, on which they spend a significant amount of time each day (8). Obesity in children and adolescents has been linked to decreased physical activity, while it is still unclear whether obesity is a cause or a result of inactivity (9). Park *et al.* concentrated on analysing changes in glucose metabolism in a sample made up of 11 IGD and 9 HC. The right middle orbitofrontal gyrus, the left caudate nucleus of the striatum (which is thought to be strongly associated with addiction and reward processing), and the right insula, which is important in the conscious desire to use drugs, all demonstrated a significant increase in resting glucose metabolism among IGD subjects (10). Stress-related glycemia increases in children with diabetes cannot be adequately controlled. Given that wide glycemic swings have been identified as one of the many variables contributing to the development of microvascular damage, it is crucial to determine the extent to which diabetic adolescents should be more conscious of glycemic variations during VG play while selecting an insulin dose (11). Children's cardiovascular reactivity and the onset of hypertension were studied by Frank Treiber and his colleagues at the Medical College of Georgia, as well as by other researchers. They hypothesised that reactivity to stressors in the laboratory may be a long-term marker in the development of hypertension and other cardiac issues (12). The ability of CBT to target and improve maladaptive cognitions that underpin gaming behaviours that cause harm and/or distress sets it apart from other therapies, including drug therapy. CBT may be more able to address comorbid problems in the context of IGD, which is still another advantage (13). The well-known treatment CBT is founded on the idea that thoughts influence moods. Patients learn new coping mechanisms and techniques for avoiding relapse as well as how to monitor their thoughts and recognise those that set off addictive feelings and behaviours (14).

So, the main objective of the study was to assess the physiological and biochemical effects of online gaming among children.

MATERIALS AND METHODS

A quantitative research approach with one group pre test and post test research design was used for the study. Before commencing the data collection, authorized setting permission was obtained from the higher authority of selected community area Veppampattu village, Thiruvallur district and then the study was conducted. A total of 60 mothers and children aged (6 to 17) years residing in Veepampattu village who met the inclusion criteria were selected as study participants by using convenient sampling technique.

The inclusion criteria for the study participants were children (6 to 17 years) who were using smart phone. The exclusion criteria for the study participants were mothers and children who don't understand Tamil and English language. The purpose of study was explained by the investigator to each of the study participants and a written informed consent was obtained from them. The demographic data was collected by structured questionnaire and the pre test and post test level of physiological and biochemical effect by monitoring the blood pressure and blood glucose. Then cognitive reconstructing therapy is given which includes following the given schedule and generalizing and analyzed by using descriptive and inferential statistics.

RESULTS AND DISCUSSION

Section A: Description of the demographic variables of mother and children

In experimental group, maximum of them were in the age group of 32-35 years, and had primary education, about 43.3% of the had primary education, 46.7% had business for father, and 56.7% mother also had own business. In control group maximum of them were in the age group of 32-35 years and 40 and above, and had primary education, about 30.0% of mothers had primary education, 46.7% had daily wages for father, and 56.7% mother also had own business.

Pictorial Representation of Age of the Child

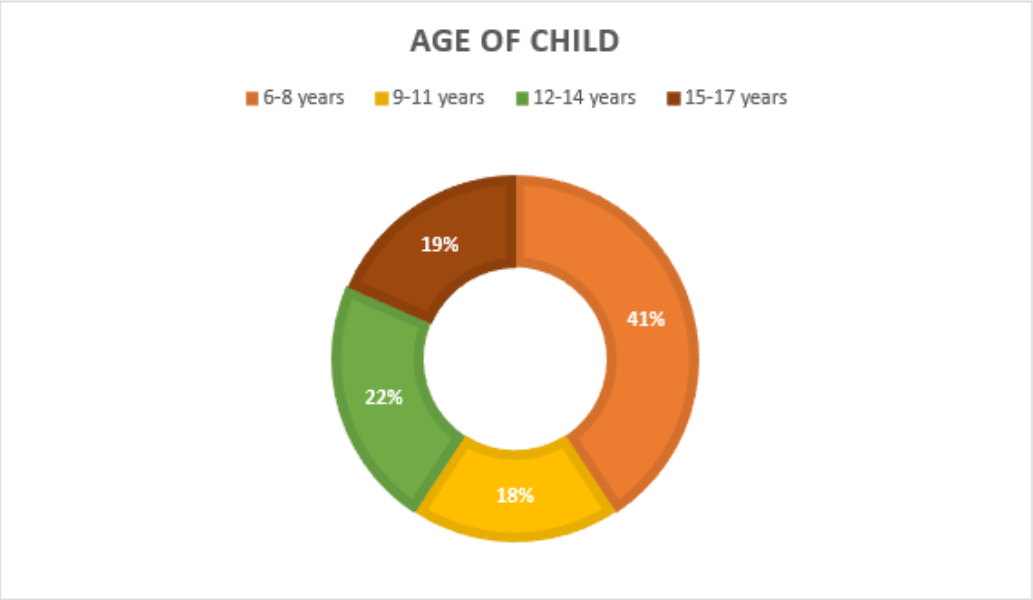

Section B: Assessment of pretest and posttest level of physiological and biochemical effect of online gaming

Table 1: Frequency and percentage distribution of physiological effect of online gaming in the experimental and control group

Group	Physiological effect	Mild		Moderate		Severe	
		No.	%	No.	%	No.	%
Experimental Group	Pre test	0	0	13	43.33	17	56.7
	Post Test	12	40.0	14	46.67	4	13.33
Control Group	Pre test	16	53.33	13	43.33	1	3.33
	Post Test	4	13.33	15	50.0	11	36.7

Table 1 depicts that Among the 60 samples in the study 30 experimental and 30 control group. In experimental group the physiological effect (blood pressure) is assessed in the pre test among 0% had mild effect, 13(43.33%) had moderate effect, 17(56.7%) had severe effect and in post test 12(40.0%) had mild effect, 14(46.67%) had moderate effect,4(13.33%) had severe effect. In the pre test among control group 16(53.33%) had mild effect,13(43.33%) had moderate effect ,1 (3.33%) had severe effect and in post test among 4(13.33%) had mild effect ,15 (50.0%) had moderate effect and 11(36.7%) had severe effect of online game addiction.

DESCRIPTION OF THE DEMOGRAPHIC VARIABLES OF AND CHILDREN

Table 2: Frequency and percentage distribution of demographic variables of in the experimental and control group.

N = 60(30+30)

Demographic Variables	Experimental Group		Control Group	
	No.	%	No.	%
Age				
6-8 years	11	36.7	9	30.0
9-11 years	5	16.7	5	16.7
12-14 years	6	20.0	9	30.0
15-17 years	8	26.6	7	23.3
Sex				
Male	19	63.3	9	30.0
Female	11	36.6	21	70.0
Education				
Primary	13	43.3	13	43.3
Secondary	9	30.0	5	16.7
Higher secondary	8	26.7	12	40.0
Frequency of playing online game				
Every day	4	133	4	13.3
Few times a week	14	46.7	11	36.7
Few times a month	10	33.3	14	46.7
Less often	2	6.7	1	3.3
Hours of playing online game				
2 hours	6	20.0	7	23.3
3 to 4 hours	17	56.7	16	53.3
More than 4 hours	7	23.3	7	23.3

In experimental group, maximum of them were in the age group 6-8 years of 36.7%, 63.3% males, 43.3% were had primary education, 46.7 of them had few times a week and plays 3 to 4 hours a day

In control group, maximum of them were in the age group 6-8 years of 30.0% ,70.0% males, 43.3% were had primary education , 46.7 of them had few times a month and plays 3 to 4 hours a day

Section B: Assessment of pre test and post test level of physiological and biochemical effect of online gaming

Table 3: Frequency and percentage distribution of physiological effect of online gaming in the experimental and control group.

Group	Blood pressure	Mild		Moderate		Severe	
		No.	%	No.	%	No.	%
Experimental Group	Pre test	0	0	13	43.33	17	56.7
	Post Test	12	40.0	14	46.67	4	13.33
Control Group	Pre test	16	53.33	13	43.33	1	3.33
	Post Test	4	13.33	15	50.0	11	36.7

Among experimental group, in pre test maximum of them had severe physiological effect of online gaming, in posttest maximum of them had mild effect of online gaming

Among control group, in pre test maximum of them had mild physiological effect of online gaming, in posttest maximum of them had severe effect of online gaming.

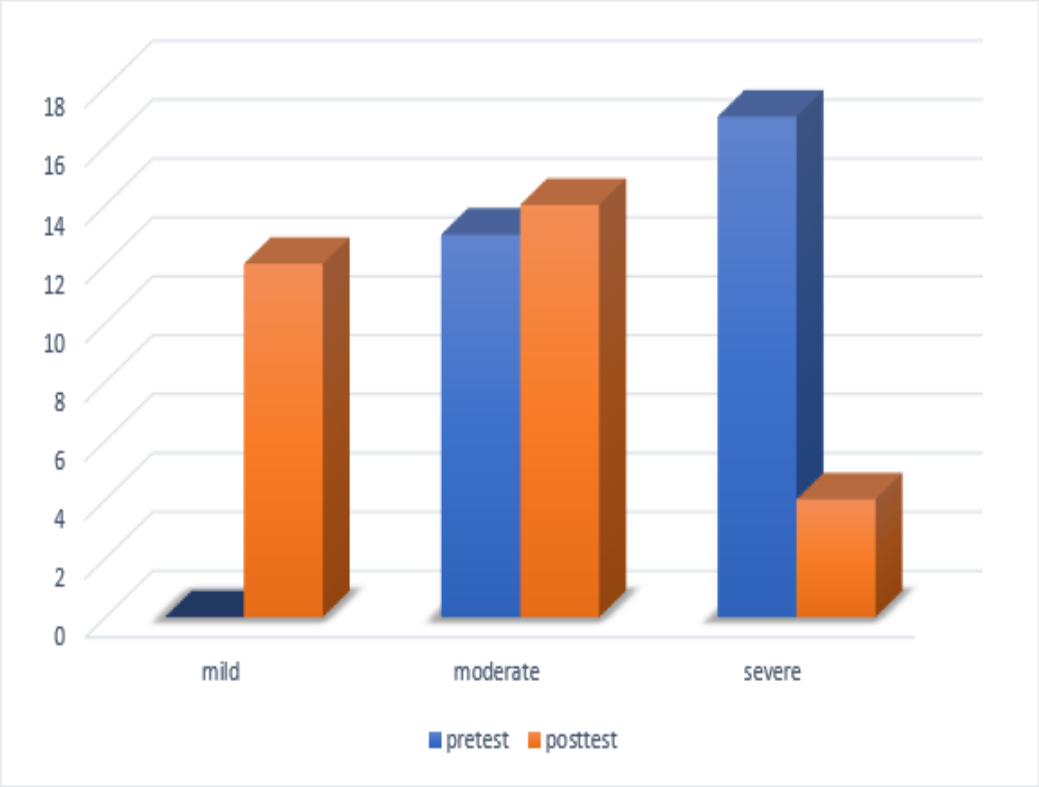

Figure 2: Percentage distribution of pretest and post test level of physiological effect the experimental group

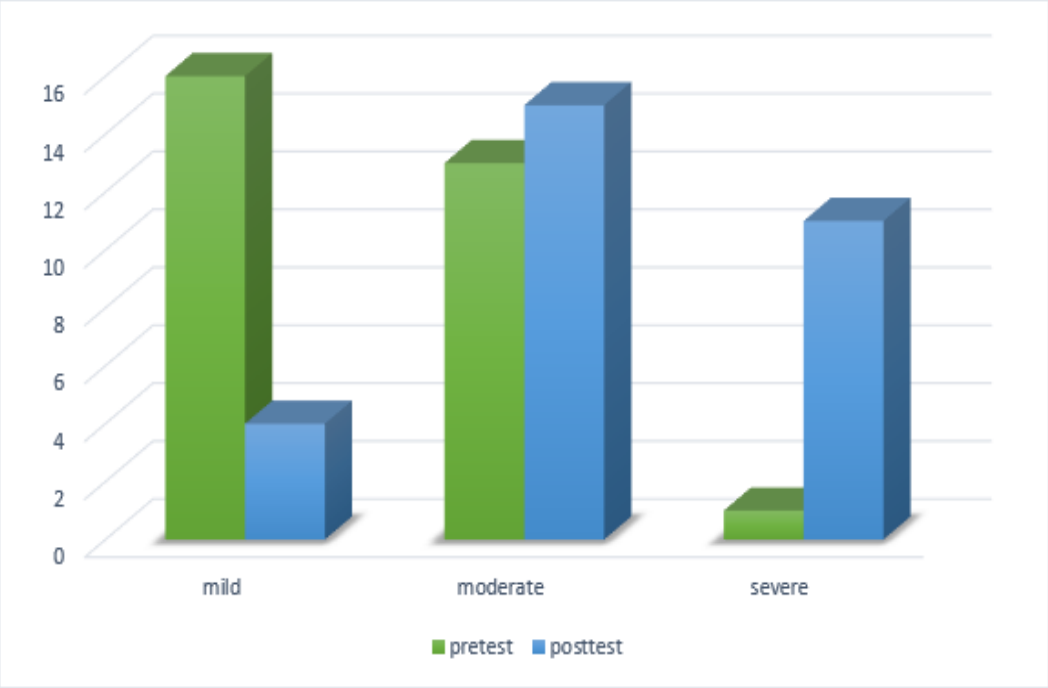

Table 2: Frequency and percentage distribution of biochemical effect of online gaming in the experimental and control group

Group	Blood glucose	Mild		Moderate		Severe	
		No.	%	No.	%	No.	%
Experimental Group	Pre test	1	3.33	16	53.33	13	43.33
	Post Test	12	40.0	13	43.33	5	16.67
Control Group	Pre test	2	6.67	12	40.0	16	53.3
	Post Test	2	6.67	14	46.67	14	46.67

Table 2 depicts that among the 60 samples in the study 30 experimental and 30 control group. In experimental group the biochemical effect (blood glucose) is assessed in the pre test among 1(3.33%) had mild effect, 16(53.33%) had moderate effect, 13(43.33%) had severe effect and in post test 12 (40.0 %) had mild effect and 13(43.33%) had moderate effect ,5(16.67%) had severe effect. Among control group biochemical effect (blood glucose) is assessed in pre test 2(6.67%) had mild effect,12(40.0%) had moderate effect ,16 (53.3%) had severe effect and.

Section C: Comparison of pre test and post test level of physiological effect after cognitive reconstructive therapy

Table 3: Mean a standard deviation of physiological effect of online gaming in the experimental and control group.

Physiological effect	Mean	S. D	Paired 't' test Value
Pre test	1.45	0.84	**t = 8.016**
Post Test	0.65	0.78	**p = 0.0001** **S*****

***p<0.001, S – Significant

The table 3 depicts that the pre test mean score of physiological effect (blood pressure) was 1.45 with standard deviation 0.84. The post test mean score of physiological effect (blood pressure) was 0.65 with standard deviation 0.78. The calculated paired `t` test value of t =8.016 was found that cognitive reconstructive therapy has significant effect on post test compared to pre test physiological effect

Table 4: Mean and standard deviation of biochemical effect of online gaming in the experimental and control group**.**

Blood glucose	Mean	S. D	Paired 't' test Value
Pre test	1.56	0.81	**t = 4.853**
Post Test	0.83	0.69	**p = 0.0001** **S*****

***p<0.001, S – Significant

The table 4 depicts that the pre test mean score of biochemical effect (blood glucose) was 1.56 with standard deviation 0.81. The post test mean score of physiological effect (blood glucose) was 0.83 with standard deviation 0.69. The calculated paired `t` test value of t =4.853 was found that cognitive reconstructive therapy has significant effect on post test compared to pre test biochemical effect.

This clearly states that cognitive reconstructive therapy has significant effect on post test compared to pretest on biochemical effect

Section D: Association of level of physiological effect with selected demographic variables

Table 5: Association of level of physiological effect with selected demographic variables

Demographic Variables	Mild		Moderate		Severe		Chi-Square Value
	No.	%	No.	%	No.	%	
Age							χ^2=7.760
28-31 years	4	13.3	4	13.3	0	0	d.f.=6
32-35 years	5	16.7	3	10.0	2	6.7	p = 0.256
36-39 years	2	6.7	5	16.7	0	0	N. S

Demographic Variables	Mild		Moderate		Severe		Chi-Square Value
	No.	**%**	**No.**	**%**	**No.**	**%**	
40 and above years	1	3.3	2	6.7	2	6.7	
Fathers' education							χ^2=4.062 d.f.=6 p = 0.668 N. S
Primary	5	16.7	4	13.3	2	6.7	
Secondary	2	6.7	2	6.7	1	3.3	
Degree	3	10.0	2	6.7	1	3.3	
Illiterate	2	6.7	6	20.0	0	0	
Mothers' education							χ^2=1.807 d.f.=4 p = 0.771 N. S
Primary	6	20.0	6	20.0	1	3.3	
Secondary	4	13.3	4	13.3	1	3.3	
Degree	-	-	-	-	-	-	
Illiterate	2	6.7	4	13.3	2	6.7	
Fathers' occupation							χ^2=2.278 d.f.=6 p = 0.892 N. S
Professional	1	3.3	3	10.0	0	0	
Business	6	20.0	6	20.0	2	6.7	
Daily wages	4	13.3	4	13.3	2	6.7	
Unemployed	1	3.3	1	3.3	0	0	
Mothers' occupation							**χ^2=10.149 d.f.=4 p = 0.038 S***
House wife	5	16.7	1	3.3	0	0	
Business	7	23.3	9	30.0	4	13.3	
Daily wages	0	0	4	13.3	0	0	
Unemployed	-	-	-	-	-	-	

*p<0.05, S – Significant, N.S – Not Significant

Results of this study show that the demographic variable such as mothers' occupation shows significant association with the physiological effect at $p < 0.05$. Then the study results shows that none of the demographic variables had shown statistically significant association with post test level of biochemical effect.

This study shows that the demographic variable such has mothers' occupation shows significant association post test level of physiological effect at $p < 0.005$.

CONCLUSION

This indicates that cognitive reconstructive therapy is effective and easy method to improve children`s behaviour. This can be applicable for changing the child's attitude and behaviour which reduces the physiological and biochemical changes in the body and reduces the stressors faced by the children.

ACKNOWELEDGEMENTS

Authors would like to appreciate all the study participants for their cooperation to complete the study successfully.

CONFLICTS OF INTEREST

Authors declare no conflicts of interest.

FINANCIAL SUPPORT AND SPONSORSHIP

None

REFERENCES

1. Krarup KB, Krarup HB. The physiological and biochemical effects of gaming: A review. Environ Res. 2020 May; 184:109344. doi: 10.1016/j.envres.2020.109344. e-pub 2020 Mar 4. PMID: 32199319
2. Aswathy, V., Devika, E., & Girish, S. (2019). A Study on Impact of Online Gaming and Its Addiction among Youth with Special Reference to Kerala. International Journal of Management, IT and Engineering, 9(6), 308-316.
3. Wang J-L, Sheng J-R and Wang H-Z (2019) The Association Between Mobile Game Addiction and Depression, Social Anxiety, and Loneliness. Front. Public Health 7:247. doi: 10.3389/fpubh.2019.00247
4. Shao, Rong & Wang, Yunqiang. (2019). The Relation of Violent Video Games to Adolescent Aggression: An Examination of Moderated Mediation Effect. Frontiers in Psychology. doi: 10.3389/fpsyg.2019.00384.
5. Wang, L., & Zhu, S. (2013). Online Game Addiction Among University Students (Dissertation). Retrieved from http://urn.kb.se/resolve?urn=urn:nbn:se:hig:diva-13757
6. Garcia, K., Jarabe, N., & Paragas, J. (2018). Negative Effects of Online Games on Academic Performance. Southeast Asian Journal of Science and Technology, 3(1), 69-72. Retrieved from https://sajst.org/online/index.php/sajst/article/view/40
7. Terry, M., & Malik, A. (2018). Video Gaming as a Factor That Affects Academic Performance in Grade Nine. Online Submission.
8. Peracchia, S., & Curcio, G. (2018). Exposure to video games: effects on sleep and on post-sleep cognitive abilities. A systematic review of experimental evidences. Sleep Science, 11(4), 302.
9. Segal, K. R., & Dietz, W. H. (1991). Physiologic responses to playing a video game. American Journal of Diseases of Children, 145(9), 1034-1036.

10. Carpita, B., Muti, D., Nardi, B., Benedetti, F., Cappelli, A., Cremone, I. M., ... & Dell'Osso, L. (2021). Biochemical Correlates of Video Game Use: From Physiology to Pathology. A Narrative Review. Life, 11(8), 775.

11. Phan-Hug, F., Thurneysen, E., Theintz, G., Ruffieux, C., & Grouzmann, E. (2011). Impact of videogame playing on glucose metabolism in children with type 1 diabetes. Pediatric diabetes, 12(8), 713-717.

12. Borusiak, P., Bouikidis, A., Liersch, R., & Russell, J. B. (2008). Cardiovascular effects in adolescents while they are playing video games: a potential health risk factor? Psychophysiology, 45(2), 327-332.

13. Stevens, M. W., King, D. L., Dorstyn, D., & Delfabbro, P. H. (2019). Cognitive–behavioral therapy for Internet gaming disorder: A systematic review and meta-analysis. Clinical psychology & psychotherapy, 26(2), 191-203.

14. Young, K. S. (2007). Cognitive behavior therapy with Internet addicts: treatment outcomes and implications. Cyberpsychology & behavior, 10(5), 671-679.

COMPARATIVE ANALYSIS OF WATER QUALITY OF HIRAKUD DAM AND MAHANADI RIVER IN THE COMMAND AREA OF HIRAKUD TOWN IN TERMS OF WATER QUALITY INDEX

Pritisha Barik, Rabiranjan Prusty and Trinath Biswal
Department of Chemistry Veer Surendra Sai University of Technology Burla- 768018, India

ABSTRACT

The physico-chemical parameters including electrical conductivity (EC), pH, total hardness (TH), chloride, fluoride, dissolve oxygen, turbidity, and sulphate of the water samples of Hirakud dam and Mahanadi River in the command area of Hirakud dam were analysed. The analysed data were then compared with standard value BIS:10500. From the analysed data of Mahanadi River, it was found that pH ranges from 6.2-8.3 mg/l indicating slightly alkaline in nature, the turbidity ranges from 2.5-4.5 mg/l, total alkalinity is 60-150 mg/l, TH varies from 90-115mg/l, sulphate ranges from 9.5-13.6 mg/l, chloride varies from 9.95-22.6 mg/l, fluoride varies in range of 0.22-0.35 mg/l, DO ranges 5.9-7.5 mg/l. On the other hand, water analysed from Hirakud dam, have pH value of 6.6-8.3 mg/l, 75-137 mg/l, TH is 98-120 mg/l, sulphate 12.6-13.8 mg/l, chloride 19.3-24.5 mg/l, fluoride 0.27-0.53 mg/l, DO is 5.7-6.4 mg/l and turbidity 2.4-4.6 mg/l. The assessment of water quality index (WQI) indicates that the WQI value for Mahanadi River is 138.8, whereas that of Hirakud dam is 179.98, Hence, both belong to category of class-E and unfit for drinking, but, however on comparison Hirakud dam water was found to be more contaminated than Mahanadi River water.

Keywords: Electrical conductivity, Total hardness, Dissolved oxygen, Alkalinity

1. INTRODUCTION

Water is present in all the three states such as gas, liquid and solid in our globe and is the basic need of all biotic community. After air, water is the second most essential compound that is present in the world, which is necessary for existence of biological world. Water is a precious resource and more than 95% water in our globe is saline water, which is present in the oceans and not considered as human consumption water resource Almost 3% of water is found in the frozen state such as ice, ice caps, glaciers etc. mainly in high altitude regions. Then, among the remaining 2% of water, a major portion is stored as in the form of ground water in aquifers under the surface of the earth's crust and very less percentage are available as surface water in rivers, ponds, canals and water reservoirs [3]. Since, very less percentage of water is available as fresh water for human use, therefore we have to save and protect our precious fresh water resources by adopting different processes or techniques [1, 2]. Not only human beings,

but also all the plants and animals require good quality of water for their survival. Fresh water is utilized in different ways, such as; agriculture, drinking, bathing, industry, laundry, aquaculture, fisheries, feed stocks, gardening, tourism, hydro power production etc. The quality of the water depends upon various factors such as local industries, mining activities, flow rate, human use and urban use [4]. The quality of water can be determined by analysing various physical, bacteriological and chemical parameters [5, 6]. River Mahanadi is the largest river of Odisha and treated as the life line of the people of Odisha. Hirakud dam is the longest earthen dam in Asia with area of 133090sq.kms, and this dam is constructed over the river Mahanadi having the length of 15 kilometers nearer to the Sambalpur town, Burla. The dam reservoir is of about 55 km length and treated as a main multipurpose river valley project after independence. Hirakud is a small town and is surrounded by a large-scale industrial sector Aditya Aluminium Pvt. Ltd. and having high density of population. It is at a distance of 299 km from capital city Bhubaneswar. In addition to industrial activities, domestic garbage, municipal sewage, solid waste like toxic heavy metal is released from industries, which consequently leads to the pollution of river water [7]. The present study leads to the impact of extensive industrialization on water quality in terms of WQI due to Hindalco industries on the water quality of river Mahanadi and Hirakud dam nearby Sambalpur city [8]. The main source of pollution of the Mahanadi River is due to industrial pollution because of the plants of Hindalco industries [9, 10]. It was observed that more than 80% of diseases are caused by the consumption of poor quality of contaminated water either directly or indirectly [11]. The standard value of water quality parameters according to the WHO is presented in Table-1

Table 1 Standard water quality parameters according to WHO [12]

Parameters	Standard Value
P^H	6.5-8.5
Chloride	250mg/l
Fluoride	0.5-1.0mg/l
Dissolved oxygen	10mg/l
Total dissolved solids	500mg/l
Sodium	20mg/l
Potassium	10mg/l
Salinity	100PSU
Hardness	200mg/l

2. STUDY AREA

Sambalpur city is located in the western part of Odisha in India at latitude21°.27' North and 83°.58' longitude, 150.75 meters above the sea level, having 299 km distance from capital city Bhubaneswar. On the eastern bank of the Mahanadi River Sambalpur

district is situated. Mahanadi River is one of the major and largest rivers in Odisha. It starts from the northern hill of Dandakaranya, which is flowing in the Raipur district of Chhattisgarh. The Mahanadi River flows through Chhattisgarh in the Eastern Ghats, then Odisha and finally enters into Bay of Bengal. The river flows through the district of Sambalpur, Subarnapur, Boudh, Jagatsinghpur, Cuttack, and Angul. The river Mahanadi forms delta with river Brahmani and Baitarani. The total area of Mahanadi River is 141,600 sq.km across and its length is 858 km. This river plays a vital role in the total irrigation system of Odisha and its tributaries are also important for different purposes. The tributaries of river Mahanadi are Seonath, Ong, Ib, Tel, Jonk, Mand etc. The Hirakud dam is constructed on river Mahanadi in Sambalpur district [13]. It forms the water reservoir of 55km long and is considered as a major multipurpose river valley project that is started just after the independence of India. It is the longest earthen dam of the world and drains an area of 133090sqkms. It is constructed in 1957 and is an iconic masterpiece and proud of our country. Hirakud dam is constructed over the river Mahanadi at about 15 kms from Sambalpur city of state Odisha. The current population of Sambalpur metropolitan region is 270,331. Therefore, due to presence of many industries and institutions, the water of Mahanadi River is continuously degrading [14]. Many canals like Samablpur canals, Bargarh canal, Sason canal are built from this dam. Many man-made activities are also taking place in this river like use of fertilizer in agriculture, washing household stuffs; domestic wastes and animal husbandry are the cause of degradation in water quality [15]. The quality of water of this river and dam is analysed by taking the parameters like EC, alkalinity, TH, chloride, fluoride and DO [16].

3. MATERIALS AND METHODS

3.1 Sample Collection

The samples are collected from 10 different location of up and down stream of Mahanadi River in Sambalpur area and also collected sample from 10 different location of up and down stream of Hirakud dam. Table-2 represents the sampling locations of Mahanadi River and Table 3 shows the sampling locations of Hirakud dam

Table 2: Sampling location of Mahanadi River

Location site	Code
P.C Bridge	A1
Kunjelpada ghat	A2
Nanda pada ghat	A3
Daleipada	A4
Sadakghat	A5
Binakhandi	A6
Upstream of Binakhandi	A7
Downstream of Binakhandi	A8
Dhanupali	A9
Maneswar	A10

Table 3: Sampling location of Hirakud Dam

Location site	Code
Remed	B1
Hindalco colony	B2
Jhankarani	B3
Sadeipali	B4
Debrigad	B5
Charbhati	B6
Budharaja	B7
Modipara	B8
Gopalmal	B9
Charbhati	B10

The sample was collected within 2-3 days before testing in the laboratory. The water samples were collected in a polyethylene bottle from different important locations of Mahanadi River nearer to Sambalpur city and both upstream and downstream of Hirakud dam. In this work, the water quality was measured in terms of physiochemical parameters such as EC, pH, fluoride, chloride, dissolved oxygen, total dissolved solids (TDS), Na, K, salinity etc. The methodology of analysis was carried out by using the following methods.

3.2 Methodology

All the analysis was done as per the standard analytical procedure (APHA 2012). pH was measured by an electrometric method using pH meter. Hardness was calculated by using EDTA titration method. The analysis of dissolved oxygen was done by Winkler's Iodometric method. Analysis of chlorides was done by argentometric titration. Fluoride

analysis was done by fluoride meter. Salinity was analysed by using a digital salinity meter. Sodium and potassium were tested in Dept. of Earth Science, Sambalpur University by using a flame photometer. The collected samples were analysed in the laboratory of Dept. of Chemistry, Dept. of Civil Engineering, VSSUT, Burla and Dept. of Earth Science, Sambalpur University within a week.

4. RESULTS AND DISCUSSION

The different physical and chemical parameters of the collected sample of the Mahanadi River and Hirakud Dam are reflected in the table-4 to Table-5.

Table 4. Physicochemical parameters of water samples in Mahanadi River in Monsoon season

Sample	pH	Fluoride (mg/l)	Chloride (mg/l)	Hardness (mg/l)	DO (mg/l)	Na (mg/l)	TDS (mg/l)	K (mg/l)	Salinity
A1	8.09	9.4	52.66	212.5	8.0	9.4	323	7.3	92
A2	7.5	8.7	41.3	160.7	7.6	6.6	334	7.1	87
A3	7.49	3.1	40.6	145.8	5.4	8.4	661	7.2	94
A4	7.45	3.0	44.2	228.2	7.2	7.7	327	6.7	59
A5	7.29	2.4	34.08	205.0	8.3	8.2	337	6.3	67
A6	7.3	5.6	43.2	201.6	7.4	9.1	453	7.1	83
A7	7.13	7.4	52.1	175.4	7.3	8.7	512	6.7	74
A8	7.81	8.0	48.4	`189.3	6.9	7.5	431	8.3	81
A9	7.42	6.8	43.5	197.1	7.6	7.8	471	6.5	79
A10	7.89	7.3	39.7	232.3	7.5	7.5	428	7.8	68

Table 5. Physicochemical parameters of water samples in Hirakud Dam in Monsoon season

Sample	pH	Fluoride (mg/l)	Chloride (mg/l)	Hardness (mg/l)	DO (mg/l)	TDS (mg/l)	Na (mg/l)	K (mg/l)	salinity
B1	6.24	2.6	34.8	324.4	8.1	426	8.2	5.3	78
B2	6.56	3.3	49.8	250.5	6.3	196	6.8	6.9	65
B3	6.82	2.3	44.02	206.7	6.7	462	6.3	7.2	72
B4	7.3	4.4	31.24	159.5	9.0	380	9.1	7.0	88
B5	7.9	3.4	44.1 4	132.4	6.7	260	7.2	5.5	93
B6	7.3	5.6	43.2	153.6	6.8	340	8.3	5.8	87
B7	6.8	6.3	53.5	165.7	7.5	312	7.4	6.7	83
B8	6.5	7.1	58.7	151.3	8.2	372	7.1	7.4	91
B9	7.1	6.5	57.9	148.8	8.0	295	6.7	7.1	94
B10	6.9	6.4	40.5	143.9	8.5	290	6.3	6.3	96

4.1 Calculation of Water Quality Index (WQI)

The WQI is a technical method that predicts the quality of any water sample by weighted mean method, which is calculated by taking the data of physico-chemical parameters of the collected water samples. This calculation was based on following derivation of formula

(1) To calculate the quality rate (Qi) the formula used is given below in equation (1)

$(Qi) = [(V_0 – V_i) / V_s – V_i]\ 100$----------(1)

Where, V_0 = weighted mean of different parameters

V_i = optimal acceptable value

V_i = 0 for all parameters except pH & DO

V_s = Standard acceptable limit of particular parameter

2) Calculation of relative unit weight (W_i) is given as follows: -

$(W_i) \alpha 1/S_i$ or $W_i = K/S_i$

$K=1/1/S_i$

Where Si = Standard value of a particular parameter

K = Proportionality constant.

3) $WQI = \frac{\sum WiQi}{\sum wi}$

Table 6. Standard Table of WQI as per WHO

WQI values	Quality of the water
0-25	A (Excellent)
26-50	B (Good)
51-70	C(Medium)
70-100	D (Poor)
Above 100	E (Worst quality and unhealthy for drinking purposes)

4.2 Water quality index of Mahanadi River and Hirakud Dam

Table 7. Water Quality Index of Mahanadi River

Name of Parameters	Mean Observed values (V_0)	Standard values (V_s)	Unit Weight (W_i)	Quality Rating (Q_i)	W_iQ_i	Remarks
pH	7.53	6.5-8.5	0.117	35.33	4.13	WQI= ∑QiWi/∑Wi 646.79/1.37 =472.1 (class =E) Very poor & unfit for drinking purpose
Fluoride	6.17	0.5-1.0mg/l	1.0	617.0	617.0	
Chloride	43.97	250	0.004	17.59	0.07	
DO	7.32	10mg/l	0.1	158.26	15.82	
TDS	427.7	500	0.002	85.54	0.17	
Hardness	194.79	200mg/l	0.005	97.39	0.48	
Na	8.09	20	0.05	40.45	2.02	
K	7.1	10	0.1	71.0	7.1	
			∑Wi =1.37		∑QiWi = 646.79	

Table 9: Water Quality Index of Hirakud Dam

Name of Parameters	Mean Observed values (V_0)	Standard values (V_s)	Unit Weight (W_i)	Quality Rating (Q_i)	W_iQ_i	Remarks
pH	6.942	6.5-8.5	0.117	-3.867	-0.45	WQI= ∑QiWi/∑Wi 502.39/1.37=366.70 (class =E) Very poor & unfit for drinking purpose
Fluoride	4.79	0.5-1.0mg/l	1.0	479.0	479.0	
Chloride	45.78	250	0.004	18.31	0.07	
DO	7.78	10mg/l	0.1	148.26	14.82	
TDS	333.3	500	0.002	66.66	0.13	
Hardness	183.68	200mg/l	0.005	91.84	0.45	
Na	7.34	20	0.05	36.7	1.83	
K	6.54	10	0.1	65.4	6.54	
			∑Wi=1.37		∑QiWi=502.39	

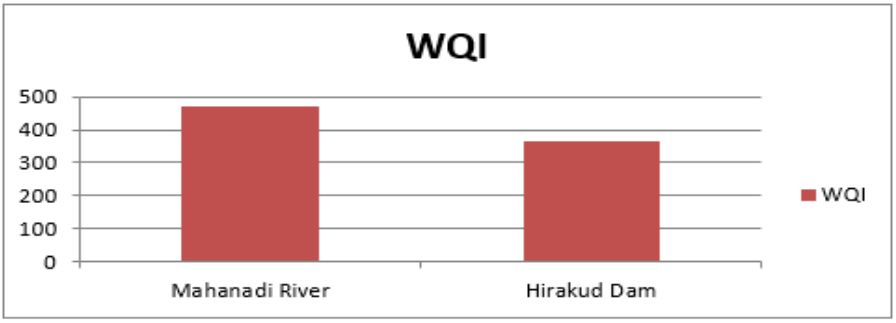

Fig.1. WQI of Mahanadi River and Hirakud Dam

In Mahanadi River area, the pH ranges from 8.09 (A1) to 7.13(A7) with an average value of 7.539 having the standard value 6.5-8.5. Fluoride ranges from 9.4mg/L (A1) to 2.4mg/L (A5), but the standard permissible limit is 0.5-1.0mg/l. The chloride concentration varies from 52.66mg/l (A1) to 30.48mg/l (A5) with an average value of 43.97mg/l but, the standard permissible limit is 250mg/l. The hardness varies from 228.2 mg/l (A4) to 145.8 mg/l (A3) with an average value of 198.79 mg/l and the standard value is 200mg/l. DO ranges from 8.3mg/l (A5) to 5.4mg/l (A3) with average 7.32mg/l and the standard value is 10mg/l. The TDS value ranges in between 661 mg/l (A3) to 323 mg/l (A1) with average of 427.7 mg/l and standard value is 500 mg/l. Sodium ranges in between 9.4 mg/l (A1) to 6.6 mg/l (A2) and potassium is 8.3 mg/l (A8) to 6.3 mg/l (A5) with an average 7.1 mg/l. Salinity is 94PSU (A3) to 59PSU(A4) with an average of 74.8 PSU and standard value of 100PSU. All the parameters are more than the permissible limit according to WHO. The WQI value of Mahanadi River water was found to be 472.1 (above 100) belongs to class- E. Hence the quality of water is very poor and totally unfit for human consumption.

In Hirakud Dam area, pH ranges from 7.9 (B5) to 6.24(B1) with an average value of 6.94. Fluoride ranges from 7.3mg/L (B1) to 2.3mg/L (B5) with average value of4.79mg/l. The chloride concentration varies from 58.7mg/l (B8) to 31.24mg/l (B4) with an average value of 44.78mg/l. The hardness varies from 324.4 mg/l (B1) to 132.4 mg/l (B5) with average value of 183.68 mg/l. DO ranges from 9.0mg/l (B4) to 6.3mg/l (B2) with an average 7.58mg/l. The TDS value ranges in between 426 mg/l (B1) to 196 mg/l (B2) with average of 333.3 mg/l. Sodium ranges from 9.1 mg/l (B4) to 6.3 mg/l (B3) with an average 7.34 mg/l and potassium 7.4 mg/l (B8) to 5.3 mg/l (B1) with average 6.52 mg/l. Salinity is 96 PSU (B1) to 65 PSU(B2) with average of 84.7 PSU. All the water parameters are within the permissible limit on accordance with WHO except Fluoride. The value WQI of Hirakud Dam water was calculated to be 360.857 which fall under the category of E-class. Although Mean value of Fluoride and WQI is less than Mahanadi River water, but still, it is unfit for drinking purpose.

5. CONCLUSION

From the analysed data, it is concluded that some parameters for the water quality of surface water in different places of Sambalpur city of river Mahanadi is beyond the permissible value and some of the parameters are within the permissible limit. The different physico-chemical parameters including pH, Fluoride, Chloride, Dissolved oxygen, TDS, Total hardness, Sodium, Potassium, Salinity of the collected samples are analysed as compared with the drinking water quality standards BIS:10500 to classify the water quality. The WQI is calculated for determining the class of the water and usability as human consumption water. The addition of waste effluents and partly solid wastes of the industry, recreational activity and urban wastes is the cause of

deterioration or degradation of the quality of water, which is directly or indirectly affecting the nearby ecosystem. In the present analysis it was found that most of the physical parameter alkalinity, total hardness and pH are found to be much beyond permissible value. From the analysed result it was found that the water of the Mahanadi River is highly polluted than the Hirakud dam. The physico-chemical data indicates that drinking water in Sambalpur regions are affected by industrial activities and MSW dumping and the water quality of surface water of Mahanadi River is now heavily polluted and alarming for the people of Sambalpur and Hirakud town and command areas of the two cities. On the basis of WQI the water of both Mahanadi River and Hirakud dam belongs to E-Class and not fit for human use. Now if pollution is not stopped, then a day will come when the water of river Mahanadi becomes unfit for human use and cause of many water-borne diseases, which will lead to the increase in rate of mortality.

REFERENCES

1. Mouillot, D., Villeger, S., Scherer-Lorenzen, M., Mason, N.W.H. (2011) Functional Structure of Biological Communities Predicts Ecosystem Multifunctionality. Journal of PLOS ONE. 6(3): 1-9
2. Bashier, E.E., Bashir, N.H., Mohamadani, A., Elamin, S.O., Abdelrahman, S.H. (2015). A challenge of sustaining water supply and sanitation under growing population: A case of the Gezira State, Sudan. International Journal of Water Resources and Environmental Engineering. 7(9): 132-138
3. Zhou, T., Nijssen, B. (2016). The Contribution of Reservoirs to Global Land Surface Water Storage Variations. Journal of Hydrometeorology. 17: 309-325
4. Kamboj, V., Kamboj, N., Sharma, S. (2017). Environmental Impact of River Bed Mining- A Review. International Journal of Scientific Research and Reviews (IJSRR). 7(1): 504-520
5. Banjara, B., Singh, R.K., Banjara, G.P. (2019) A study on physico-chemical parameters of river, urban and rural ponds of Raipur district. International Journal of Development Research. 9(1): 24986-24989
6. Aziz, S.Q., Saleh, S.M., Omar, I.A. (2019). Essential Treatment Processes for Industrial Wastewaters and Reusing for Irrigation, ZANCO Journal of Pure and Applied Sciences. 31(3): 269-275
7. Obinnaa, I.B., Ebere, E.C. (2019). A Review: Water pollution by heavy metal and organic pollutants: Brief review of sources, effects and progress on remediation with aquatic plants. Analytical Methods in Environmental Chemistry Journal. 2(3); 5-38

8. Sakr, N.A., Abu-Elkheir, M., Atwan, A., Soliman, H.H. (2018). Current trends in complex human activity recognition. Journal of theoretical and applied information technology. 96(14): 4564-4583

9. Khan, M., Tarique, M. (2015). Industrial Pollution in Indian Industries: A Post Reform Scenario. Journal of Energy Research and Environmental Technology (JERET). 2(2): 182-187

10. Abatenh, E., Gizaw, B., Tsegaye, Z. (2018). Contamination in a Microbiological Laboratory. International Journal of Research Studies in Biosciences (IJRSB). 6(4): 7-13

11. Saklani, N., Khurana, A. (2019). Global Warming: Effect on Living Organisms, Causes and its Solutions. International Journal of Engineering and Management Research. 9(5) :24-26

12. Levallois, P., Villanueva, C.M. (2019). Drinking Water Quality and Human Health: An Editorial. International journal of Environmental Research and Public Health. 16(631), 1-9

13. Beura, D. (2015). Floods in Mahanadi River, Odisha, India: Its Causes and Management. International Journal of Engineering and Applied Sciences (IJEAS). 2(2): 51-55

14. Singh, V.K., Chauhan, N.S., Kushwaha, D. (2015). An overview of hydro-electric power plant. ISST Journal of Mechanical Engineering. 6(1): 59-62

15. Ogbuewu, I.P., Odoemenam, V.U., Omede, A.A., Durunna, C.S., Emenalom, O.O., Uchegbu, M.C., Okoli, I.C., Iloeje, M.U. (2012). Livestock waste and its impact on the environment. Scientific Journal of Review. 1(2): 17-32

16. Salahuddin, H., I. (2020). Analysis of Lower Lake Water in Bhopal Region of Madhya Pradesh, India. International Journal of Lakes and Rivers. 13(1): 17-25

 ISBN: 978-81-959870-7-8

A CASE STUDY ON CHROMIUM EFFLUENT TREATMENT PLANT OF LEATHER PROCESSING UNITS

Iti Dubey and Meenu Srivastava
College of Community & Applied Sciences, MPUAT, Udaipur, Rajasthan, India

ABSTRACT
In Kanpur, CETP units have been installed to treat the enormous effluents discharge from various leather processing units. Researcher collects the data in terms of its location area, year of establishment and number of units attached for treatment of effluents and their effluent treatment capacity per day. Result of the study indicate that majority of leather units were connected to CETP of Bajidpur in Jajmau area of Kanpur. Some remaining large scale leather units not involved in combined units are also there which have their own Chromium Effluent Treatment Plant (CETP).

Keywords: Waste Treatment; CETP; Leather Processing Unit.

1. INTRODUCTION
The main purpose of CETP is to decrease the treatment price for individual units along with caring for the environment. Further, as a communal entity, CETP can get the subsidies from Central and State Govt., which are otherwise deprived for establishment of the individual effluent treatment plant.

The release of crude tannery effluents and other wastes is a matter of great worry to the society. Various NGOs and citizen forums in states where leather clusters are found, started showing their disapproval against detrimental effects of the effluents on human health and environment. There is need to implement proper treatment technology for the tannery effluents.

Schjolden (2000) remarked that in Kanpur, the number of tanneries had doubled over the past 15 years. Most of the tanners in Jajmau area has expanded their production capacity. Initially they started only with leather tanning. Almost half of them have expanded to production of leather, leather components and products, like shoe uppers or shoes, bags, saddlery and harness goods. The diversification of production is also more common amongst the medium and large firms. Here, 100% have engaged in the production of leather products of some kind, either directly in the same company as the tannery, or as a separate unit owned by the same family or group.

In Kanpur, leather tanning particularly blossomed during British colonial rule, when many cantonments were located in this area, and the need for boots, saddlery and harness equipment was high. Most of the tanneries are located in Jajmau, an area south- east of the city, close to the military cantonment area, and on the southern bank of the river

Ganges. Today, the area of Jajmau is crowded, not only with tanneries, but also with the houses of the people living there, mostly these are tannery workers who suffers from various health problems. Chromium from leather tanning can make its way into air, soil, food and water, and the most common forms of exposure are through inhalation of dust or fumes and ingestion of or contact with contaminated water. Workers in tanning facilities can inhale airborne chromium and can also be exposed through dermal contact.

Common Effluent Treatment Plant (CETP) is the concept of treating effluents by means of a collective effort mainly for a cluster of small-scale industrial units.

The main objectives of CETP are –

- To reduce the treatment cost for individual units while protecting the environment.
- To minimize the problem of lack of technical assistance and trained personnel as less plants require less people.
- To solve the problem of deficiency of space as the centralized facility can be planned in advance to ensure that suitable space is vacant.
- To reduce the problems of viewing for the pollution control boards.
- To organize the disposal of treated wastes and mud and to advance the reprocessing and recycle options.

Method

The study was carried out in Kanpur city because it is known as third largest tanning center in India. The researcher purposively identified and prepared a list of 10 leather processing industries within Kanpur which have been registered since last 20 years and have CETP for waste recovery. Prior permission was taken from the respective head of the selected leather industry to allow to do survey for the study.

The survey method was used to elicit desired information about CETP through structured interview schedule. The obtained data was statistically analyzed and presented in terms of frequency and percentage. The developed schedule was pre-tested on ten non sample subjects. The collected data was analyzed for statistical treatment in the light of objective of study.

Results:

In Kanpur, CETP units have been installed to treat the enormous effluents discharge from various leather processing units.

Table 1 presents the data regarding details of CETPs installed in terms of its location area, year of establishment and number of units attached for treatment effluents and their effluent treatment capacity per day. It can be seen from the table that first unit of common effluent treatment plant (CETP) was established in the year 1994 at, Bajidpur

in Jajmau area of Kanpur and its treating capacity is 36 million liter per day (MLD). Jajmau is the main area where there are more than 400 tannery units. Another CETP was established in 2004 at Banthar area in Unnao in which 25 units are attached, its capacity is 4.15 MLD. It was also found that few leather units have installed their own CETP, one of them is Mirza International Ltd. Kanpur, which established its CETP in the year 2013 and its effluent treatment capacity is 1.65 MLD.

Table 1: Establishment year, capacity of CETPs, and units attached *

Area	Year of establishment	Unit attached	Capacity (Million liter/day)
Bajidpur, Jajmau, Kanpur	1994	260 UNIT	36 MLD
Banthar, Unnao, Kanpur	2004	25 UNIT	4.15 MLD
Magarwara, Unnao, Kanpur	2013	Only Mirza units (Private plant)	1.65 MLD

*Source: http://www.bantharpollutioncontrol.org/technicaloverview.html

Majority of leather units (66.67%) selected by researcher for survey work were connected to CETP of Bajidpurin Jajmau area of Kanpur. Remaining leather units (33.33%) which were large scale and involved in both leather processing and production units have their own Chromium effluent treatment plant (CETP).

Land area details of CETPs

It is apparent from Table 2 that total area covered under CETPs (42 MLD, including all the three CETP reported in Table-1) is 120.58 acres, Salt & Sludge Area (12.45 acres)

, Common Chrome Recovery Plant, CCRU -(11.52 acres) and Green Area, Admin Building, Future expansion and Substation covered 42.95,11.37,17.0 and 10.02 acres respectively.

Table 2 :Land area details of CETPs

Land Use	Area (in Acre)
CETP 42 MLD area	120.58
Salt & Sludge Area	12.45
Common Chrome Recovery Plant (CCRU)	11.52
Green Area	42.95
Admin Building	11.37
Future Expansion	17.0
Sub station	10.02
Other	9.51

Raw materials/chemicals required for effluent treatment

Regarding raw materials required for tannery effluent treatment, Table- 3 depicts that lime, alum, polyelectrolyte and soda ash are main chemicals needed.

Table 3:Raw materials required for tannery effluent treatment

Material	Unit	Quantity
Lime	Tons/day	186
Alum	Tons/day	117
Polyelectrolyte	Kg/day	158
Soda Ash	Tons/day	128

Composition of the feed to the treatment plant

The feed consists of leather effluent of different parameters (pH, COD, BOD etc.) from different leather processing units.

Parameters of effluent treated water

Table 4 clearly shows the detail of various parameters of effluent treated water in terms of estimated values of pH, BOD, COD, TSS, TDS and total chrome. The pH value of treated water was observed as 6.5 to 9.5, BOD 1000 to 1800 mg per litre, COD 2000 to 4000 mg per litre and TSS as 2000 to 3000 mg per litre.

Table 4 : Parameters of Effluent Treated water

Parameters	Estimated Values*
pH	6.5-9.5
BOD	1000 – 1800 mg/l
COD	2000 – 4000 mg/l
TSS	2000 - 3000 mg/l
Total Cr	40—100 ppm
TDS	5000-10000 mg/l

***Source: http://www.bantharpollutioncontrol.org/ technicaloverview.html**

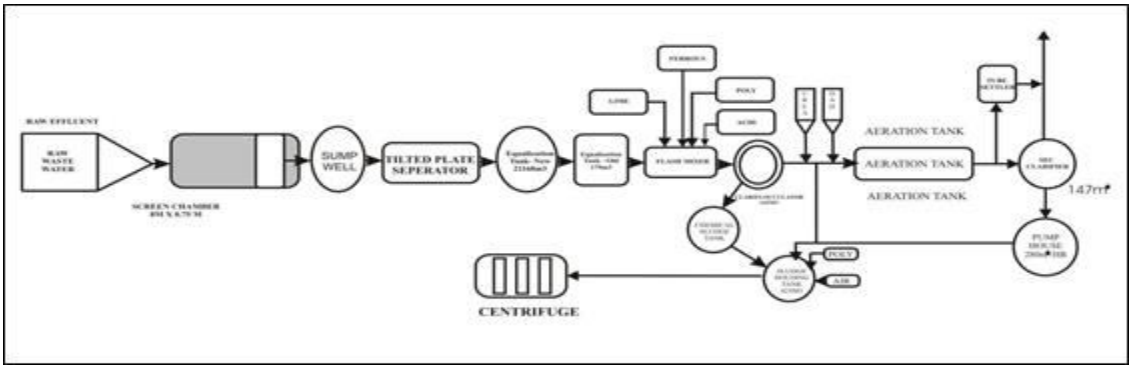

Fig.1: Flow chart of Common Effluent Treatment Plant

Effluent treatment process

The effluent treatment plant has primary, secondary and tertiary treatment systems. The primary treatment system includes Pre-treatment Chamber, Equalization Tank, Flash Mixture Tank and Clariflocculator and the secondary treatment system consists of Aeration tank - I, Clarifier - I, Aeration Tank - II and Clarifier - II. The tertiary treatment is carried out in two units, namely Pressure Sand Filter and Activated Carbon Filter.

Plant operation

The effluent is collected through open drain from various processing unit at one place, and is called CETP inlet and treated by following stages.

1. Screen chamber

The waste water passes through the screen chamber which comprises of mild steel bars. The purpose of installation of screen is to arrest large floating materials, plastic pieces, rags etc. so that these do not get entangled with pump impellers and other machinery of the plant. This is a manually cleaning screen & should be cleaned as often as required to prevent surcharging of waste water in the drain.

2. Sump well

The raw waste water passing through the screen gets collected in the wet well of the pump house. In the dry well of pump house centrifugal pump have been installed to pump the raw waste water to the equalization tank to equalize the waste water characteristics and to neutralize the pH of waste effluent.

3. Tilted plate separator

The waste water pumped from sump well is lifted to the tilted plate separator to remove any oil and grease from the waste water. Then oil less waste water is transfered to the equalization tank.

4. Equalization tank

The effluents pH varies from time to time. The effluents are stored for 8 to 12 hours in the equalization tank. Jet air blower has been installed in the equalization tank for homogenous mixing of effluents and neutralization by acid (H_2SO_4 or HCl) dosing to decrease the BOD load.

5. Flash Mixer:

Effluent with pH 8-9 is transferred to chemical dosing house for chemicals dosing, where coagulants are added to the effluents. These are-

Lime (450 - 500 ppm) – to raise the pH up to 8-9. Ferrous sulphate (800 – 900 ppm) – to remove colour and Anionic Polyelectrolyte (1-2 ppm) – to settle the suspended matter

6. Clarriflocculator:

This chemical dosed effluent is transferred to clarriflocculator. In the clarriflocculator, the water is circulated continuously by stirrer. This is also known as primary clarifier. Overflowed water is taken out to the aeration tank. The solid particles are allowed to settle down, and collected separately in chemicals sludge tank which is then passed to sludge holding tank for thickening.

7. Aeration tank

Chemically treated effluent from clariflocculator, flows to Aeration tank for biological treatment. Biological treatment removes organic matter from the waste water. For effective treatment of waste water, oxygen is required for growth of microorganisms. A lso for mixing in the aeration tank, floating type of mechanical aerators have been provided. The detention period in aeration tank is 17 hrs. During this time a healthy flocculent sludge is formed which brings about oxidation of the dissolved organic matter. BOD removal to the extent of 99% could be achieved with efficient operation.

8. Secondary clarifier

Biological sludge is collected here and treated effluent is disposed safely.

9. Centrifuge (Sludge thickener)

The effluents are taken to centrifuge for thickening & solidification centrifuge action, to separate the solids and liquids with a polyelectrolyte (cationic type) dosing. The sludge thickener centrifuge reduces the water content in the effluent wastes. The effluent is then reprocessed and sludge is collected at the bottom and disposed at the dumping site.

Case study of CETP at Mirza International Ltd.

Some of the leather units like Mirza International Limited (Tannery Division) Unnao, Kanpur has installed its own Effluent Treatment Plant in the year 2013 to treat the tannery waste water. The plant is designed to treat the effluent at the rate of 1.65 ML per day. Fig shows the flow diagram of ETP.

Fig 2 : Flow diagram of ETP

To prevent contamination of ground water and air, in ETP of Mirza International, tannery discharge is treated biologically. The free discharge meets the country's pollution Board Standards.

Table 5 highlights the treated values of tannery waste after being treated at CETP which is much lower than the permissible standard values as per environment norms and treated water can safely be discharged in river, for agriculture purpose or for cleaning wash rooms and floor etc.

Table 5 : Treated vale and standard (permissible value) of Tannery effluents

Effluent after treatment	Treated value	Standard
$Chrome^{+3}$	0.3 mg /l	1.0 mg /l
BOD	25 mg/l	30 mg/l
COD	180 mg/l	250 mg/l

CONCLUSION

Their chrome recovery unit is also very efficient as stated by them. It recovers more than 99.5% chromium that would otherwise be discharged as waste. The recovered chromium is re-used with BCS resulting in safeguarding the environment and reducing cost.

In response to the question asked about the approximate amount of the treated effluent disposed per day, it was reported by the respondent of private CETP owner of selected leather unit as 12.60 K.L. Further, it was confirmed by them that the capacity of CETP at their leather unit is sufficient to treat the waste water.

ACKNOWLEDGEMENTS

This work was supported by department of textiles and apparel designing, college of community and applied sciences, MPUAT, Udaipur. We also acknowledge the leather unit for permitting us to perform survey for the present research.

REFERENCES

1. Dubey, I. 2019 .Occupational health hazards of leather industry workers of Kanpur. M.Sc. thesis in Department of Textile and Apparel Designing, College of Home science , Maharana Pratap University of Agriculture and Technology, Udaipur.
2. Koka ,V. 2012.Occupational health hazards of textile workers of Pali district. Ph.D. thesis in Department of Textile and Apparel Designing, College of Home science, Maharana Pratap University of Agriculture and Technology, Udaipur.
3. Schjolden, A. 2000. Leather tanning in India: Environmental regulations and firms compliance, Working Papers, No. 21. ISSN 0804-5828 retrieved from http://s3.amazonaws.com/zanran_storage/www.cicero.uio.no/ContentPages/18864935.pdf on December 12 ,2018.
4. http://www.bantharpollutioncontrol.org/technicaloverview.html
5. http://www.bantharpollutioncontrol.org/ technicaloverview.html
6. http://shodhganga.inflibnet.ac.in/bitstream/10603/156680/9/09_chapter%203.pdf

SUBSTITUTIONAL EFFECT OF TiO_2 ON THE OPTICAL AND STRUCTURAL PROPERTIES OF SODIUM CADMIUM BORATE GLASSES

Ravinder Singh and Sonam Raheja*
School of Engineering & Technology, Apeejay Stya University, Sohna, Palwal road, Village Silani, Sohna (Gurugram), Haryana-122103, India

ABSTRACT

Glass compositions $20Na_2O.(20-x)CdO.60B_2O_3:xTiO_2$ (x = 0,1, 2, 3, 4 and 5 mol %) were synthesized using standard melt-quench method. In order to comprehend the function of TiO_2 in these glasses, researchers have looked at their optical and structural properties. With increasing concentration of TiO_2 in these glasses the volume of non-bridging oxygens *(NBOs) is found to increase causes to decrease the energy band gap (E_g). Decreasing values of ΔE suggests the structural stability of these glasses. The presence of TiO_4 and TiO_6 units has been confirmed from IR analysis. Decreasing trend of optical basicity and energy band gap is explained in terms of polarizability, which is found less in these glasses. The refractive index of Ti doped glasses is found in the range of 2.24 – 2.27.*

Keywords: Oxide glasses; Borate Glasses; Optical Properties; Structural Properties

1. INTRODUCTION

The use of oxide glasses in the field of optoelectronics and optoelectronic communication devices has been increased during the past two decades. In oxide glasses, borate glasses containing transition metal oxides (TMOs) are one of the most popular and glass forming material because of its compositional and structural flexibility[1]. Multi valences cations like transition metals and rare earth cations are widely used common additives that are incorporated to the borate glasses because of their ability to modify the magnetic, electrical, attenuation, and optical properties of those glasses[2], [3]. It has been reported that TiO_2 is an interesting transition metal oxide among all transition metals to have exhibited non-linear optical (NLO) effects in glass systems. Titanium dioxide TiO_2 is considered a precious dopant because it is used to enhance the glass's optical properties, because of its low coordination numbers, trivalent and tetravalent, titanium cations may share in glass's matrix not only as a glass's modifier, TiO_6, but also as a glass's former as TiO_4 [4]. Normally, it was found that TiO_2 exist in Ti^{4+} state forming TiO_4 units and sometimes with TiO_5 (comprising of trigonal bipyramids) structural units in the glass network. There is possibility for the reduction of Ti^{4+} ions into Ti^{3+} ions during synthesis and annealing process [5]. The valency of TiO_2 in the glass matrix depends on many factors like chemical composition and melting temperature. Morinaga *et al.* reported that Ti^{3+} is absent in high

concentration alkali borate glasses even the melting temperatures of glass is 1500°C [6]. It has been reported that the addition of small amount of Titanium oxide in borate glasses enhances the glass forming ability, chemical durability, thermal stability, high refractive indices, excellent transparency in the visible–IR region and intense UV absorption [6], [7]. These glasses are found good for their suitability as low loss optical fiber in optical communication devices, refractive index dispersion and eligible for tunable laser devices and optical amplifier media [8]–[11]. Production of such type of oxide glasses need some additives to improve physicochemical properties of theses glasses. In the present composition Na_2O introduced to lower the melting point [4]. Na_2O react with B_2O_3 to modify borate structure from tri-angular boron to tetrahedral coordination and have unique properties due to two coordination states in their network structure [12]. Upon addition of Na_2O to the B_2O_3 covalent network causes considerable change, resulting in the creation of anionic sites occupied by modifying Na_2O. Cadmium oxide CdO is introduced to enhance the efficiency of the borate glass and shorten the time taken for solidification of glasses during the quenching process. Oxide glass containing CdO have high chemical stability and less thermal expansion [13]. The aim of present study to investigate the optical properties of sodium cadmium borate glasses with TiO_2 act as dopant material.

2. Materials and Experimental Method

The composition of the glass series is shown in Table 1. Six glass samples were prepared with the increasing concentration of TiO_2 in steps of 1 mol% replacing CdO. Glass samples were synthesized via conventional melt quenching technique. Analytical grade reagents of sodium carbonate (Na_2CO_3), boric acid (H_3BO_3), cadmium oxide (CdO) and titanium oxide (TiO_2) were used as starting materials. The raw materials were weighed and taken in quartz mortar pestle to mix it well. The well mixed powder was taken into porcelain crucible and then melted in an electric muffle furnace for 1 hour at 1373 K temperature. To assure the homogeneity of the sample, the melts were stirred regularly after 15 min. The melt was quenched between two stainless steel plates to obtain glass sample of thickness around 1.0 – 1.5 mm. The obtained samples were annealed for 1 hour at 673K for further removal of impurities in the glass sample.

The glass samples were grounded and optically polished to record the optical absorption spectra by UV/VIS/NIR spectrophotometer (Model-Varian Cary-5000) in the wavelength range 200–3300 nm. The energy band gap (E_g) (direct/indirect), band tailing parameter were calculated by using the data obtained from UV–Vis–NIR spectrophotometer

IR transmission spectra of the glasses under study were recorded at RT on a Bruker Alpha-T spectrophotometer in the spectral range of 400-4000 cm^{-1} by ATR (Attenuated Total Reflection).

The calculated values of optical basicity (Λ) and refractive index (n) taken from our previous article are displayed in Table 2 [7].

Table 1: Sample code and composition ratio.

Glass Code	Na_2O (mol%)	CdO (mol %)	B_2O_3 (mol%)	TiO_2 (mol%)
NCBT0	20	20	60	0
NCBT1	20	19	60	1
NCBT2	20	18	60	2
NCBT3	20	17	60	3
NCBT4	20	16	60	4
NCBT5	20	15	60	5

3. RESULTS AND DISCUSSION

Some important physical parameters Optical basicity (Λ_{th}), refractive index (n) have already been calculated and described in our previous article [7]. Here we have used those parameters to correlate with the other optical parameters listed in the Table 2.

Table 2: Optical basicity (Λ_{th}),refractive index (n), cut-off wavelength ($\lambda_{cut\text{-}off}$), optical band gap (E_g), band tailing parameter (B) and Urbach energy (ΔE) for NCBT $20Na_2O.(20\text{-}x)CdO.60B_2O_3:xTiO_2$ (x = 0,1, 2, 3, 4 and 5 mol %) glasses..

Code	Λ_{th}	n	$\lambda_{cut\text{-}off}$	E_g (r=2)	E_g (r=3)	B	ΔE
Unit			(nm)	(eV)	(eV)		eV
NCBT0	0.719	2.36	358	3.07	2.90	1.03	0.76
NCBT1	0.716	2.24	338	3.55	3.36	1.97	0.24
NCBT2	0.714	2.24	345	3.50	3.31	2.87	0.19
NCBT3	0.713	2.25	348	3.47	3.32	4.54	0.18
NCBT4	0.711	2.26	350	3.46	3.34	7.45	0.14
NCBT5	0.709	2.27	357	3.38	3.35	10.32	0.12

UV-VIS-NIR Spectroscopy

The optical absorption spectra for NCBT doped with TiO_2 glasses was recorded at room temperature in the spectrum range of 250– 500 nm. As shown in the Fig.1. The spectrum of the doped and un-doped glasses does not exhibit any absorption band. It is observed that the fundamental absorption edge ($\lambda_{cut\text{-}off}$) of the glasses is not sharply defined and indicates their glassy nature [14]. To find the optical transitions and electronic band structure of a material, investigation of the optical absorption edge is a very useful method. In the present glasses it has been observed that with the increasing concentration of TiO_2, the optical absorption edge shifted towards higher wavelength

due to the structural changes in the glass network [15]. The absorption coefficient α(ν) can be determined near the edge from the relation as given below [16].

$$\alpha(\nu) = \frac{1}{d} ln\left(\frac{I_o}{I_t}\right) \quad (1)$$

where d is the thickness of the sample; I_o and I_t are the intensities of the incident and transmitted beams, respectively.

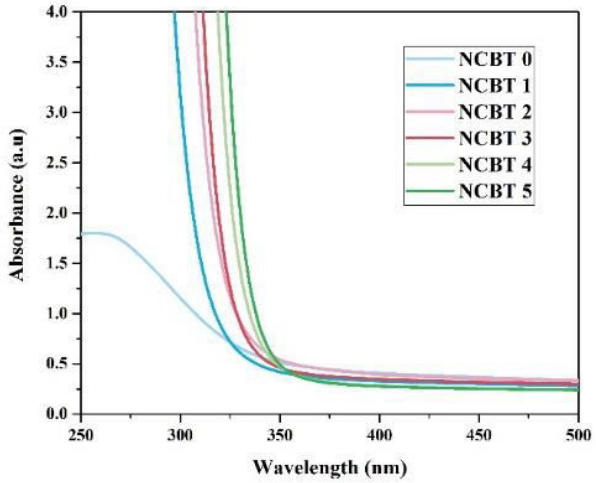

Fig.1: Optical absorption spectra for NCBT glasses.

The optical energy band gap (E_g) was calculated from the slopes of the linear regions of the Tauc's plots of $(\alpha h\nu)^{1/2}$ against (hν) for r=1/2 corresponding to direct allowed and direct forbidden transitions respectively [17], as shown in Fig.2. similarly, for r=1/3 from the plot $(\alpha h\nu)^{1/3}$ Vs (hν) as shown in Fig.3. The values of E_g were calculated from the slopes of the linear regions of these curves. The band gap of the glasses under study depends on the NBO's (non-bridging oxygens) concentration. The addition of TiO_2 concentration creates NBO's in the glass network causes to decrease the band gap of glasses under study [18]. However, the optical band gap energy (E_g) increases with the addition of TiO_2 content as compared to TiO_2 free glass is attributed to the structural changes that took place in the glass after the addition of TiO_2. The gradual addition of TiO_2 leads to remarkable decrease in the energy band gap. This decrease is concurrent with the red shifting of the absorption edge. Based on the IR spectra, the Ti^{3+} absorption band showed gradual dwindling with a shift toward a higher wavenumber (decrease in the Ti^{3+} concentration). It is well known that the Ti^{3+} may act as a modifier in the glass network [19], [20]. The exponential increase of the absorption coefficient α(ν) with photon energy (hν) in accordance with the empirical relation (2) as shown below [21].

$$\alpha(\nu) = \alpha_o \exp(h\nu/\Delta E) \quad (2)$$

Here, α_o is a constant, ν is the frequency of the radiation and ΔE is the Urbach energy. Urbach energy provides a measure for the disorder in amorphous and crystalline materials. Smaller is the value of Urbach energy, greater is the structural stability of the glass system. In the present glass system, the values of ΔE are decreasing with increasing concentration of Ti. Band tailing parameter (B) is calculated from the slope of the linear region of the Tauc's plot (r=2) and Urbach energies (ΔE) are calculated by taking the reciprocals of the slopes of linear regions of the curves ln(α) verses hν as shown in Fig.4. The values of Band Tailing parameter (B) and Urbach energy (ΔE) are presented in the Table.2.

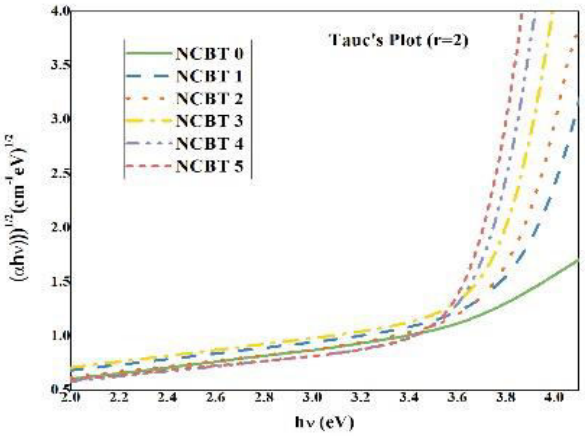

Fig.2: Dependence of (α) $(\alpha h\nu)^{1/2}$ vs (hν) for NCBT glasses.

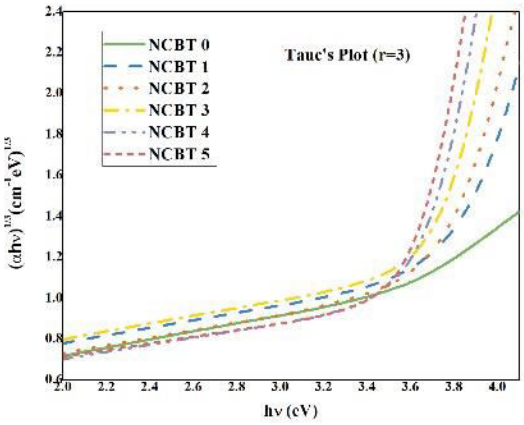

Fig.3: Dependence of (α) $(\alpha h\nu)^{1/3}$ vs (hν) for NCBT glasses.

 ISBN: 978-81-959870-7-8

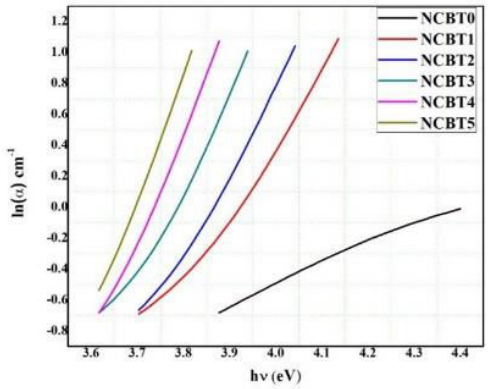

Fig.4: Urbach plots of TiO_2 doped NCBT glasses.

FTIR Spectroscopy

The FTIR spectroscopy was performed to investigate the glass structure and also ascertain the presence and participation of some required groups in the glass network. The FTIR spectra of NCBT glasses is shown in the Fig.5. It is observed that the IR vibrations are mainly active in 400 -1600 cm^{-1}. The borate groups are mainly active in three regions; the first band was observed at 697 cm^{-1} between the region from 600 to 800 cm^{-1} which is attributed to B–O–B bending modes in $[BO_3]$ and $[BO_4]$ units. The intensity of this band is found to increase with the addition of TiO_2 concentration up to (2 mol%). Sigaev *et al.*, suggested that the two well-resolved bands at 740 cm^{-1} (identified due to vibrations of TiO_4) and 650 cm^{-1} (referred to the symmetrical stretching vibrations of TiO_6) were created with the successive addition of TiO_2 into the borate network [22], [23]. In this study, a well resolved band is obtained at ~704 cm^{-1} due to TiO_4, which has been completely merged with the B–O bending vibrations of bridging oxygen atoms in B–O–B bonds. As the concentration of TiO_2 goes beyond from (3 mol %), the intensity of the band is found to increase due to higher concentration of B–O–Ti linkages. Consequently, the increment of TiO_2 in the glass sample causes discontinuation in the network chain. The second band arises at 898 cm^{-1} between the region from 800–1200 cm^{-1} which is due to the stretching modes of $[BO_4]$ tetrahedral borons. The intensity of the band was increased with shifting of meta center towards higher wave number at ~911 cm^{-1} with the addition of the TiO_2 concentration up to (2 mol %) beyond this concentration up to (3 mol %) the intensity goes decreased and after (3 mol %) of TiO_2 concentration the intensity was increased, The effect of introduction of TiO_2 and alkali oxides into B_2O_3 glass can cause conversion of sp^2 planar BO_3 units into more stable sp^3 tetrahedral BO_4 units and may also create non-bridging oxygens. The third band was found at 1528 cm^{-1} between the range 1200–1600 cm^{-1} due to the asymmetric stretching relaxation of the B–O band of trigonal BO_3 units.

Based on the above explanation, the intensity of this band was decreased with the addition of TiO_2 up to (2 mol %) concentration in the glass network, due to the decrease in the concentration of BO_3 units. Beyond this concentration the intensity of BO_3 units was increased. After that the peak intensity was increased due to no more formation of NBOs in the network structure. According to the equation (3) the transformation occurred from TiO_4 tetrahedra to TiO_6^{2-} octahedra by converting BO_4^- units to BO_3 units [18], [24], [25].

$$TiO_4 + 2BO_4^- \rightarrow TiO_6^{2-} + 2BO_3 \qquad (3)$$

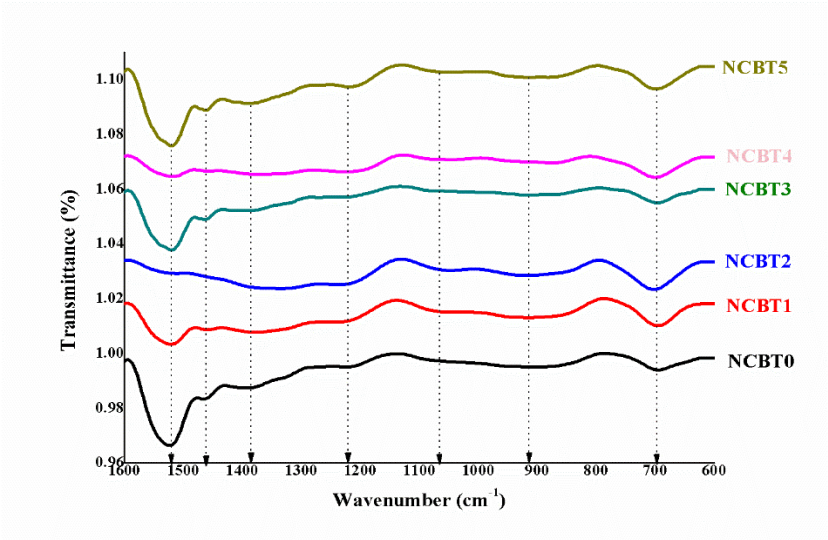

Fig.5: FTIR spectra of NCBT glasses doped with TiO_2.

4. CONCLUSION

Glass system with the composition $20Na_2O.(20\text{-}x)CdO.60B_2O_3:xTiO_2$ ($0 \leq x \leq 5$ mol%) have been prepared. The following conclusions have been drawn:

1. $\lambda_{cut\text{-}off}$ is found to shift towards higher wavelength with the increasing concentration of TiO_2 indicates large transmission window in UV-VIS region.
2. Decrease in E_g indicates the presence of NBOs in the glass structure, increasing with the TiO_2 doping. However, overall bandgap is found to increase in comparison to the Ti free glass, makes this composition suitable for optical applications.
3. Decreasing value of ΔE suggest that more defects are creating in the glass structure and the composition having higher concentration of TiO_2 has greater tendency to convert weaker bonds into defects. Structural stability is increasing with TiO_2 concentration.
4. FTIR study reveals the transformation occurred from TiO_4 tetrahedra to TiO_6^{2-} octahedra by converting BO_4^- units to BO_3 units.

5. The decreasing values of both optical basicity and energy band gap suggests the small single bond strength and small polarizability of these glasses.

The increasing value of refractive index can be explained that the less polarizable cations in the glass matrix do not effectively slow down the light as it travels through the vitreous network, which would cause the 'n' to rise.

ACKNOWLEDGEMENTS

Authors are thankful to Armament Research Board, DRDO, New Delhi for providing the financial assistance to carry out the work through Grant-In-Aid scheme of ARMREB, Project No.: ARMREB/MAA/2018/205.

REFERENCES

[1] S. Sanghi, S. Rani, A. Agarwal, and V. Bhatnagar, "Influence of Nb_2O_5 on the structure, optical and electrical properties of alkaline borate glasses," Materials Chemistry and Physics, vol. 120, no. 2, pp. 381–386, Apr. 2010, doi: 10.1016/ j.matchemphys. 2009. 11.016.

[2] M. S. Sadeq and H. Y. Morshidy, "Effect of mixed rare-earth ions on the structural and optical properties of some borate glasses," Ceramics International, vol. 45, no. 15, pp. 18327–18332, Oct. 2019, doi: 10.1016/j.ceramint.2019.06.046.

[3] S. S. Rojas, J. E. De Souza, K. Yukimitu, and A. C. Hernandes, "Structural, thermal and optical properties of CaBO and CaLiBO glasses doped with Eu^{3+}," Journal of Non-Crystalline Solids, vol. 398–399, pp. 57–61, Sep. 2014, doi: 10.1016/ j.jnoncrysol. 2014. 04.026.

[4] H. M. Gomaa, S. M. Elkatlawy, I. S. Yahia, H. A. Saudi, and A. M. Abdel-Ghany, "Influence of the gradual increase of TiO_2-impurities on the structural and optical properties of some calcium sodium borate glasses," Optik, vol. 244, p. 167543, Oct. 2021, doi: 10.1016/j.ijleo.2021.167543.

[5] A. P. Reddy, M. C. S. Reddy, A. S. S. Reddy, J. Ashok, N. Veeraiah, and B. A. Rao, "Photo-induced non-linear optical studies on gallium alkali borate glasses doped with TiO_2," Appl. Phys. A, vol. 124, no. 11, p. 755, Oct. 2018, doi: 10.1007/s00339-018-2178-0.

[6] B. Nagamani and C. Srinivasu, "Physical parameters and structural analysis of titanium doped binary boro silicate glasses by spectroscopic techniques," Materials Today: Proceedings, vol. 18, pp. 2077–2083, Jan. 2019, doi: 10.1016/j.matpr.2019.06.263.

[7] S. Raheja, R. Singh, and M. Uddin, "Electrical Characterization of Sodium Cadmium Borate Glasses Doped With TiO_2," J. Inst. Eng. India Ser. D, vol. 103, no. 2, pp. 497–503, Dec. 2022, doi: 10.1007/s40033-022-00350-0.

[8] A. S. Abouhaswa, Y. S. Rammah, S. E. Ibrahim, and A. A. El-Hamalawy, "Structural, optical, and electrical characterization of borate glasses doped with SnO_2," Journal of Non-Crystalline Solids, vol. 494, pp. 59–65, Aug. 2018, doi: 10.1016/ j.jnoncrysol. 2018. 04.051.

[9] S. Thomas, S. N. Rasool, M. Rathaiah, V. Venkatramu, C. Joseph, and N. V. Unnikrishnan, "Spectroscopic and dielectric studies of Sm^{3+} ions in lithium zinc borate glasses," Journal of non-crystalline solids, vol. 376, pp. 106–116, 2013.

[10] M. Pal, B. Roy, and M. Pal, "Structural Characterization of Borate Glasses Containing Zinc and Manganese Oxides," Journal of Modern Physics, vol. 2, no. 9, Art. no. 9, Sep. 2011, doi: 10.4236/jmp.2011.29129.

[11] M. Djamal *et al.*, "Spectroscopic study of Nd^{3+} ion-doped Zn-Al-Ba borate glasses for NIR emitting device applications," Optical Materials, vol. 107, p. 110018, 2020.

[12] M. A. Marzouk, F. H. ElBatal, and H. A. ElBatal, "Effect of TiO_2 on the optical, structural and crystallization behavior of barium borate glasses," Optical Materials, vol. 57, pp. 14–22, Jul. 2016, doi: 10.1016/j.optmat.2016.04.002.

[13] J. Anjaiah, C. Laxmikanth, P. Kistaiah, and N. Veeraiah, "Dosimetric and kinetic parameters of lithium cadmium borate glasses doped with rare earth ions," Journal of Radiation Research and Applied Sciences, vol. 7, no. 4, pp. 519–525, Oct. 2014, doi: 10.1016/j.jrras.2014.08.009.

[14] Y. B. Saddeek, K. A. Aly, K. H. S. Shaaban, A. M. Ali, and M. A. Sayed, "The Effect of TiO_2 on the Optical and Mechanical Properties of Heavy Metal Oxide Borosilicate Glasses," Silicon, vol. 11, no. 3, pp. 1253–1260, Jun. 2019, doi: 10.1007/s12633-018-9912-2.

[15] R. Nadjd-Sheibani and C. A. Hogarth, "The optical properties of some borate glasses," J Mater Sci, vol. 26, no. 2, pp. 429–433, Jan. 1991, doi: 10.1007/BF00576538.

[16] S. Rani, S. Sanghi, A. Agarwal, and N. Ahlawat, "Influence of Bi_2O_3 on optical properties and structure of bismuth lithium phosphate glasses," Journal of Alloys and Compounds, vol. 477, no.1, pp. 504–509, May 2009, doi: 10.1016/j.jallcom.2008.10.048.

[17] N. Deopa and A. S. Rao, "Photoluminescence and energy transfer studies of Dy^{3+} ions doped lithium lead alumino borate glasses for w-LED and laser applications," Journal of Luminescence, vol. 192, pp. 832–841, Dec. 2017, doi: 10.1016/j.jlumin.2017.07.052.

[18] Y. S. M. Alajerami, S. Hashim, W. M. S. Wan Hassan, and A. T. Ramli, "The effect of titanium oxide on the optical properties of lithium potassium borate glass," Journal of Molecular Structure, vol. 1026, pp. 159–167, Oct. 2012, doi: 10.1016/ j.molstruc. 2012. 05.047.

[19] P. S. Prasad, M. S. Reddy, V. R. Kumar, and N. Veeraiah, "Spectroscopic and dielectric studies on $PbO–MoO_3–B_2O_3$ glasses incorporating small concentrations of TiO_2," Philosophical Magazine, vol. 87, no. 36, pp. 5763–5787, Dec. 2007, doi: 10.1080/ 14786430701733016.

[20] T. Satyanarayana *et al.*, "Role of titanium valence states in optical and electronic features of $PbO–Sb_2O_3–B_2O_3:TiO_2$ glass alloys," Journal of Alloys and Compounds, vol. 482, no. 1, pp. 283–297, Aug. 2009, doi: 10.1016/j.jallcom.2009.03.185.

[21] M. A. Hassan and C. A. Hogarth, "A study of the structural, electrical and optical properties of copper tellurium oxide glasses," J Mater Sci, vol. 23, no. 7, pp. 2500–2504, Jul. 1988, doi: 10.1007/BF01111908.

[22] V. N. Sigaev *et al.*, "Structure of lead germanate glasses by Raman spectroscopy," Journal of Non-Crystalline Solids, vol. 2–3, no. 279, pp. 136–144, 2001.

[23] A. A. Ali, Y. S. Rammah, and M. H. Shaaban, "The influence of TiO_2 on structural, physical and optical properties of $B_2O_3 –TeO_2 – Na_2O – CaO$ glasses," Journal of Non-Crystalline Solids, vol. 514, pp. 52–59, Jun. 2019, doi: 10.1016/j.jnoncrysol.2019.03.030.

[24] J. Anjaiah, C. Laxmikanth, P. Kistaiah, and N. Veeraiah, "Dosimetric and kinetic parameters of lithium cadmium borate glasses doped with rare earth ions," Journal of Radiation Research and Applied Sciences, vol. 7, no. 4, pp. 519–525, Oct. 2014, doi: 10.1016/j.jrras.2014.08.009.

[25] H. Doweidar, K. El-Egili, R. Ramadan, and M. Al-Zaibani, "Structural units distribution, phase separation and properties of $PbO–TiO_2–B_2O_3$ glasses," Journal of Non-Crystalline Solids, vol. 466–467, pp. 37–44, Jul. 2017, doi: 10.1016/j.jnoncrysol.2017.03.040.

PARTIAL REPLACEMENT OF BITUMEN WITH WASTE PLASTIC FOR FLEXIBLE PAVEMENT

Farooq Ahmed Maniyar, Ameerhusain Jamdar and Farhan Kazi
Department of Civil Engineering, NK Orchid College of Engineering & Technology, Solapur, India

ABSTRACT
Nowadays plastic waste is one of the major concerns in our world. Plastic disposal is the major risk to the environment and the termination of this plastic is very unfavourable to the environment. Plastic being a non-biodegradable material does not decay over time and even if dumped in barren lands finds its way back in the environment through air and water erosion; can choke the drains and drainage channels. The use of plastic waste in a bituminous mix increases its properties and also strengthens it. The bitumen modified plastic improved the tensile strength of the road by making it more durable and flexible and also prevented pothole formation. The layer of molten plastic fills the space between the gravel and bitumen and holdsup rain water from seeping in and causing structural damage. Use of plastic waste in road makes it more hindrance in nature. Use of plastic waste in road construction enhances the properties of flexible pavement and gives a water proof surface as plastic is water resistant material. In addition, it will also be a solution to plastic disposal as road construction is the basic part of the developing countries. In current study, conventional and modified bituminous is blended with various plastic percentage are prepared using Low Density Polyethylene (LDPE), High Density Polyethylene (HDPE) and Polyethylene Terephthalate (PET) at normal mixing and compaction of temperature. The waste plastic is shredded and coated over aggregated in a furnace at 120^{o}C and mixed with hot bitumen at a temperature of 120-130^{o}C and resulted mix is used for pavement.

Keywords: Low Density Polyethylene (LDPE), High Density Polyethylene (HDPE), Polyethylene Terephthalate (PET), Pavement.

INTRODUCTION
The plastic roads include transition mats to ease the passage of tyres up to and down from the crossing. Both options help protect wetland haul roads from rutting by distributing the load across the surface. But the use of plastic-waste has been a concern for scientists and engineers for a quite long time. Recent studies in this direction have shown some hope in terms of using plastic-waste in road construction i.e., Plastic roads. A Bangalore-based firm and a team of engineers from R. V. College of Engineering, Bangalore as shown in figure 1.1, have developed a way of using plastic waste for road construction. An initial study was conducted in 1997 by the team to test for strength and durability. Plastic roads mainly use plastic carry-bags, disposable cups and PET bottles that are collected from garbage dumps as an important ingredient of the construction material. When mixed with hot bitumen, plastics melt to form an oily coat over the aggregate and the mixture is laid on the road surface like a normal tar road.

Figure 1.1 Road Constructed from Waste Plastic

1.1 PLASTICS

Plastic is a versatile packing material and a friend to common man while plastic has many valuable uses, we have become addicted to single-use or disposable plastic —with severe environmental consequences. In total, half of all plastic produced is designed to be used only once and then thrown away today we produce about 300 million tons of plastic waste every year, that's nearly equivalent to the weight of the entire human population. Plastic carry bags, packaging material, bottles, cups, and various other items have slowly replaced everything made of other material because of advantage of plastic.

Figure 1.2 Polyethylene Terephthalate (PET) Plastic

MATERIALS AND METHODS

2.1 Types of Plastics

i. Polyethylene Terephthalate (PET)

ii. HDPE, High-Density Polyethylene

iii. PVC, Polyvinyl Chloride

iv. LDPE, Low-Density Polyethylene

v. PP, Polypropylene

vi. PS, Polystyrene

Plastics are durable and degrade very slowly; the chemical bonds that make plastic so durable make it equally resistant to natural processes of degradation. Since the 1950s, one billion tons of plastic have been discarded and may persist for hundreds or even thousands of years. Perhaps the biggest environmental threat from plastic comes from nurdles, which are the raw material from which all plastics are made. They are tiny pre-plastic pellets that kill large numbers of fish and birds that mistake them for food. Prior to the ban on the use of CFCs in extrusion of polystyrene (and general use, except in life-critical fire suppression systems; see Montreal Protocol), the production of polystyrene contributed to the depletion of the ozone layer; however, non-CFCs are currently used in the extrusion process. Thermoplastics can be remelted and reused, and thermoset plastics can be ground up and used as filler, although the purity of the material tends to degrade with each reuse cycle. There are methods by which plastics can be broken back down to a feedstock state.

2.2 BITUMEN

The Indian bitumen market was valued at $2.8 billion in 2018, and is projected to reach $3.6 billion by 2026, growing at a CAGR (compound annual growth rate) of 2.8% from 2019 to 2026.

According to IS: 334 – 1951, bitumen is a black to dark brown sticky material, composed principally of high molecular weight hydrocarbons. It is a semi-solid hydrocarbon product of crude oil distillation, which is produced by removing the lighter fractions (such as liquid petroleum gas, petrol, and diesel) from heavy crude oil during their fining process. The physical properties of bitumen include adhesion, resistance to water, hardness, ductility, and higher softening point.

Figure 2.1 VG-30 Grade of Bitumen

2.3 AGGREGATES

Construction aggregate, or simply aggregate, is a broad category of coarse particulate material used in construction, including sand, gravel, crushed stone, slag, recycled concrete and geo-synthetic aggregates as shown in figure 1.4. Aggregates are the mostly mined materials in the world. Aggregates are a component of composite materials such as concrete and asphalt concrete; the aggregate serves as reinforcement to add strength to the overall composite material. Due to the relatively high hydraulic conductivity value as compared to most soils,

aggregates are widely used in bituminous mix. All bituminous and concrete surfacing are principally composed of aggregates, they play an important role in the behaviour of the pavement surfacing.

Figure 1.4 Aggregate Used for the construction of Flexible Pavement

2.4 DESIGN OF FLEXIBLE PAVEMENT USING IRC-37:2001 AND IRC-37:2018

The California bearing ratio (CBR) test is penetration test meant for the evaluation of subgrade strength of roads and pavements. The results obtained by these tests are used with the empirical curves to determine the thickness of pavement and its component layers. This is the most widely used test method for the design of flexible pavement.

The value of CBR for the present study has been calculated using IRC-37: 2001 for the following dimensions/data:

1. Two Lane Single Carriage Way
2. Initial Traffic in the year of completion of construction in terms of the number of commercial vehicles per day = 400 CV/Day
3. Traffic Growth (average annual growth rate) = 7.5% [Clause no. 3.3.2.2]
4. Design Life = 15 years [Clause no. 3.3.3.2]
5. Vehicle Damage Factor (VDF) = 2.5
6. CBR of Sub-grade Soil = 15% [Obtained]
7. Lane Distribution Factor = 0.75 [75%, Clause no. 3.3.5]
8. Cumulative number of Standard Axles (N) to be catered for in the design in terms of msa (million standard axles) [Clause no. 3.3.6.1]

$$N = \frac{365[(1+r)^n - 1]}{r} A.D.F$$

Where,

r = Annual Growth Rate of Commercial Vehicles (for 7.5% annual growth rate, r = 0.075)

D = Lane Distribution Factor (0.75)

F = Vehicle Damage Factor (2.5)

A = Initial Traffic in the year of completion of construction in terms of the number of commercial vehicles per day (400)

n = Design life in years (15)

$N = 365*[(1+0.075)^{15}-1]/0.075*400*0.75*2.5 = 7.2\times10^{6} = 7.2$ msa

As per IRC-37:2018 (page no. 41) for 7.2 msa value of the Pavement Thickness is 502 mm.

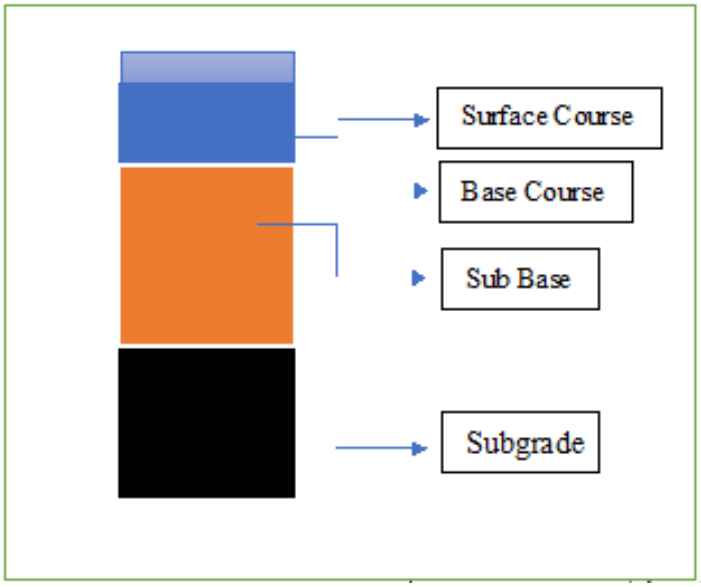

Figure 3.3 Pavement Composition

9. Total Pavement Thickness for CBR 15% and Traffic 7.2 msa = 502 mm

10. Pavement Composition

a. Surface Course = 30 mm

b. Base Course = 50 mm

c. Sub Base = 250 mm

d. Sub Grade = 172 mm

RESULTS AND DISCUSSION

3.1 RESULTS OF TESTS CONDUCTED ON AGGREGATE

Table 3.1 Results of Tests on Aggregate

Properties	Test	Specification	Result	IS-Code
Particle Shape	Flakiness & Elongation Index	Max.35% (Combined)	21.41%	IS:2386 (Part I)
Strength	Los Angeles Value	Max. 35%	11.43%	IS: 2386 (Part IV)

Strength	Aggregate Impact Value	Max. 35%	8.09%	IS: 2386 (Part IV)
Strength	Aggregate Crushing Value	Max. 35%	21%	IS: 2386 (Part IV)

Summary of Table 3.1 is:

a. Flakiness & Elongation Index of the Aggregate is 21.41%.

b. Los Angeles Value of the Aggregate is 11.31%.

c. Aggregate Impact Value of the Aggregate is 8.09%.

d. Aggregate Crushing Value of the Aggregate is 21%.

3.2 RESULTS OF TESTS CONDUCTED ON BITUMEN

Table 3.2 Results of Tests on Sub-Soil

Properties	Test	Specification	Result	IS-Code
Penetration	Penetration Test	50-70	56.67cm	IS:1203-1978
Softening Point	Softening Point Test	40-50	48.75℃	IS:1205-1978
Ductility	Ductility Test	40 minimum	76.7 cm	IS:1208-1978

Summary of Table 3.2 is:

a. Penetration Value of the Bitumen lies between 50-70.

b. Softening Point of the Bitumen is 48.75℃.

c. Ductility Value of the Bitumen is 76.7 cm

3.3 RESULTS OF MARSHALL STABILITY TEST

Table 3.4 Results of Marshall Stability Test

Properties	Observationof Marshall Test (O.B.C)	Observation table of Marshall Stability Test with (PET).
Stability Value	1532.21	1781.02
Flow Value	2.97	3.61
Bulk Density	2.35	2.24
Va	4.03	4.48
Vb	11.99	12.10
1VMA	16.05	17.25
VFB	74.10	74.01

- **Percentage of bitumen by weight % is 4.75**

Observations from Marshall Test (O.B.C.) and Marshall Stability Test with PET are shown in the Table 3.4.

Based on experimental work results for PET modified Bituminous mixtures compared with conventional Bituminous mixtures; the following conclusions can be drawn:

i. PET can be conveniently used as a modifier for Bituminous mixes for sustainable management of plastic waste as well as for improvement in performance of Bituminous mix.

ii. The optimum amount of PET to be added as a modifier of Bituminous mix was found to be 15 % by weight of optimum Bitumen content of the Bituminous mix.

iii. The Rate of PET Modifier of Bituminous Mix was found to be less as compared to the conventional Bituminous Mix. This can be the advantage for the disposal of plastic waste, which is the major problem to the environment.

iv. For a unit km the amount of bitumen can be replaced by 15% to the Optimum Bitumen Content which will lead to economical during the construction of Flexible Pavement.

CONCLUSION

The expansion of plastic waste adjusts the properties of bitumen. The utilization of plastic wastes in development of roads draws out a superior execution as there is better authoritative of bitumen with plastic. The recurrence of purge spaces is likewise diminished because of expanded holding and contact territory between plastic wastes and aggregates or bitumen. This eventually helps in lessening the absorption of moisture and oxidation of bitumen by entangled air. Henceforth, the roads can hold up under substantial activity, in this way expanding their toughness. The process is easy and does not need any new machinery. Plastic increases the aggregate impact value and improves the quality of flexible pavements. Wear and tear of the roads has decreased to a large extent. Plastic coating on aggregates is used for the better performance of roads. This helps to have a better binding of bitumen with plastic wasted coated aggregate due to increased bonding and increased area of contact between plastic and bitumen. The plastic coating also reduces the voids. This prevents the moisture absorption and oxidation of bitumen by entrapped air. This has resulted in reducing rutting, raveling and there is no pothole formation. The roads can withstand heavy traffic and show better durability.

In short, we can conclude that, using plastic waste in mix will help reduction in need of bitumen by around 15%, increase the strength and performance of road, avoid use of anti-stripping agent, avoid disposal of plastic waste by incineration and land filling and ultimately develop a technology, which is eco-friendly. Increased traffic conditions will and are reducing the life span of roads. Plastic roads are means of prevention and ultimately will be the cure.

REFERENCES

[1] V. A. Salimath and F. A. Maniyar (2019) Improvement of Subgrade Soil Characteristics by Utilizing Lime and Rice Husk Ash, International Journal of Engineering, Research and Technology, Vol. 8(6), 219-223.

[2] Khan Amjad, Gangadhar, Murali Mohan Murali and Rayka Vinay, (1999) "Effective Utilization of Waste Plastics in Asphalting of Roads", Report, R.V. College of Engineering, Bangalore.

[3] Al-Hadidy A.I., Yi-qiu Tan (2009), “Effect of polyethylene on life of flexible pavements”, Construction and Building Materials, Vol. 23(3), 1456-1464.

[4] Annette R. Hill, Andrew R. Dawson, Michael Mundy, (2001), "Utilisation of aggregate materials in road construction and bulk fill", Resources, Conservation and Recycling, Vol. 32, School of Civil Engineering, University of Nottingham, Australia, pp 305–320.

[5] Aravind K., Das Animesh, (2007), "Pavement design with central plant hot-mix recycled asphalt mixes", Construction and Building Materials, Vol. 21, Dept. of Civil Engg., Indian Institute of Technology Kanpur, India, pp 928–936.

[6] R. Vasudevan *et al.*, (2012), "A technique to dispose waste plastics in an eco-friendly way-Applicationin construction of flexible pavements", Department of Chemistry, Thiagarajar College of Engineering, Madurai, Tamil Nadu, India, Construction and Building Materials, Vol. 28(1), 311-320.

[7] Sangita *et al.*, (2011), "Effect of waste polymer modifier on the properties of bituminous concrete mixes", Construction and Building Materials, Vol. 25(10), Central Road Research Institute, New Delhi, India, pp 3841–3848.

[8] M. Wahlstroem *et al.*, (2000), "Environmental quality assurance system for use of crushed mineral demolition wastes in road constructions", Waste Management, Vol. 20(2), pp 225-232.

[9] J. R. Jimenez, (2011), "Utilisation of unbound recycled aggregates from selected CDW in unpaved rural roads", Resources, Conservation and Recycling, Vol. 58, Construction Engineering Area, University of Córdoba, Córdoba, Spain, pp 88–97.

[10] A. N. Dhodapkar *et al.*, (2008), "Use of waste plastic in road construction", Indian Highways, Technical paper journal, 31-32.

ABOUT THE EDITORS

Dr. Aarti Trehan
Associate Professor
Chemistry Department
Arya Kanya Mahavidyalaya
Shahabad M 136135, Kurukshetra
(Haryana) India

Dr. Aarti Trehan, Associate Professor of Chemistry at Arya Kanya Mahavidyalaya, Shahabad (M), Kurukshetra with over 30 years of research and teaching experience, got her doctorate from Panjab University as CSIR fellow and master's from Kurukshetra University. She has organized and actively participated in many seminars, workshops, conferences, webinars etc. and has more than 12 research publications to her credit in journals of repute. She is engaged in numerous academic and administrative activities in her college and university. She acted as Member, Board of Studies, Kurukshetra University. Her present interests include Educational Reforms and Sustainable Growth.

Dr. Rajesh Trehan
Associate Professor and Head
Department of Chemistry
DYSP Govt. P. G. College,
Nahan-173001 (H.P.) India

Dr. Rajesh Trehan got his doctorate from Panjab University, Chandigarh; master's (M.Sc., M.Phil.) from Kurukshetra University, Kurukshetra and is presently working as Associate Professor and Head of Chemistry Department at DYSP Govt. P. G. College, Nahan (H.P.). He has over 30 years of teaching and research experience at various premier government institutions; has more than 40 publications in national and international journals of repute and authored five books on varied topics. Dr. Trehan has organized and participated in many seminars, conferences, workshops, webinars of national and international level in various capacities and successfully completed three research projects of DST, CSIR & USAID. He was awarded fellowships of DST & CSIR (JRF, SRF open) in Chemical Sciences and is actively associated with many academic societies, clubs, associations etc. He got professional trainings on various analytical techniques from reputed institutions and performed numerous administrative and academic duties at college and university levels. He was also associated with Indira Gandhi National Open University (IGNOU) and SCERT. His current interests are material sciences, analytical chemistry, skill enhancements in chemistry and environmental sciences.

ABOUT THE BOOK

The modern world relies on development through technological advances all the time. Every day we are enriched by new discoveries and modern technologies that improve the comfort of our lives. We anticipate that chemistry will continue to define the directions of technological change during the 21st century, as the availability of various chemical raw materials is the basis of many inventions. In response to consumer demand and the problems faced by the world, chemistry is constantly developing and adjusting its technological capacity and will always appear at the basis of new discoveries or inventions. Chemistry will help us solve many future problems, including sustainable energy and food production, managing our environment, providing safe drinking water, promoting human and environmental health. Chemistry will continue to surprise us with new discoveries and will remain on the centre stage of recent advances for a long time to come.

The present work is a compilation of thirteen chapters showing the recent trends of research on varied topics from different parts of the globe predicting the role of chemistry in recent technological advances.

NEX GEN PUBLICATIONS
ISBN 978-81-959870-7-8
9 788195 987078

India | UAE | Nigeria | Uzbekistan | Montenegro | Iraq | Egypt | Thailand | Uganda | Philippines | Indonesia

www.nexgenpublication.com